DISSERTATION

A MULTI-SCALE ANALYSIS OF VEGETATION AND IRRIGATION HETEROGENEITY EFFECTS ON ECOHYDROLOGICAL FUNCTION AND ECOSYSTEM SERVICES IN A SEMI-ARID URBAN AREA

Submitted by

Edward A. Gage III

Graduate Degree Program in Ecology

In partial fulfillment of the requirements

For the Degree of Doctor of Philosophy

Colorado State University

Fort Collins, Colorado

Summer 2014

Doctoral Committee:

Advisor: David Cooper

Jay Ham
Stephanie Kampf
Michael Ryan

ABSTRACT

A MULTI-SCALE ANALYSIS OF VEGETATION AND IRRIGATION HETEROGENEITY EFFECTS ON ECOHYDROLOGICAL FUNCTION AND ECOSYSTEM SERVICES IN A SEMI-ARID URBAN AREA

An ever-increasing proportion of humanity resides in cities, yet the factors driving resource use and shaping urban sustainability remain poorly understood. In arid and semi-arid climates, water is a limited and costly resource, and future supplies are threatened by increases in population and climate change. A majority of summertime household water use in many western cities goes to irrigating vegetation, and this can be viewed as a significant cost or, from an ecosystem services perspective, "disservice". However, urban vegetation also provides a wide variety of important provisioning and regulating ecosystem services. While the general value of green spaces to ecological services is widely recognized, the importance of specific structural and compositional characteristics on ecosystem services and disservices is unknown. Such information is essential for achieving ecological resiliency in the face of an uncertain future.

This dissertation research focused on three broad objectives: (1) quantifying the compositional and structural variation in urban vegetation and characterizing consequences for water use patterns; (2) evaluating heterogeneity in irrigation practices and its relationship to water use by the two most common classes of urban vegetation, turfgrass and trees; and (3) quantifying a key ecosystem service, land surface temperature (LST) amelioration, in relation to vegetation composition, structure, and residential water use patterns. Because scale is a critical consideration in evaluating ecohydrological patterns and processes, I conducted my analyses at a range of spatial scales, from that of individual city parks to the city of Aurora, Colorado (> 200 km^2).

To develop high resolution land cover data essential for subsequent analyses, I compared the accuracy of different remote sensing classification approaches for mapping urban land cover (LC) and

structure. Specifically, I compared classification accuracy of LC maps derived from lidar and 4-band multispectral data using three different approaches: (1) an object-oriented segmentation (OBIA) and Random Forest classification approach; (2) a pixel wise classification using Random Forests; and (3) a traditional pixel-wise maximum likelihood classification. I mapped six classes: trees, buildings, low-vegetation, low-impervious, bare soil, and water. Overall classification accuracy for the Random Forest analysis was 92.7% (K_{hat} = 0.90), outperforming both the pixel-wise Random Forest classification (87.2% overall accuracy; K_{hat} = 0.83) and maximum likelihood classification (84.7% overall accuracy; K_{hat} = 0.80). The lidar-derived normalized difference surface model (nDSM) had the highest variable importance measure in both the pixel-wise and OBIA Random Forest analyses, highlighting the value of lidar height information for discriminating urban land cover classes.

To inform improved urban water conservation and planning, I evaluated spatial patterns and correlative relationships among physical land cover properties, socioeconomic and demographic characteristics, and single-family outdoor residential water use. Using the high resolution land cover maps and lidar-derived vertical structural data I developed, land cover composition and vertical structural characteristics for over 45,000 single-family detached residential parcels was analyzed. These data were combined with socioeconomic and demographic datasets from the 2010 US Census and local government agencies, and used in Random Forest regression analyses of outdoor water use from residential water meter records, with separate analyses conducted using parcels and census block groups as sampling units. To assess the relative importance of physical (e.g., land cover composition, three-dimensional structure) and socioeconomic variables in predicting outdoor water use, I evaluated conditional variable importance measures from Random Forest analyses and compared the predictive accuracy of models developed using subsets of explanatory variables. Random Forest models of outdoor water use developed using the subset of land cover variables had the highest predictive accuracy, followed by models developed using vertical structural variables, and lastly, the subset of socioeconomic/demographic variables. At both the parcel and census block group scale, I found statistically significant spatial clustering in outdoor water use, with neighborhood age, land cover, and vertical structure differentiating high and low water use clusters. High

water use clusters occurred in the oldest neighborhoods and had higher mean tree canopy cover and tree height than low water use clusters.

Water use can be viewed as an ecological disservice--a cost incurred to maintain irrigated urban vegetation--but assessments of cost and benefit should consider a wider suite of ecosystem services. One such service provided by irrigated vegetation is amelioration of the urban heat island formation through moderation of land surface temperature (LST). Using land cover maps and lidar-derived vertical structural data (e.g., tree and building height), I evaluated the relative importance of land cover compositional and vertical structural variables in predicting LST derived from Landsat 5 TM thermal band data. After aggregating data using 2010 census blocks, I analyzed LST using the Random Forest machine learning algorithm. Three variable importance measures were used to evaluate the relative value of variables in predicting LST. Along with NDVI, tree height and the mean height difference between trees and buildings had the highest variable importance for predicting LST and were found to contribute significantly to model accuracy. Models incorporating vertical structural variables explained an average of 11.5% more variation in LST than models developed using only land cover class variables. These results highlight the importance of vertical structure for LST patterns.

Finally, I evaluated water use by irrigated *Poa pratensis* turf and several common urban tree species in five city parks and recreational areas in Aurora. Two separate approaches were used to assess turf water use. Drainage lysimeters were installed in each study site and monitored to yield monthly and seasonal estimates of turf ET. Secondly, I used an infrared gas analyzer to quantify instantaneous ET from a small chamber sampled along a gradient of irrigation application and soil moisture availability. These measurements were related to qualitative measures of turf condition and quantitative analyses of digital photographs. To measure tree transpiration, I installed thermal dissipation sap flow sensors in study site trees. Irrigation application data was analyzed using a network of catch cans and interpolated to produce maps of application. Turf water use was highly variable within and between individual study sites. This was primarily due to variability in irrigation application caused by inefficiencies in sprinkler systems and heterogeneity introduced by localized sprinkler interception by tree trunks. Tree water use varied

depending on the specific water use metric in question (e.g., sap flux density, individual tree water use, and canopy-area normalized water use), tree species, and tree functional type. Ring-porous species had higher sap flux density values, but after factoring in the greater sapwood area of diffuse-porous species and conifers, they had whole tree and canopy-area adjusted water use on average below that of conifers or diffuse-porous trees. Collectively, these results highlight the variability in plant water use characteristics, variability that must be addressed in order to advance the broader understanding of urban water use in the Colorado Front Range.

ACKNOWLEDGMENTS

I am grateful for the all of the support I've received during the course of my degree program. Foremost, I thank my advisor, David Cooper. I am forever indebted for his mentorship and friendship through the years. David has the rare ability to think about both the "big picture" and fine details like the pubescence on a sedge's perigynium. He has helped me immeasurably improve my abilities as a scientist, writer, and thinker. Thanks also to my graduate committee for their keen observations and help in improving the style and substance of my dissertation.

Thanks to the City of Aurora and the Aurora Water Resources Department for funding and logistical support. I particularly wish to thank Dawn Jewell and Dan Gallen, whose support made possible the establishment and maintenance of field studies. The Aurora Parks and Open Space Department and their staff provided access to study sites and logistical support for sampling. Dan Ault and Branden Effland of Deere and Ault Engineers provided broad technical support for field analyses and deserve special acknowledgement. Thanks also to John Dingess, who provided insightful comments on the initial field research design. My thanks to the Colorado Water Resources Institute for their student research grant which provided additional funding.

I want to extend my deepest gratitude to all those who helped collect data in the field. Andrew Carlson played a particularly important role, displaying great patience in the field and a MacGyver-like ability to improvise solutions to problems large and small. Members of the Cooper lab have also been rock solid as friends and colleagues – it has been a privilege to learn beside so many talented and smart people. Particular thanks to Sarah Bisbing, Jeremey Shaw, Kristen Kaczynski, Dave Miller, Andrea Borkenhagen, Derek Schook, Betsy Bultemea, Cristina McCernen, Erick Carlson and all the other folks with whom I've shared office space, comradery, and many stimulating conversations through the years.

Lastly, I thank my incredible family for all their love and support. They, more than anyone, made this possible. Amy, Benjamin, and Juliana—you've made me sane and brought the lion's share of joy in my life through the years. Thank you. Lastly, my deepest thanks to my parents. As they've done throughout my entire life, they've given freely their love and support for me and I am forever grateful.

TABLE OF CONTENTS

LIST OF TABLES

LIST OF FIGURES

1. INTRODUCTION

The world is rapidly urbanizing, and for the first time in history, a majority of humans reside in cities (Clark 2003). This trend is predicted to continue (Cohen 2006), although the consequences for the global environment and future human well-being remain uncertain (Galea 2002). Adding greater resiliency to cities in the face of climate change, increasing populations, and resource scarcity is a critical societal challenge (Cromwell et al. 2007, Devitt and Morris 2009, Ahern 2013, Wu 2014). The importance of urban green spaces to the livability and sustainability of cities is broadly recognized (Jabareen 2006, Tzoulas et al. 2007, Pickett et al. 2011, Pickett et al. 2013). However, the identification of specific design and management approaches best able to provide desired ecosystem services has been stymied by the great compositional and structural complexity present in cities.

For my dissertation, I examined urban vegetation and its role in influencing water use and derived ecological services. I focused on three broad objectives: (1) quantifying the compositional and structural variation in urban vegetation and evaluating consequences for water use patterns; (2) evaluating fine-scale and landscape-scale heterogeneity in irrigation practices and plant water use; and (3) quantifying the provisioning of a key ecosystem service, land surface temperature (LST) amelioration, in relation to vegetation composition, structure, and irrigation patterns. As a whole, the dissertation is aimed at improving general understanding of the importance of urban heterogeneity on basic dimensions of urban function and sustainability, focusing on the particular role of urban vegetation.

Scale is a critical consideration in evaluating ecological and hydrologic patterns and processes (Wood et al. 1988, Levin 1992, Blöschl and Sivapalan 1995, Pickett and Cadenasso 1995). Therefore, I conducted my analyses at a range of spatial scales. Remote-sensing analyses were used to improve understanding of landscape-scale land cover and vertical structural characteristics in my study area. In addition, I conducted separate analyses at the field scale ($10^2 – 10^3$ m^2). While conceived of as distinct analyses and not a direct up- or down-scaling of a particular response measure, approaches were meant to

be complementary, thereby contributing to a broader understanding of urban vegetation effects on ecohydrological processes.

Some comments about my use of terminology are warranted. The main topics in this document fall within several distinct disciplinary domains. For example, Chapter 2, which details remote sensing analyses used to develop land cover data sets used elsewhere in the dissertation, falls squarely within the scope of a remote sensing or geography journal. In contrast, Chapter 5 focuses on plant water use and irrigation patterns and delves into topics traditionally pursued the fields of agronomy or ecology. Each chapter is written in the context of a particular schema, so some foundational knowledge and terminology is unavoidable. However, wherever possible, I try to avoid the use of jargon wherever a plain language alternative will suffice.

In Chapter 2, I present a remote sensing analysis of urban land cover and structure, the product of which was used in analyses presented in subsequent chapters. Specifically, I compare several approaches for classifying land cover using high-resolution multispectral imagery and lidar data. Because of their high structural complexity and spectral heterogeneity, traditional pixel-wise techniques for classifying remote sensing data often perform poorly in urban settings. However, my analysis demonstrates how, by incorporating height information from lidar data and applying efficient machine learning algorithms in an object-oriented image analysis (OBIA) framework, it is possible to markedly increase classification accuracy.

I use this land cover data set in chapter 3 to analyze outdoor residential water use data derived from water meter data provided by the city of Aurora, with the objective clarifying the influence of land cover composition, vertical structure, and socioeconomic characteristics on outdoor water use. This analysis was conducted at the scale of individual parcels, US Census Bureau census blocks, and census block groups. Land cover maps and lidar surface models developed in Chapter 2 were used to characterize parcel-level characteristics and relate these to outdoor irrigation. To evaluate the effects of spatial aggregation and to access socioeconomic data from the US Census Bureau and local government not available at the parcel scale, I aggregated parcel-level data to the census block and block-group scales.

At each spatial scale, I modeled outdoor water use using the Random Forest (RF) algorithm and used conditional variable importance metrics to evaluate the importance of different factors on model performance. Lastly, I used spatial statistical measures of local spatial autocorrelation to evaluate whether there were distinct clusters of high and low residential water use and to evaluate whether these were correlated with particular land cover and structural characteristics.

In arid and semi-arid regions, water use by and applied for urban vegetation is a limited and expensive resource, and from an ecosystem services framework perspective, can be considered a "disservice", i.e., a cost rather than a benefit is incurred (Pataki et al. 2011b). However, irrigated vegetation also provides beneficial services. One such service is moderation of land surface temperature (LST) and amelioration of the Urban Heat Island phenomenon. In chapter 4, I present presents results of landscape-scale analyses of land surface temperature (LST) patterns derived from Landsat thermal imagery in relation to patterns of urban vegetation. Specifically, I asked what land cover composition, vertical structural characteristics, and socioeconomic and demographic variables were most useful for predicting LST across my study area. I used Random Forests to evaluate the importance of different predictor variables on LST and GIS analyses to evaluate the spatial characteristics of LST.

Finally, I present field–scale analyses of tree and turf plant water use and irrigation practices for 5 urban parks and recreation areas. To evaluate spatial patterns of irrigation application, I deployed and monitored a network of catch cans, from which I generated application maps using spatial interpolation approaches in a GIS. Drainage lysimeters were used to quantify ET of *Poa pratensis* turf. I supplemented these data with survey measurements of instantaneous transpiration made using an infrared gas analyzer. Tree water use was measured using thermal dissipation (TDP) sapflow sensors. I found that plant water use was highly variable, and for turfgrass, water use patterns were strongly influenced by irrigation application and soil moisture availability.

In the pages that follow, I attempt to further understand the complex role urban vegetation plays in the urban environment by identifying and quantifying the key structural and functional characteristics of urban vegetation most important to urban ecohydrological function and related ecosystem services. Together, these studies provide a broad perspective on the role of urban vegetation and its management in the urban water balance of a semi-arid urban area, and of the importance of vegetation and anthropogenic subsidies of water on the provisioning of ecosystem services.

2. A COMPARISON OF OBJECT-ORIENTED AND PIXEL-WISE APPROACHES TO URBAN LAND COVER MAPPING USING LIDAR AND MULTISPECTRAL REMOTE SENSING DATA

Introduction

Land cover composition and spatial structure is highly variable in urban areas, with important consequences for ecological and hydrologic functioning (Oke 1989, McDonnell et al. 1997, Walsh et al. 2005). Vertical structural attributes including the height and lateral spacing of trees and buildings influence boundary layer roughness, energy and mass transfer processes, thereby affecting microclimate (Oke 1989, Mitchell et al. 2008). Given its broad importance, accurate land cover data is essential. However, the great heterogeneity present in cities makes accurate and fine-scale land cover classification using remotely sensed data difficult.

Many different land cover classification approaches have been developed. Among the key factors differentiating these approaches is source and general characteristics of the underlying data. Data used in classifications may originate from either airborne or satellite platforms, and can span a wide variety of data types beyond simple imagery, including radar, lidar, and hyperspectral imagery (Jensen and Cowen 1999, Huang et al. 2008, Weng et al. 2008). The choice of data used for classification is driven by many factors including spatial resolution, spectral resolution (i.e., the number and spectral width of bands), cost of acquisition, and spatial and temporal availability of data.

High spatial resolution images (< 1m ground surface distance), collected via either aircraft or space-borne platforms, are widely available in urban areas and are commonly used for land cover classification (Thanapura et al. 2007, Tooke et al. 2009, Myint et al. 2011). However, most high spatial resolution satellite products have low radiometric resolution, with 3 or perhaps 4 bands of information. Image fusion, whereby dissimilar types of data are combined for analysis (e.g., optical remote sensing data and radar), can help overcome these limitations (Lach et al. 2009, Yang et al. 2009, Malinverni et al. 2011). Increasingly, Lidar data are being incorporated into land cover mapping, often combined with

multispectral imagery (Priestnall et al. 2000, Seo 2003, Zhou and Troy 2008, Goodwin et al. 2009, Shugart et al. 2010). The height information from lidar can improve classification accuracy as well as providing insights into structural characteristics lacking in data describing simple compositional class (Holland et al. 2008). Effective and low-cost approaches and tools are needed to fully utilize the broad promise of these data for understanding the urban environment.

Remote sensing data have traditionally been classified using pixel-based classification approaches. These include unsupervised and supervised classification techniques utilizing hard and soft classifiers (Myint 2006, Doan and Foody 2007, Malinverni et al. 2011, Hansen and Loveland 2012). Regardless of the algorithms used, in all pixel-wise land cover mapping approaches, individual pixels are the units classified. In contrast, image segments—groups of contiguous pixels sharing some measure of spectral and spatial homogeneity—are the units classified in object-oriented image analysis (OBIA). OBIA utilizes not just the spectral characteristics of images, but also the spatial and contextual information of objects and their surroundings (Yu et al. 2006, Jobin et al. 2008, Pascual et al. 2008). Unlike conventional pixel-based classifiers such as minimum distance or maximum likelihood, object-oriented classification algorithms start by grouping neighboring pixels into meaningful multi-pixel objects based on spectral and spatial characteristics of pixel groups. These approaches can have higher classification accuracies than pixel-based methods (Kressler et al. 2002, Herold et al. 2003, Al Fugara et al. 2009), and are increasingly favored by analysts, particularly those working in spatially and spectrally complex urban landscapes (Kressler et al. 2002, Lackner and Conway 2008, Voss and Sugumaran 2008). New and developing open-source and low cost software and analysis tools offer great promise for expanding analysis options, but there remains uncertainty about best classification practices, particularly in cities.

With both pixel-wise and OBIA approaches, the analyst has to choose from numerous statistical classifiers. Examples include hard and soft (i.e., “fuzzy”) classifiers, each of which has many variants and different workflows depending on the specific software application used for classification. Pixel-wise classifications using a maximal likelihood classifier represent one of the earliest classifiers used to

classify remote sensing data (Campbell and Wynne 2002). While the technique is easily accessible and computationally efficient, its main value is as a benchmark to evaluate the efficacy of more modern classification approaches.

My goal with this research was to compare the mapping accuracy of several approaches for urban land cover classification using lidar and multispectral imagery. Specifically, I asked: (1) how does classification accuracy differ between land cover products derived from object-oriented analyses and those derived using traditional per-pixel frameworks? (2) How do different classification algorithms perform? (3) What variables derived from the raw lidar and multispectral imagery are most useful predicting land cover class membership?

Methods

Study area and data sets

My study area was Aurora, Colorado, a rapidly growing suburb with a population of approximately 325,000 residents in the Colorado Front Range (Figure 2-1). The pre-settlement land cover was shortgrass steppe, but much of this was converted to dryland and irrigated agriculture in the mid-19th century (West 1998). The region has had rapid population growth in recent decades, development away from the urban core in Denver and into Aurora.

My classification approach consisted of several general steps: (1) data preprocessing; (2) image segmentation (for the object-oriented approach only); (3) image classification; and (4) error analysis. The final land cover classification was the product of an iterative process, and preliminary classification runs were used to identify deficiencies in training data sets and improve the accuracy of subsequent classifications. An overview of the analysis approach is presented in Figure 2-2.

Small-footprint multiple-return lidar point cloud and intensity data were collected by Sanborn Map Company in April 2008 for portions of the Denver Metro region using a 1064 nm laser with a pulse repetition frequency of 50 kHz. Approximately 2.3 points/m^2 were collected. I used the LASTools library of lidar processing tools (Rapid Lasso, GmB; www.rapidlasso.com) to create separate 0.5 m resolution

raster grids based on first returns, bare Earth, and lidar intensity point data. A normalized digital surface model (nDSM), which represents the height of features above the ground surface, was created by subtracting the bare Earth surface from the first return surface.

Four-band (blue, green, red, near infrared) multispectral imagery were collected in April 2008 as part of a regional imagery and lidar data acquisition. To increase processing efficiency and reduce storage volume, the original 0.125 m GSD imagery was resampled using bilinear interpolation to a 0.25 m^2 pixel size (0.5 m GSD). To reduce information redundancy, a principal components analysis (PCA) was run using the original four bands and the first two bands were retained for use in image segmentation and classification. The red and near-infrared bands were used to calculate the Normalized Difference Vegetation Index (NDVI) and the green and near-infrared bands were used to calculate an analogue of the Normalized Difference Water Index (McFeeters 1996).

Image segmentation

Image segmentation, the process of completely partitioning an image into non-overlapping segments, is a critical step in object-oriented image analysis (Schiewe 2002, Chen et al. 2009). Data layers used for the segmentation (Table 2-1) were composited into a single multiband raster in ArcGIS (ESRI; Redlands, CA, USA) and exported for use as input into the segmentation software. Batch image segmentation of individual tiles was conducted using the software package BerkeleyImageSeg (BIS; Berkeley, CA, USA; http://berkenviro.com/berkeleyimgseg/). Each of the data layers had equal weight in the segmentation. BIS employs a segmentation method using region merging based on object heterogeneity of shape and spectral values (Benz et al. 2004). The algorithm begins with initial seed pixels and progressively merges areas based on homogeneity criteria determined by three image segmentation parameters: threshold, shape rate, and compactness. The threshold value controls the maximum size of image segments, while the shape rate and compactness parameters are weights used to determine segment shape by influencing the relative importance of segment compaction and spectral homogeneity in the region growing process. Using batch utilities in the BIS program that allow for the segmentation and evaluation of large numbers of parameter combinations, I evaluated segmentation

performance using the d* metric, which evaluates segmentation fidelity to the boundaries of training segments (Clinton et al. 2010) and through qualitative assessments of over- and under-segmentation using a single, small (2000 x 2000 pixels) test section of my study area. The final image segmentation used a threshold setting of 16, a shaperate value of 0.1, and a compactness level of 0.5 (Figure 2-3). Following the final image segmentation, the mean and standard deviation values for each image segment was calculated using zonal statistics tools in ArcGIS for each of the data layers used in the segmentation. Attribute data were then exported to the R statistical package for classification.

Image classification

A training data set was developed for use in classification development and assessment by manually selecting and assigning class identity to 2100 image segments spanning each of my intended classes: low vegetation (primarily irrigated turf, but also including other vegetation types such as remnant unirrigated shortgrass steppe communities), trees and tall shrubs, low impervious (asphalt, concrete, and other impervious materials), buildings, bare ground, and water. Training segments were chosen to represent the broad range of characteristics present in each class and for their fidelity to the true image object boundaries visible in the high-resolution imagery and lidar datasets.

I developed a classification model using the Random Forests algorithm in the statistical program R (Liaw and Wiener 2002). Random forests is an ensemble classifier widely used in machine learning applications because of its strong predictive ability and robustness to high dimensional and nonparametric data sets (Breiman 2001). I constructed 500 trees (mtree = 500) with a split of 2 (ntree = 2). Out of bag (OOB) error estimates were constructed providing an estimate of relative model performance. The importance of individual variables was assessed by evaluating two variable importance measures: mean decrease in accuracy and mean decrease in the Gini index.

Classification accuracy assessment

To quantify the accuracy of the resulting classification (Figure 2-4), I created a validation point data set by generating a spatially-balanced equal probability random sample of 500 points using the

ArcGIS v10.1 Geostatistical Analyst extension. For each point, I examined high-resolution imagery and manually assigned class identity. This validation data set was then compared to classification output from the Random Forest analysis and used to calculate overall accuracy, producer's accuracy (i.e., omission error), user's accuracy (i.e., commission error), and kappa coefficient (Congalton and Green 1999).

Comparison to pixel-based analyses

To provide a reference for evaluating the performance of the object-oriented classification, I conducted a pixel-based analysis of my study area using a traditional Maximum Likelihood classifier in ArcGIS 10.1. I used the same primary and derived raster layers used in the object-oriented analyses and training set polygons. The same validation data set used to evaluate the final object-oriented Random Forest classification was used to calculate error assessment measures including user's and producer's accuracies, overall accuracy, the confusion matrix, and the kappa coefficient.

Results

Object-oriented classification

The object-oriented Random Forest method produced an overall accuracy of 92.7% and a Cohen's kappa coefficient of 0.90, indicating a strong agreement between prediction and validation data unlikely entirely from chance (Figure 2-4). Analysis of the confusion matrix revealed that the highest producer's accuracy was for the water class (100%), followed low-impervious class (95.4%), low-vegetation (94.9%), buildings (88.6%), trees (87.5%), and bare soil (77.1%) (Table 2-2). The tree class had the highest user's accuracy (95.5%), followed by buildings (94.9%), and the low-impervious and low-vegetation classes, each with a user's accuracy of approximately 93%. User's accuracies for bare soil and water classes were significantly lower than other classes at 81.8% and 81.0%, respectively.

Two lidar-derived variables, mean segment nDSM and mean segment lidar intensity, had the highest variable importance measures in the final Random Forest classification (Figure 2-5). The specific ranking of the three most important multispectral image-derived variables differed depending on the variable importance measure used, but for both importance measures (mean decrease in accuracy and

mean decrease in Gini index), the two PCA bands and the NDWI-analogue had the highest variable importance. For any particular explanatory variable used in the Random Forest classification, it was the mean segment values rather than standard deviations that had the highest importance. This was expected given the nature of the segmentation process, which seeks to maximize homogeneity within the specified shape and compactness parameters.

Pixel-based classifications

My pixel-based land cover maps had lower overall classification accuracy than the object oriented Random Forest classification. The pixel-wise Random Forest classification had an overall classification accuracy of 87% and a kappa statistic (K_{hat}) of 0.83 (Table 2-3). The low vegetation and building classes at the highest producer's accuracies (90.1% and 90.5%, respectively), while the low vegetation and low impervious classes had the highest user's accuracies (92.9% and 91.4%). Bare ground had the lowest producer's and user's classification accuracy (74.3% and 66.7%).

As with the object oriented analysis, the most important variables in class prediction for the pixel-wise Random Forest classification were derived from lidar layers. The relative importance of variables differed depending on whether the importance measure is the decrease in accuracy or decrease in Gini metric. For example, 2011 NDVI was the third most important variable using the accuracy criterion, but was only the sixth most important variable when using the Gini criterion. The first principal components were of relatively low importance using both measures.

Overall classification accuracy was lowest for the land cover map produced from the pixel-wise maximum likelihood classification (84.7%). The kappa statistic (K_{hat}) of 0.80 was lower than for both the object-oriented Random Forest and pixel wise Random Forest classification products (0.90 and 0.83, respectively). Producer's accuracies from the maximum likelihood classification ranged from 68.6% (bare ground) to 88.5% (trees/shrubs), while user's accuracies ranged from 54.5% (bare ground) to 94.4% (low vegetation). The proportion of the assessment area comprised of each land cover class differed among classification approaches (Table 2-5). For example, the object-oriented Random Forest classification had the highest low vegetation cover (40.3%) compared to the pixel wise Random Forest and maximum

likelihood classification products (35.4% and 33.0%). The bare ground class was predicted with the lowest frequency for the object-oriented classification, while tree cover was most abundant in the maximum likelihood classification.

Discussion

Classification accuracy using both the object-oriented and pixel-wise Random Forest approaches exceeded the widely used minimum accuracy standard of 85% (Anderson et al. 1976), while the maximum likelihood classification was below this threshold. Accuracy was comparable to classifications performed elsewhere using similar data sets. For example, using orthoimagery and lidar data and an object-oriented Random Forest analysis approach, Guan et al. (2013) achieved an overall classification accuracy of 92.1% and 89.6% for land cover maps developed for Niagara Falls, NY and Mannheim, Germany, respectively. Working in Philadelphia, PA, O'Neil-Dunne et al. (2012) used lidar data and multispectral imagery in an object-based urban land cover analysis, producing a classification with an overall accuracy of 95%. As in my study, bare soil was the most problematic class in their analysis, with a producer's accuracy of 57% and a user's accuracy of 70%.

The pixel-based maximum likelihood approach performed most poorly, with a lower Kappa statistic and overall accuracy. In contrast to machine learning algorithms like the Random Forest approach, the maximum likelihood classifier is parametric, and assumptions regarding the distribution of predictors are typically violated, degrading classification performance. In addition to lower quantitative accuracy metrics, both pixel-based classifications suffered from a significant "salt and pepper" effect not present in the object-oriented Random Forest classification (Figure 2-6). These effects can be partially ameliorated using various filtering techniques, but the aesthetic presentation of the land cover, important to consumers of the data, is unavoidably degraded relative to the object-oriented maps.

My analyses clearly demonstrate that incorporating lidar data into classifications provides significant benefits (Schiewe 2002, Chen et al. 2009, Ke et al. 2010, O'Neil-Dunne et al. 2012, Guan et al. 2013). The lidar-derived nDSM had the greatest variable importance measure in Random Forests analyses and exploratory classifications run without inclusion of lidar data had significantly lower accuracy, owing

in great part to increased confusion between high and low vegetated and impervious classes. My results clearly demonstrate the utility of nDSM data for separating classes, particularly trees and buildings.

The primary imagery used in this analysis was the 2008 4-band data set, collected in spring prior to leaf emergence. The leafless phenology did not prevent accurate tree identification, since lidar data were effective for distinguishing this class. However, because vegetation was still emerging from dormancy, contrasts with bare soil class were less pronounced than they would have been after leaf expansion and growth. I achieved small gains in overall accuracy by introducing additional information on vegetation vigor via NDVI data from the summer of 2011. However, I also observed the introduction of different types of errors associated with differences in imagery resolution and registration. I limited data used in the segmentation to imagery and lidar data sets and their derivatives collected contemporaneously in 2008, and limited used of the 2011 data to the classification stage.

Accuracy is a primary concern in land cover classification. However, other factors such as data storage and processing requirements must also be addressed. The computational efficiency of segmentation algorithms are affected by the number of bands, pixel size, and analysis extent. The analyst may choose, as I did in this analysis, to resample imagery to a slightly coarser resolution to increase computational efficiency and reduce storage overhead. Tiling of analyses is essential when processing large areas. If software and hardware resources for parallel processing of data sets are available, considerable efficiencies can be gained (O'Neil-Dunne et al. 2012).

The approach I used resulted in high classification accuracy. Random Forests is robust and flexible, allowing the fusion of different data types and usability for both pixel-wise and object-oriented work flows (Watts and Lawrence 2008, Smith 2010, Rodriguez-Galiano et al. 2012, Guan et al. 2013). As an ensemble method, interpretation of Random Forest output is less straightforward than an approach such as single-tree regression (Strobl et al. 2009). However, variable importance measures do provide greater insights into the predictive value of different data sets than black box methods like artificial neural networks (Witten et al. 2011).

The efficacy of any specific classification approach is best viewed in the context of the aims and purposes of the classification, as well as the available data and resources for analysis. Results from this study clearly demonstrate the utility of lidar data for improving classification accuracy, but given the high cost of lidar acquisition and the currently limited availability of free or low-cost lidar archives, such data may not be available. Classifications adequate for many purposes are still possible using only optical imagery, but results will be less accurate. This study also illustrates the advantages of an object-oriented analysis approach. Commercial software packages like eCognition offer many algorithms for segmentation and classification, but can be prohibitively expensive. However, as with many aspects of technology and software development, lower cost and open-source alternatives are rapidly gaining functionality, so limitations will gradually disappear.

Errors in analyses can arise from several sources. While considerable care was taken in selecting parameters for image segmentation, over-segmentation and under-segmentation errors cannot be completely avoided. Training data used to develop and refine the classification model do not necessarily encompass the full range of characteristics present within each class, a source of potential error in the process. There is also a temporal component to consider; land cover patterns change over time, and in the case of urbanization, changes can be dramatic. As with all aspects of the classification process, there are trade-offs to consider including accuracy, efficiency, and cost.

Conclusions

Accurate high resolution land cover data are essential to evaluate the effects of urbanization and to manage urban form and function to the greatest benefit. This study demonstrates the advantages of object-oriented analysis approaches in urban land cover analyses. The fusion of lidar and optical imagery allows for high classification accuracy, a challenge in structurally and spectrally complex urban environments. Random Forests is a powerful classification algorithm, particularly when used in an object-based analysis framework. However, even when it is applied in a pixel-wise analysis approach, it outperforms traditional parametric classifiers. While pixel-wise maximum likelihood classifiers are more accessible than ever before, having been incorporated into the most popular commercial GIS program.

However, results clearly demonstrate the value of using more robust machine learning approaches. These are easily accessible through open-source software platforms like R and provide an easy means of improving classification workflows.

Table 2-1. Data sets used in classification. All data layers were resampled to 0.5 m GSD.

Data layer	Description
Multispectral imagery	Collected April, 2008. Blue, green, red, near-infrared bands. A primary data set used to generate image derivatives (e.g., NDVI). Original GSD 0.15 m; resampled to 0.5 m
Normalized Difference Vegetation Index (NDVI)	Derived using red and near-infrared bands: NDVI = (NIR - R)/(NIR + R)
Normalized Green/NIR index (NGI)	Derived using green and near-infrared bands: NGI = (G - NIR)/(G + NIR)
Principal Components Analysis (PCA) bands	Derived using the 4 primary multispectral bands. The first two PCA bands (PCA1 and PCA2) were retained for use in segmentation and classification
Lidar LAS files	Collected April, 2008. Raw lidar data. A primary data set used to generate the first return and bare ground points used in nDSM calculation
Normalized Digital Surface Model (nDSM)	Calculated as the difference between bare Earth and first return surfaces
Lidar intensity	Primary lidar data layer
NDVI 2011	Derived from 1 m NAIP imagery. Not used in segmentation, only in classification

Table 2-2. Confusion matrix for object-oriented Random Forest classification of urban land cover.

	Ground truth							
Class	*Bare*	*Bldg*	*LowImp*	*LowVeg*	*Tree/shrub*	*Water*	Count	**% User Accuracy**
Bare	**27**	0	2	4	0	0	33	**81.8**
Bldg	0	**93**	3	0	2	0	98	**94.9**
LowImp	3	8	**230**	1	3	0	245	**93.9**
LowVeg	5	1	6	**243**	6	0	261	**93.1**
Tree/shrub	0	3	0	1	**84**	0	88	**95.5**
Water	0	0	0	7	1	**34**	42	**81.0**
Count	35	105	241	256	96	34	**767**	
% producer accuracy	**77.1**	**88.6**	**95.4**	**94.9**	**87.5**	**100.0**		
Overall accuracy: 92.7% K_{hat} **= 0.903**								

Table 2-3. Confusion matrix for pixel-wise Random Forest classification of urban land cover.

	Ground truth							
Class	*Bare*	*Bldg*	*LowImp*	*LowVeg*	*Tree*	*Water*	Count	% User accuracy
Bare	**26**	0	7	6	0	0	39	**66.7**
Bldg	0	**95**	9	4	11	0	119	**79.8**
LowImp	3	4	**210**	1	2	6	226	**92.9**
LowVeg	1	3	12	**233**	6	0	255	**91.4**
Tree	0	3	3	9	**77**	0	92	**83.7**
Water	5	0	0	3	0	28	36	**77.8**
Count	35	105	241	256	96	34	**767**	
Producer accuracy	**74.3**	**90.5**	**87.1**	**91.0**	**80.2**	**82.4**		
Overall accuracy: 87.2% K_{hat} **= 0.83**								

Table 2-4. Confusion matrix for pixel-wise maximum likelihood classification of urban land cover.

	Ground truth							
Class	*Bare*	*Bldg*	*LowImp*	*LowVeg*	*Tree*	*Water*	Count	% User accuracy
Bare	**24**	0	9	10	1	0	44	**54.5**
Bldg	0	**89**	14	4	10	1	118	**75.4**
LowImp	3	6	**204**	1	0	5	219	**93.2**
LowVeg	3	2	8	**220**	0	0	233	**94.4**
Tree	0	8	6	18	**85**	0	117	**72.6**
Water	5	0	0	3	0	**28**	36	**77.8**
Count	35	105	241	256	96	34	**767**	
Producer accuracy	**68.6**	**84.8**	**84.6**	**85.9**	**88.5**	**82.4**		
Overall accuracy: 84.7% $\mathbf{K_{hat} = 0.80}$								

Table 2-5. Comparison of class abundance (% of the assessment area) for each classification approach.

Class	Random Forest OBIA	Random Forest Pixel-wise	Maximum likelihood
Bare	0.5	4.2	3.7
Bldg	12.6	16.8	15.6
LowImp	32.1	28.2	25.3
LowVeg	40.3	35.4	33.0
Tree	13.7	14.7	21.7
Water	0.8	0.7	0.7

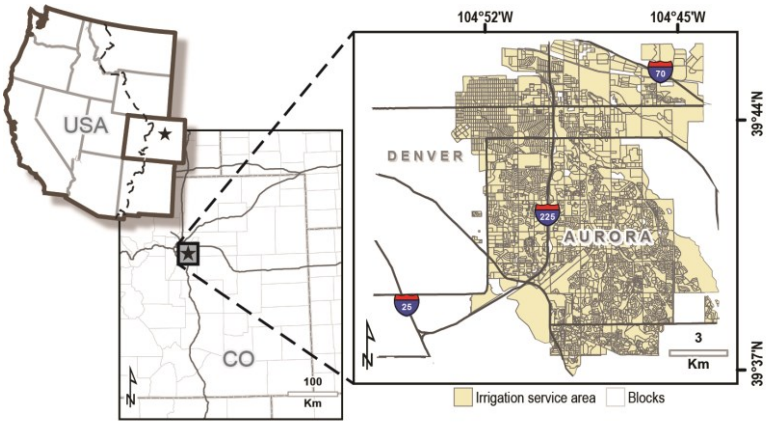

Figure 2-1. Map of Aurora, Colorado study area.

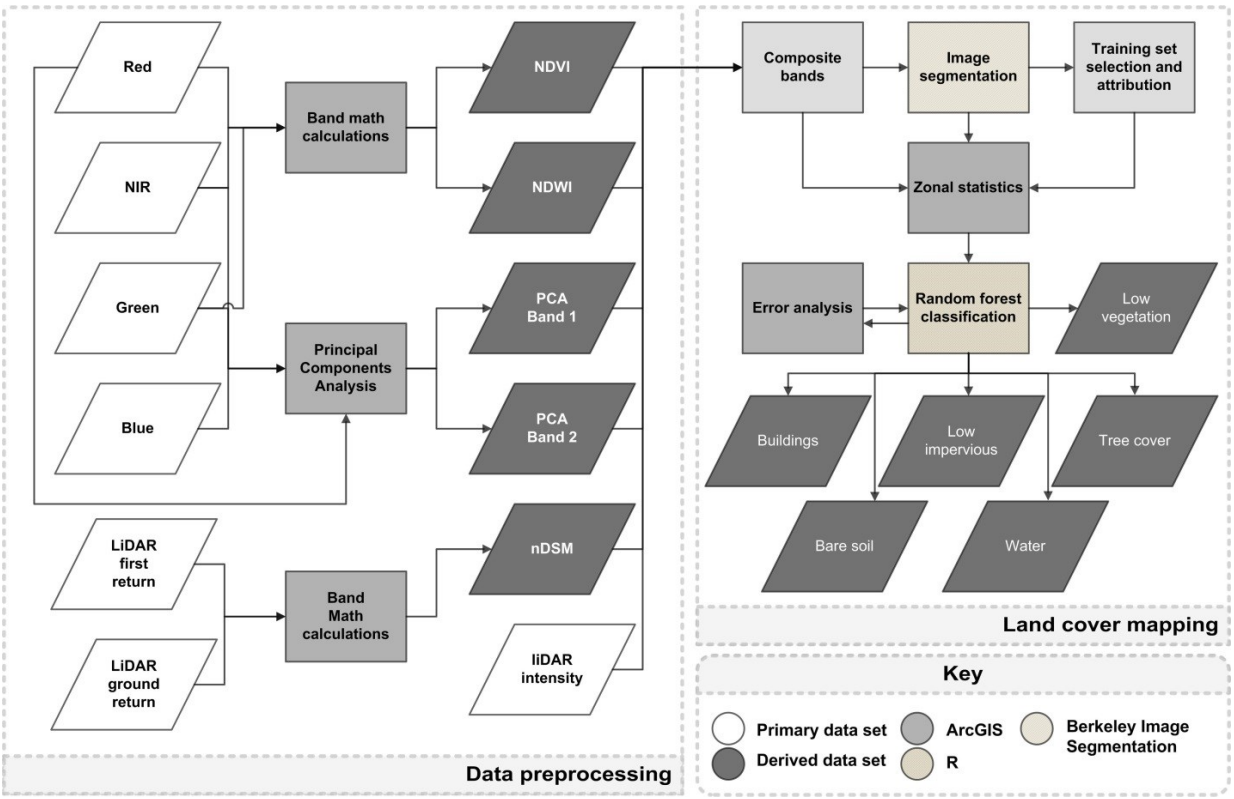

Figure 2-2. Flow chart illustrating main steps in analysis (NDVI = Normalized Difference Vegetation Index; NDWI = Normalized Difference Water Index-analogue; nDSM = Normalized Digital Surface Model).

Figure 2-3. True color image of portion of study area (panel A); PCA band 1 (panel B); PCA band 2 (panel C); NGI (panel D); lidar intensity (panel E); lidar-derived nDSM (panel F).

Figure 2-4. Example of final land cover classification. Low vegetation consists primarily of irrigated turfgrass, but also includes other vegetation cover types such as unirrigated remnant shortgrass steppe communities. The low impervious class includes land cover materials such as asphalt and concrete.

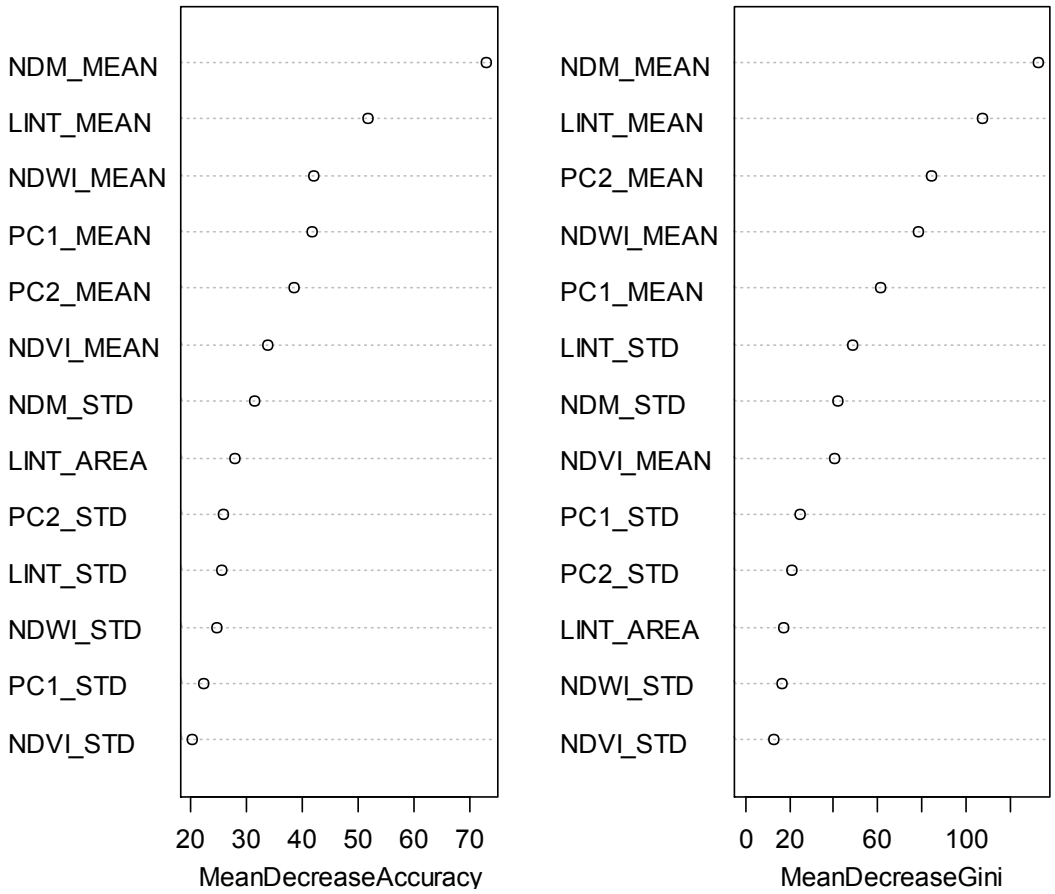

Figure 2-5. Variable importance plots from Random Forest classification of image segments. MeanDecreaseAccuracy measures how much the inclusion of a predictor in the model reduces classification error, while a low Gini (i.e. higher decrease in Gini) indicates that a particular predictor variable plays a greater role in partitioning the data into the defined classes.

Figure 2-6. Comparison of LC maps from maximum likelihood pixel-wise classification (Panel A) and object-oriented Random Forest analysis (panel B). Circles illustrate examples of common classification errors with both the pixel-wise approaches: power lines and cars. Also of note is the greater "salt and pepper" effect in the pixel-wise classification.

3. THE INFLUENCE OF LAND COVER, VERTICAL STRUCTURE, AND SOCIOECONOMIC FACTORS ON OUTDOOR WATER USE IN A COLORADO FRONT RANGE URBAN AREA

Introduction

Water is an essential yet limited resource in most regions of the world. The costs of securing and delivering water to cities in arid and semi-arid regions are high and rising due to pressures such as drought and population increases (Hansen et al. 2002, Brookshire et al. 2004, Brown 2006). In addition, climate changes threaten the future of these water supplies (Barnett et al. 2008). In many cities in the western US, the majority of water use during the summer is for outdoor irrigation, and planners and water managers increasingly recognize the importance of water conservation for urban sustainability (St. Hilaire et al. 2008, Ferguson et al. 2013). However, patterns of residential outdoor water use are complex, and there is considerable uncertainty about the drivers of household irrigation practices. While the effects of pricing strategies and other economic factors on residential water use have been examined (Kenney et al. 2008, Grafton et al. 2011), little is known about how the varying patterns in ecological, physical, and socioeconomic characteristics across cities affects outdoor irrigation use.

Domestic water use is influenced by climate, urban design, land development history, and socioeconomic and demographic factors (Corbella and Pujol 2009, House-Peters and Chang 2011). The importance of each factor depends on the whether indoor, outdoor, or total household water use is evaluated and the spatial scale of analysis (Wentz and Gober 2007, Balling et al. 2008, House-Peters and Chang 2011). Important factors at the scale of individual parcels may include its area and the type of vegetation being grown, as well as socioeconomic factors such as household income (Harlan et al. 2009, Larson et al. 2010). At broader spatial scales (e.g., US Census tracts), factors such as the built area and density are significant predictors of water use (Polebitski and Palmer 2009). While residential water use has been correlated with a number of explanatory variables (Arbués et al. 2003, Wentz and Gober 2007, Polebitski and Palmer 2009) few studies have compared the relative importance of land cover

composition, structure, and socioeconomic/demographic characteristics on water use, all factors that will drastically change with urbanization in the region.

Understanding the spatial pattern of outdoor water use, whether random, dispersed or clustered, has important implications for water planning and conservation. Spatial statistical techniques can provide an objective means of characterizing water use patterns across large areas. Distinct geographic trends were found for total county, municipal, and agricultural water use in Oregon, USA (Franczyk and Chang 2009). In British Columbia, spatial statistical analyses were used to identify distinct neighborhood effects on residential water use (Janmaat 2013). An understanding of the spatial characteristics of water use can provide information critical to predicting future changes in water demand, but few studies have examined the spatial patterns of outdoor water use in semiarid regions.

The relative abundance and spatial organization of land cover (LC) classes such as trees, turfgrass, buildings, and pavement shapes a city's physical structure, influencing biophysical and ecological processes, environmental quality, and aesthetics (Smardon 1988, Dimoudi and Nikolopoulou 2003). The fine-scale analysis of urban LC has been limited by a lack of high resolution land cover data. The National Land Cover Database (NLCD) derived from 30-m pixel Landsat imagery is widely available in the US is too course for the analysis of individual household-scale land cover. High-resolution satellite imagery and new classification techniques allow the analysis of land cover patterns at the scale of individual residential parcels and whole cities. Both scales are critical for understanding patterns and potential drivers of water use, but have not been undertaken in semi-arid cities.

Vertical structural of the urban forest varies among neighborhoods of different age and those with distinct tree species composition. Other characteristics of landscape structure such as increases in average building size and density in recent decades have also occurred in many cities (Wheeler 2008). Vertical structure influences evapotranspiration and energy exchange rates and processes (Oke 1989), but it has not been incorporated into landscape-scale analyses of urban water demand because suitable data have been lacking. Lidar remote sensing data can be used to quantify fine-scale vertical structure across

landscapes (Lefsky et al. 2002, Shugart et al. 2010), and evaluate the importance of vertical structure on outdoor water use patterns.

Land-use and socioeconomic/demographic factors may also influence residential water use (Balling and Cubaque 2009, Boone et al. 2010). For example, larger homes and those with higher assessed values have been reported to use more water (Harlan et al. 2009). However, an analysis of single family residential water consumption in an Oregon suburb found that outdoor water use was positively correlated with head of household education level and the size of the property's outdoor space (House-Peters et al. 2010). However, the relative importance of socioeconomic factors on residential outdoor water use versus land cover composition and vertical structure of remains poorly understood.

Objectives

In this study, I analyzed the influence of land cover composition, vertical structure, and socioeconomic/demographic variables on outdoor water use at different spatial scales. My data set of more than 40,000 single-family parcels provides a suitable data set for analyzing broad-scale patterns of outdoor water use and allowed me to ask the following questions: (1) What land cover, vertical structure, and socioeconomic & demographic factors best predict outdoor water use? (2) Are single-family parcels with similar outdoor water use clustered spatially, and if so, what are the characteristics of high and low-use clusters? (3) How do patterns of outdoor water use vary with urban neighborhood age and the scale of analysis? The results of analyses provide improved context for understanding the relationships between urban land cover vegetation characteristics and irrigation practices, which is an important component of urban water use.

Methods

Study area

My study area was Aurora, Colorado, a rapidly growing suburb with approximately 325,000 residents located east of Denver in the Colorado Front Range urban corridor. The land historically was short grass steppe, but beginning in the mid-19th century, most areas were converted to agricultural crops

to support Denver and surrounding areas. Human population increased through the 20th century and has led to the urbanization of remnant steppe and agricultural lands. Dominant contemporary land uses include low to high density single and multi-family residential, retail, commercial and light industrial. Urban forests, irrigated lawns parks and residential areas, and unirrigated communities are the dominant urban vegetation types. The climate is semiarid, with the majority of precipitation occurring from April-September, often from large convective thunderstorms (Doesken et al. 2003). The 30-year normal annual precipitation is 402 mm, but during 2005 and 2006, the two years examined in the study, 321 mm and 213 mm was recorded (National Weather Service; Station ID: KDEN). Approximately 75% of Aurora's water goes to residential consumers, with the remainder going to municipal, commercial, and agricultural users (Kenney et al. 2008).

Outdoor water use

I used data from individual parcel water meter records for calendar years 2005 and 2006 provided by Aurora Water for my analyses. Outdoor water use was quantified by subtracting mean winter household water use, when little to no outdoor water use occurs, from March through November monthly water use totals. I focused my analyses to detached, single-family parcels in Arapahoe County. Because total outdoor water use may be influenced by parcel area and vegetation cover I derived two additional response variables for my analyses. Total water used (m^3) was divided by parcel area (m^2) in ArcGIS to produce a parcel-adjusted depth of application (I_{parcel}; in m^3 water/m^2 area). I divided the total volume of water used by the area covered by vegetation in each parcel to produce $I_{vegetation}$. To eliminate outliers caused by errors in meter records or GIS datasets, I statistically normalized I_{parcel} and $I_{vegetation}$ for 2005 and 2006 and filtered out parcels with z scores more than 3 standard deviations from the mean as outliers (Balling and Cubaque 2009). The final analysis included 46,588 parcels.

Physical, socioeconomic, and demographic variables

I used a 0.5 m resolution land cover (LC) developed in Chapter 2 for assessing the physical structure of each parcel. Five LC classes were mapped: trees, buildings, low vegetation, low impervious,

and “other” (bare soil, water). Using parcel boundary GIS data from the Arapahoe County tax assessor and zonal statistics tools in ArcGIS, I calculated the proportion of parcels covered by each LC class, as well as several lidar-derived vertical structural variables such as tree height (Table 3-1). For census block groups, I calculated the mean and maximum variable value of all parcels in a given block group.

I used 2009 appraised property values from the Arapahoe County assessor's office as an indicator of socioeconomic status of individual parcels. At the scale of US Census Block Groups, primary variables for demography such as the mean age of residents, household size, and marital status were used (2010 Decennial Census Summary File SF 1; www.factfinder2.census.gov)(Table 3-2). To evaluate the effect of differences in the age of residential development on patterns of outdoor water use and different explanatory variables, I utilized historical land use and land cover data from the Colorado Front Range Comprehensive Urban Ecosystem Study (CUES) project [http://rockyweb.cr.usgs.gov/cues/COcuesHome.html]. These data are derived from analyses of historical aerial photographs and geospatial data depicting land-use for 1937, 1957, 1977, and 1997. To extend this analysis to the years of my water use data, I used zoning and parcel data to identify parcels built between 1997 and 2007.

Spatial statistical analyses

I quantified the patterns of outdoor water use, LC composition and vertical structure, and socioeconomic variables using spatial statistics metrics. Using ArcGIS I calculated the Getis-Ord Gi* statistic, which identifies statistically significant spatial clusters of high or low values by comparing measured patterns to those expected by random chance (Getis and Ord 1992). A fixed inverse Euclidean distance threshold of 500 m was used for parcel-scale analyses, while a 1000 m threshold was used for block groups because of the courser spatial scale.

I calculated the Anselin Local Moran's I statistics as a complimentary measure of local spatial pattern using ArcGIS. The statistics produced are a measure of local autocorrelation, with high positive z-scores indicating that the surrounding features have similarly high or low values, and low negative z-score indicating spatial outliers (Anselin 1995). To examine potential land cover and vertical structure

correlates of high and low water use clusters, I compared explanatory land cover and socioeconomic variables between statistically significant ($p < 0.05$) clusters of high values (HH), low values (LL), as well as spatial outliers with high values surrounded by low values (HL), and spatial outliers where low values are surrounded primarily by high values (LH).

Random Forest analyses of outdoor water use

I used Random Forest (RF) models developed using the "randomForest" package (Liaw and Wiener 2002) in R (ver. 15.3)(R Core Team 2013) to analyze the relative importance of land cover composition and structural variables on parcel water use. Separate regression models were developed using I_{parcel} and $I_{vegetation}$ as response variables. Model predictive accuracy, assessed using out-of-bag (OOB) error estimates (Strobl et al. 2009) produced by the algorithm were used to compare model predictions for subsets of explanatory variables, such as vertical structure variables, LC composition, and socioeconomic/demographic variables. Each model was run using 500 trees and an mtry set to the square root of the number of variables (Diaz-Uriarte and Alvarez de Andres 2006, Hapfelmeier and Ulm 2013).

I compared conditional variable importance values generated using the "cforest" algorithm in the R "party" package to provide an additional measure of the relative importance of land cover structure, vertical structure and socioeconomic factors on model prediction. Conditional variable importance metrics can be more robust than traditional variable importance measures (Strobl et al. 2007). While RF variable importance measures help identify important factors, they do not identify whether correlations are positive or negative. To better understand the relationship between explanatory and response variables, as well as the correlation structure among explanatory variables, I calculated and plotted Pearson partial correlation coefficients.

Results

Land cover, vertical structure, and socioeconomic patterns

The most abundant LC class was low vegetation with a mean cover of 34.6%, followed by buildings at 26.2%, and 17.7% for trees. LC class values were significantly different between parcels of

different age (Figure 3-1). For example, mean tree cover was 28.6% in parcels developed prior to 1938, compared to 8.6% for parcels developed between 1997 and 2007. Cover of the low vegetation class was less variable, ranging from a low of 33.0% in parcels built between 1978 and 1998 and a maximum of in 37.9% in parcels built between 1938 and 1958. Buildings occupied 34.3% of the youngest parcels, and only 23.8% of parcels in the oldest neighborhoods, reflecting a trend of a decreasing tree cover and increasing home sizes in the newest neighborhoods.

Mean tree height had a similar pattern to tree cover, with the youngest neighborhoods having the lowest mean and maximum tree heights at 3.1 and 6.8 m, compared with 4.8 and 13.7 m for the oldest neighborhoods. Mean tree and building heights were spatially autocorrelated as indicated by the statistically significant global Moran's I and Getis-Ord General G statistics ($p < 0.0001$). Maps created using the output from spatial autocorrelation analyses showed significant clustering of high and low outdoor water use areas and of physical and socioeconomic explanatory variable values (Figure 3-2, 3-3). For example, mean tree height in the older north-central portion of Aurora was average for the study areas, while clusters of low height trees occurred in the newer portions of the study area (Getis Gi^* statistics). Appraised property values in 2009 were much higher in the newest neighborhoods with a mean of $213,336, compared with $104,865 for parcels built between 1938 and 1958.

Spatial trends in parcel-scale land cover composition and vertical structure were still present following aggregation of parcel-scale data into census block groups. Aggregation reduced fine scale heterogeneity evident in parcel-scale maps, but did not eliminate broader patterns of land cover variation seen in the parcel data set. Block groups in the older northwest portions of the city had higher mean tree height, with a mean of approximately 5.3 m, versus a low of 2.7 m in block groups in the newest parts of the study area supporting lower tree cover. The negative correlation between both tree canopy cover, tree height, and outdoor water use was the same when evaluated with either $I_{vegetation}$ or I_{parcel}.

Parcel outdoor water use

Mean total outdoor water application per parcel in 2006 was 412.8 m^3, which was 4% greater than 396.5 m^3 applied in 2005. After normalizing for parcel area, mean irrigation application (I_{parcel}) was

0.56 m in 2005 and 0.58 m in 2006, while irrigation normalized by vegetated area ($I_{vegetation}$) was 1.09 m and 1.14 m. At the parcel scale, $I_{vegetation}$ was negatively correlated with % vegetation (Pearson correlation = -0.62), the opposite of the correlation with % impervious cover (correlation = 0.62). I found significant spatial clustering of high (high Getis Gi^* z scores; low p-value) and low water application parcels (negative Getis Gi^* z scores; low p-value) in analyses of 2005 and 2006 $I_{vegetation}$ (Figure 3-2). Distinct clusters of high water use parcels occur in the eastern and central portions of the study area, and low water use in the north as indicated by both local Moran's I and Getis Gi* analyses of $I_{vegetation}$. Similar spatial trends were observed with analyses of I_{parcel}.

Mean outdoor water use among parcels in high water use clusters during 2005 was 1.89 m, which was significantly greater than the mean of 0.53 m in low use clusters (Kruskal-Wallace test, $p < 0.001$; Figure 3-3). When high use spatial clusters are broken down by neighborhood age, the youngest parcels built between 1998 and 2007 had the highest mean water use of 2.27 m compared with 1.70 m in parcels built prior to 1938 (Table 3-3). Low water use clusters had significantly higher maximum and mean tree height (Kruskal Wallace, $p < 0.0001$), while the mean % impervious cover in high water use clusters was 57.8%, nearly twice that of low water use clusters.

Block group water use

Spatial trends in water use and land cover/vertical structure across study area census blocks were similar to those observed at the parcel scale (Figure 3-4). Block group scale $I_{vegetation}$ was positively correlated with vegetation class cover and tree height in 2005 and 2006 (Figure 3-5). As with the parcel level analysis, mean block group-scale $I_{vegetation}$ was slightly lower in 2005 than 2006, at 1.07 m and 1.11 m. Mean parcel area-adjusted application rates (I_{parcel}) were 0.55 m in 2005 and 0.58 m in 2006. Global Moran's I for vegetated area-adjusted water use was positive and statistically significant in 2005 (Moran's $I = 0.31$; $z = 5.5$; $p < 0.0001$), and 2006 (Moran's $I = 0.33$; $z=5.8$; $p < 0.0001$), indicating a tendency for clustered rather than dispersed outdoor water use among census blocks (Figure 3-5).

Random Forest analyses of parcel outdoor water use

The fully parameterized Random Forest model of parcel water use explained 58.4% of the variance in $I_{vegetation}$ in 2005 and 54.2% in 2006. Models that used only land cover variables predicted most of the variance, 55.7% in 2005 and 53.8% in 2006, highlighting the strong predictive value of land cover, particularly %vegetation and %impervious surface. Models that used vertical structure variables explained 37.2% and 34.8% of variation in 2005 and 2006, suggesting that vertical structure was less important in predicting water use. The % impervious land area and vegetation variables had the highest conditional variable importance in Random Forest analyses of $I_{vegetation}$ in both study years, followed by parcel area, % building, and % low vegetation (Figure. 3-6). The highest ranked vertical structural variable was mean building height.

Random Forest analyses of block group outdoor water use

The Random Forest model predicting block group water use from all vertical structure, land cover, and socioeconomic/demographic explanatory variables had high predictive accuracy of 84.6% and 82.1% in 2005 and 2006. This was closely followed by the model including only land cover variables, which predicted 81.5% and 79.8% of $I_{vegetation}$ in 2005 and 2006. The model comprised of only vertical structure variables explained 66.7% of $I_{vegetation}$ for 2005, while the model with the poorest predictive ability used socioeconomic and demographic factors alone, which explained 43.2% of water use variance in 2005.

Land cover variables were most important for predicting water use among land cover, census and vertical structure categories, with the three top variables being % impervious cover, % vegetation, and % building (Figure 3-7). Vertical structure characteristics, particularly mean building height and mean/max tree height also had high conditional variable importance. Socioeconomic factors were of low importance, with appraised property value and mean family size with the highest conditional variable importance values among socioeconomic variables. Variables from the US census contributed little to model predictive performance (Figure 3-7).

Discussion

Residential outdoor water use is highly variable across urban environments. Some homeowners apply more water than needed to satisfy the demands of parcel vegetation, while others apply little or no water. The patterns of water use I observed were not random, but exhibited distinct clustering, both at the parcel and block group scales. Clusters of high water use parcels had significantly lower tree and low vegetation cover. While aggregation of parcel data to census block groups eliminated fine-scale heterogeneity, the same clustering pattern was observed at the coarser spatial scale. The clustering of outdoor water use parcels indicates that outdoor water use is relatively similar among households in a neighborhood, irrespective of land cover, structure, and socioeconomic characteristics. These results add to an emerging consensus from studies suggesting that water use is a spatially structured phenomenon (Wentz and Gober 2007, Franczyk and Chang 2009, House-Peters et al. 2010).

Analyses of land cover and structure in relation to parcel age revealed large differences in land cover, vertical structure, and water use among neighborhoods of different age. Total tree cover and height were significantly higher in older neighborhoods. This reflects the fact that most tree species get larger as they age, and there have been shifts in landscape design and species preferences over time towards smaller species of trees. Shifts in home and lot characteristics, such as an increase in building size and height, contribute to aesthetic and functional differences between neighborhoods of different age. Understanding how these variables change through time as landscapes age provides useful analyses for forecasting future changes in water demand.

Urban areas are highly coupled natural and human systems, and patterns and processes particular to each domain can influence water demand (House-Peters and Chang 2011). A number of interacting socioeconomic, demographic, and physical variables are correlated with water use, and their relationships to each other are commonly non-linear with strong spatial dependency. The RF approach is well suited to addressing variables with these characteristics and has the benefit of producing importance measures useful for screening large numbers of variables and identifying more manageable subsets of data prediction (Hastie et al. 2009, Hapfelmeier and Ulm 2013).

The three different response measures--total water use, water application normalized by parcel area, and water use by vegetated area--differed in how well they related to parcel water use. Total water volume used is the least intuitive for understanding irrigation behavior, because the area irrigated must be factored in. Parcel area is calculated from a single GIS layer. However people generally restrict watering to vegetated areas, and parcel-area normalized application (I_{parcel}) does not account for the proportion of land covered by vegetation or impervious surfaces.

Normalizing water use by vegetated area provides the most relevant measure of water consumption rates, and is similar to measures used in agriculture and landscape management. For example, irrigation recommendations are usually provided in application units (cm) normalized to vegetated area. This metric is most informative for evaluating water use efficiency and estimating hydrologic fluxes such as groundwater discharge and evapotranspiration (St. Hilaire et al. 2008, Healy and Scanlon 2010). However, unlike parcel area, the calculation of vegetated area, and individual vegetation classes (e.g. trees, turf) requires high-resolution land cover information, which has not been available. The expanding constellation of satellites collecting hyperspatial (<1 m GSD) imagery and the increased availability of lidar enable the development of land cover classifications sufficiently precise for parcel scale analyses. While my use of $I_{vegetation}$ was based on projected canopy area, not basal area, it was still a useful approach for normalizing water application. Areas where trees overhang impervious surfaces such as buildings or driveways are not usually purposefully watered, but the leaf area still contributes important ecosystem services such as rainfall interception (Berland and Manson 2013).

In addition to increasing classification accuracy of land cover maps, lidar data allows the explicit analysis of vertical structure characteristics at several scales. While land cover variables generally had greater predictive value than vertical structural characteristics in my RF analyses, measures of vertical structure improved model accuracy and were more important than socioeconomic and demographic variables. In addition, vertical structure is important to processes such as precipitation interception, ET, and land surface temperature (Oke 1982, Xiao et al. 1998).

Urban water demand is increasing and additional water sources to supply growth are limited and expensive (Kenney et al. 2008). Where increasing regional populations occur and climate change effects are being measured, there is a particularly strong impetus for communities to promote water conservation. Outdoor water use comprises over half of domestic household water consumption in many regions (Mayer et al. 1999), therefore efforts targeted at improving irrigation efficiency are critical. This is especially true since irrigation practices are often only weakly correlated with the actual water needs of urban vegetation.

Targeted outreach to inefficient water users has been shown to improve conservation efforts (Nieswiadomy 1992). My work informs conservation efforts by enabling targeted outreach in portions of the irrigation service area with the highest outdoor water use rates. The approach I took using local measures of spatial autocorrelation (Anselin Moran's I; Getis Gi*) helped identify clusters of high and low water use. This can facilitate more effective water conservation by concentrating outreach in clusters of high use that tended to be newer neighborhoods with smaller trees and lower tree cover in my study area.

Household outdoor water use is a complex phenomenon, influenced by numerous demographic, behavioral, and social factors (Russell and Fielding 2010, Fielding et al. 2012). My results highlight the importance of the parcel physical structure, including vegetation area, composition, and vertical structure. Across an urban areas, variables describing in land cover composition and vertical structure variables may be particularly useful for explaining water use patterns. These are relatively easily incorporated into predictive models and may perform better than socioeconomic and demographic variables. Residents are "the fundamental local actors making landscaping decisions in front and backyards" (Cook et al. 2012); however, my results indicate significant neighborhood effects on residential water use, not just individual household factors.

These analyses highlight the importance of tree cover and height to patterns of water use. Trees influence water use by reducing watering requirements of turf through shading (Feldhake et al. 1983, Litvak et al. 2013), and moderate urban land surface temperature (Shashua-Bar et al. 2011). Because of

their deeper rooting habit and laterally extensive root systems, trees also are often better able to seasonally maintain their water balance from natural precipitation. Cool-season turfgrasses may rapidly decline in condition with low soil moisture (Githinji et al. 2009), prompting a resident to water, whereas trees may show no obvious effects until severe water stress occurs. The study area encompasses neighborhoods with diverse physical and social structural characteristics. The ontogeny of cities is complex and strongly conditioned by local physical and historical factors. While no two cities are identical, the methods developed here are broadly relevant to many urban areas around the world.

Table 3-1. Explanatory (italicized) and response variables used in parcel-scale analyses.

Variable	Category
Low Impervious cover	Land cover composition
Building cover	Land cover composition
Tree cover	Land cover composition
Low vegetation cover	Land cover composition
Other cover	Land cover composition
Total vegetation cover	Land cover composition
Total Impervious cover	Land cover composition
Max vegetation height	Vertical structure
Mean vegetation height	Vertical structure
Max building height	Vertical structure
Mean building height	Vertical structure
Max tree height	Vertical structure
Mean tree height	Vertical structure
Development age	Socioeconomic/demographic
Appraised value	Socioeconomic/demographic
Parcel area	Socioeconomic/demographic
Total 05 outdoor water use	Response
Total 06 outdoor water use	Response
Parcel-adjusted 05 application (I_{parcel})	Response
Parcel-adjusted 06 application (I_{parcel})	Response
vegetation-adjusted 05 application ($I_{vegetation}$)	Response
vegetation-adjusted 06 application ($I_{vegetation}$)	Response

Table 3-2. Explanatory (italicized) and response variables used in census block group-scale analyses. Land cover compositional and vertical structural variables represent statistical averages of parcels contained within individual census block groups.

Variable	Category
Low impervious cover	Land cover composition
building cover	Land cover composition
Tree cover	Land cover composition
Low vegetation cover	Land cover composition
Other cover	Land cover composition
Total vegetation cover	Land cover composition
Total impervious cover	Land cover composition
Maximum vegetation height	Vertical structure
Mean vegetation height	Vertical structure
Maximum building height	Vertical structure
Mean building height	Vertical structure
Maximum Tree height	Vertical structure
Mean Tree height	Vertical structure
Parcel area	Socioeconomic/demographic
Population difference 2000-2010	Socioeconomic/demographic
2010 population density	Socioeconomic/demographic
Mean block population size	Socioeconomic/demographic
Mean block household size	Socioeconomic/demographic
Appraised value	Socioeconomic/demographic
Log appraised value	Socioeconomic/demographic
% male	Socioeconomic/demographic
% female	Socioeconomic/demographic
% household age 5-17	Socioeconomic/demographic
% household age 18-21	Socioeconomic/demographic
% household age 22-29	Socioeconomic/demographic
% household age 30-39	Socioeconomic/demographic
% household age 40-49	Socioeconomic/demographic
% household age 50-64	Socioeconomic/demographic
% household age 65+	Socioeconomic/demographic
% owner occupied	Socioeconomic/demographic
% vacant	Socioeconomic/demographic
% single male	Socioeconomic/demographic
% single female	Socioeconomic/demographic
% household married with children	Socioeconomic/demographic
% household married with no children	Socioeconomic/demographic
Parcel-adjusted 05 application	Response
Parcel-adjusted 06 application	Response
Vegetation-adjusted 05 application	Response
Vegetation-adjusted 06 application	Response

Table 3-3. Summary statistics for measures (n, median, interquartile range, and mean) of outdoor water application for parcels in spatial clusters of high and low water use clusters identified by Anselin Local Moran's I analysis of 2005 data.

Neighborhood age	Number of parcels		Median $I_{vegetation}$ (m)		$I_{vegetation}$ (m) IQR		Mean $I_{vegetation}$ (m)	
	High	***Low***	***High***	***Low***	***High***	***Low***	***High***	***Low***
pre-1938	11	144	1.47	0.46	0.28	0.31	1.70	0.47
1938-1958	47	2581	1.92	0.53	0.81	0.34	2.20	0.52
1958-1978	828	7057	1.89	0.54	0.70	0.29	2.06	0.53
1978-1998	3650	753	1.87	0.43	0.78	0.27	2.09	0.42
1998-2007	2469	44	1.94	0.37	1.07	0.32	2.27	0.33

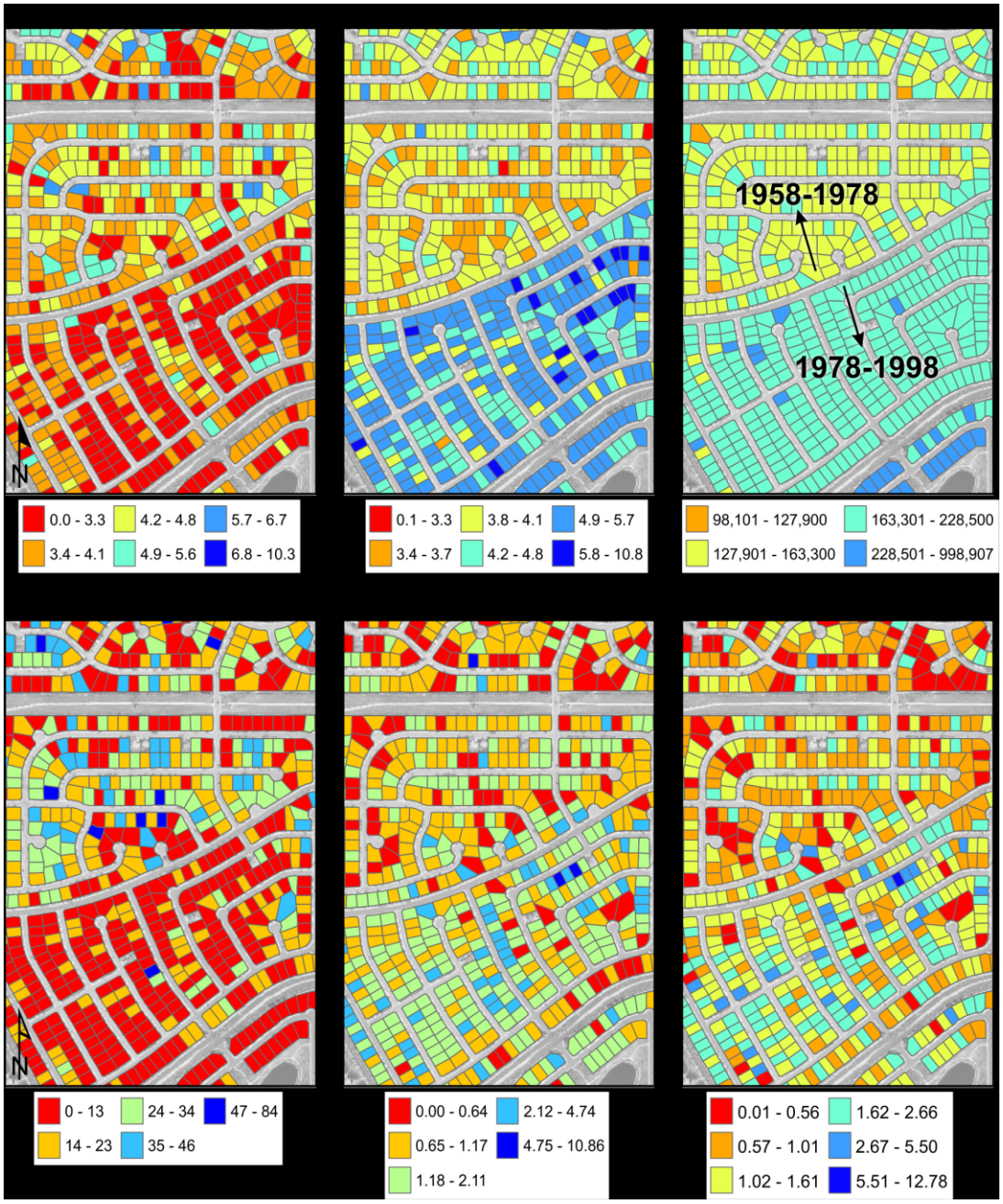

Figure 3-1. Parcel level variation in water use and land cover variables for a representative neighborhood spanning two developments of different age.

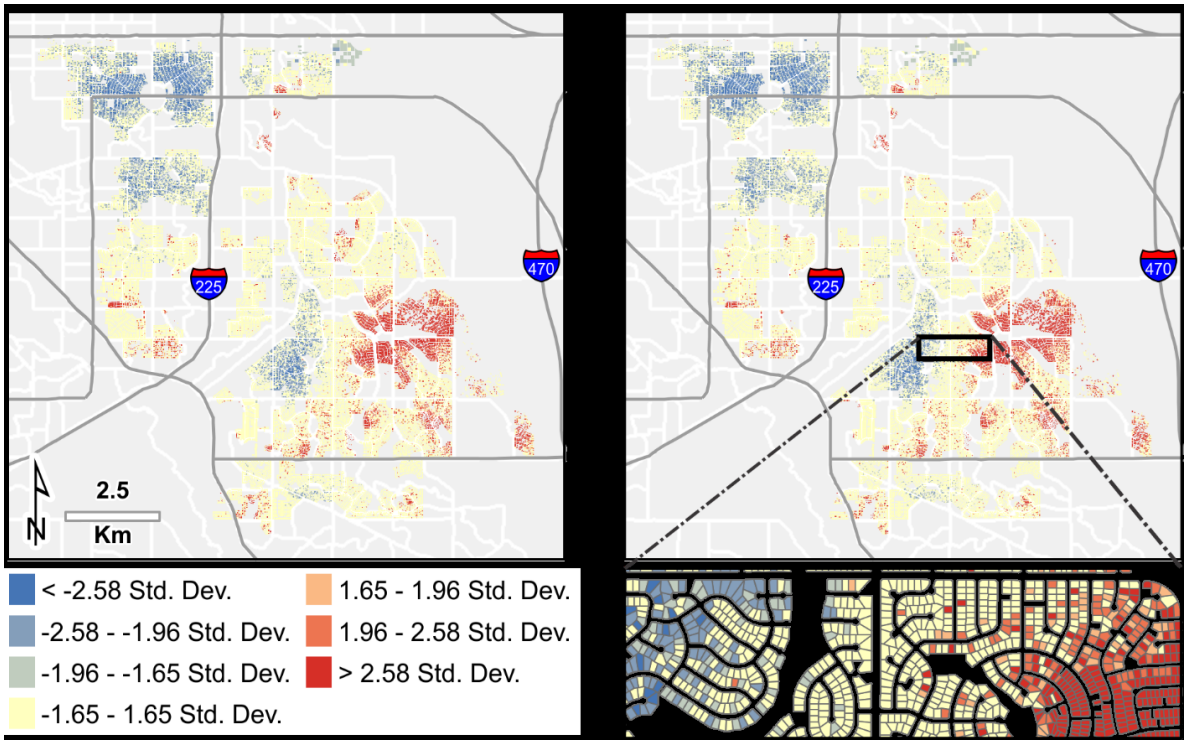

Figure 3-2. Maps of deviation in Getis-Ord Gi* scores for 2005 and 2006 for parcel-level outdoor water use (I vegetation). Very high or low z-scores indicate spatial clustering.

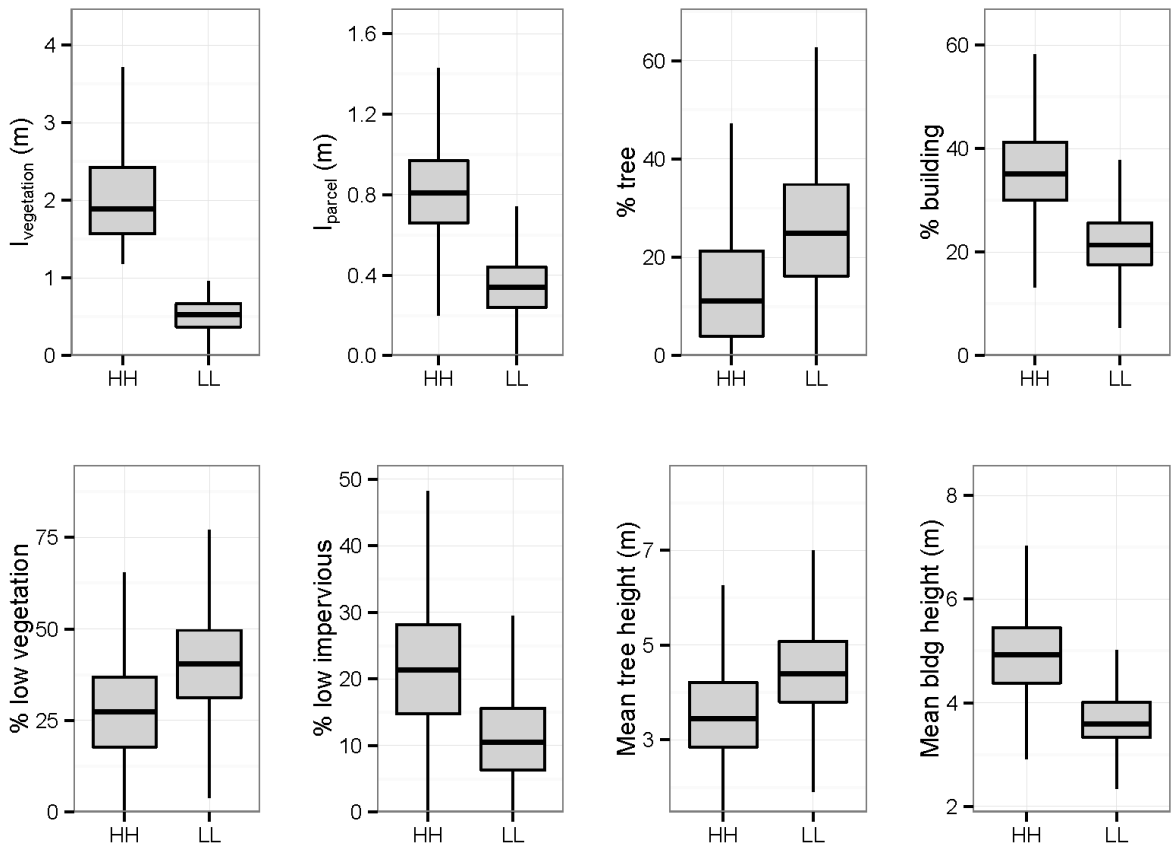

Figure 3-3. Box and whisker plots for vegetated cover-adjusted application ($I_{vegetation}$), parcel area-adjusted application (I_{parcel}), parcel-scale land cover composition and vertical structure variables, calculated for parcels in statistically significant clusters of high and low 2005 outdoor water use identified using Anselin Local Moran's I statistics (HH: high value in cluster of high values; LL: low value in cluster of low values).

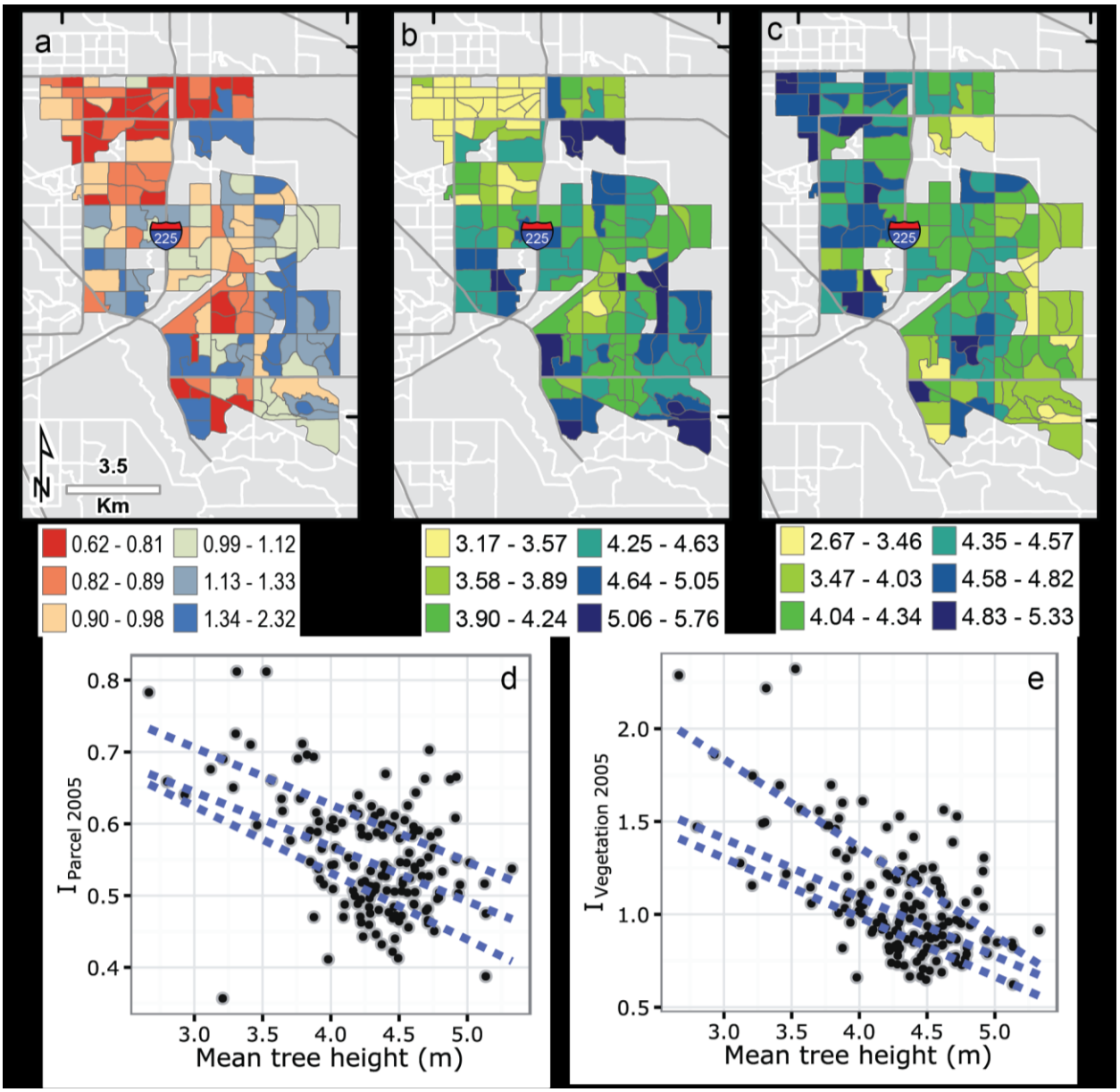

Figure 3-4. Parcel-level data aggregated by 2010 Census block group (n = 155): Water use ($I_{vegetation}$) in 2005 (panel a); mean parcel building height (panel b); mean parcel tree height (panel c). Scatterplots of block group-scale 2005 I_{parcel} (panel d) and $I_{vegetation}$ (panel e) and mean tree height (m). Dashed lines represent from top to bottom the 75th, 50th, and 25th conditional quantiles.

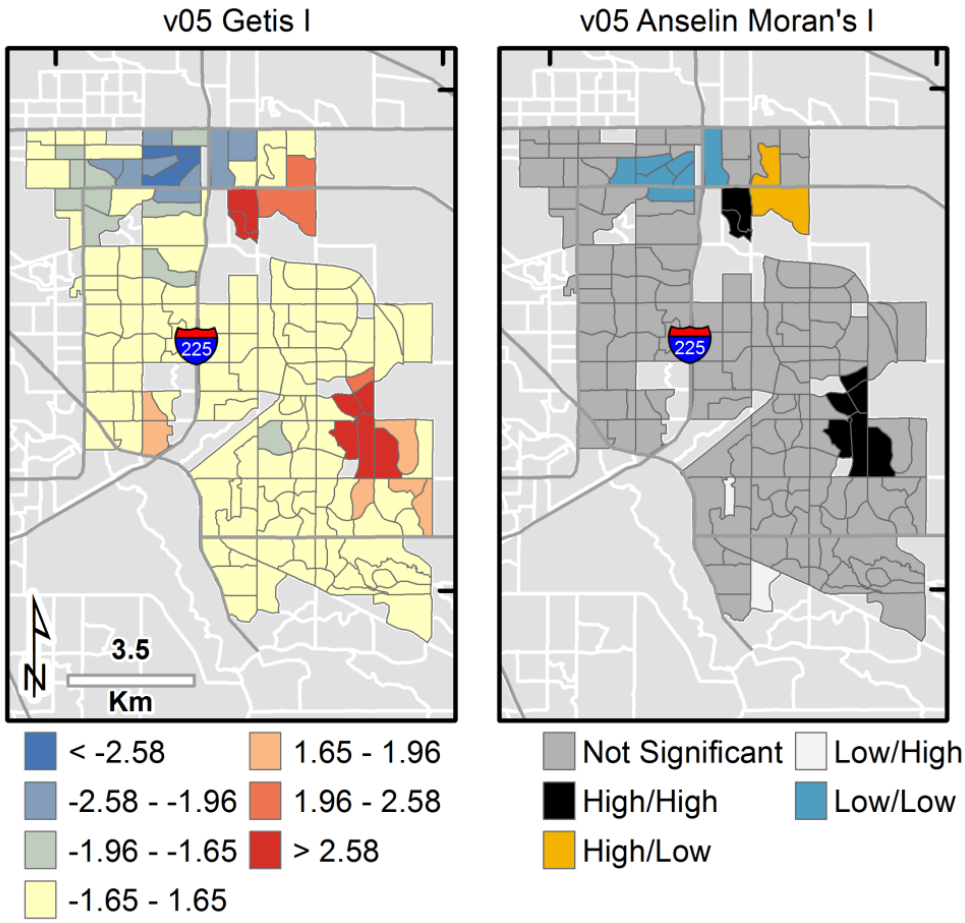

Figure 3-5. Spatial pattern analysis of 2005 block group $I_{vegetation}$: Left panel: Getis-Ord Gi* z-scores; right panel: Anselin Moran's I clusters (high/high; low/low) and spatial outliers (low/high; high/low).

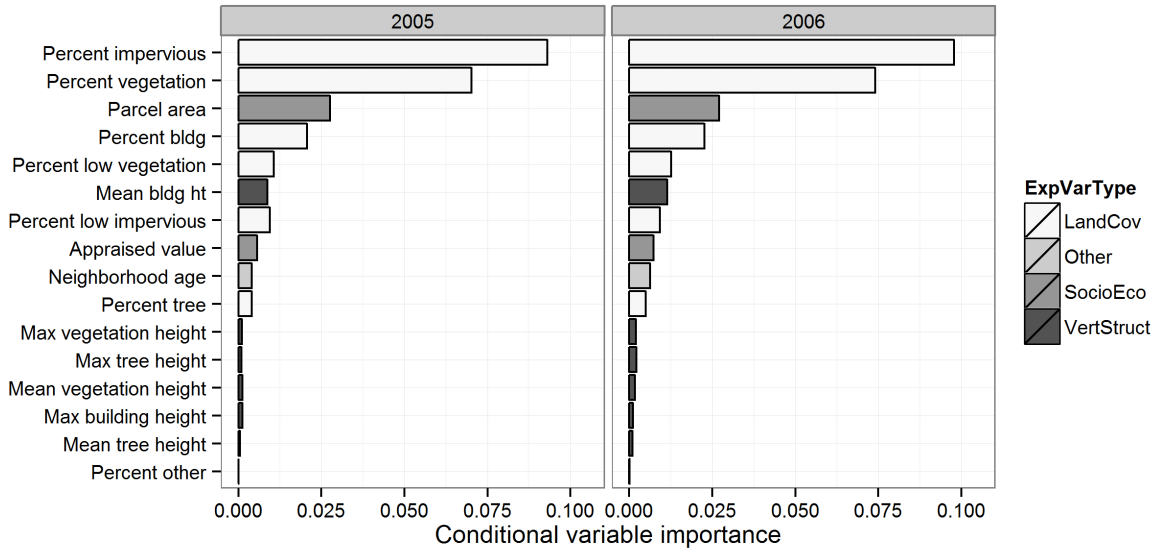

Figure 3-6. Conditional variable importance plot of explanatory variables used in Random Forest regression of parcel-scale vegetated area-adjusted irrigation ($I_{vegetation}$) for 2005 (left panel) and 2006 (right panel).

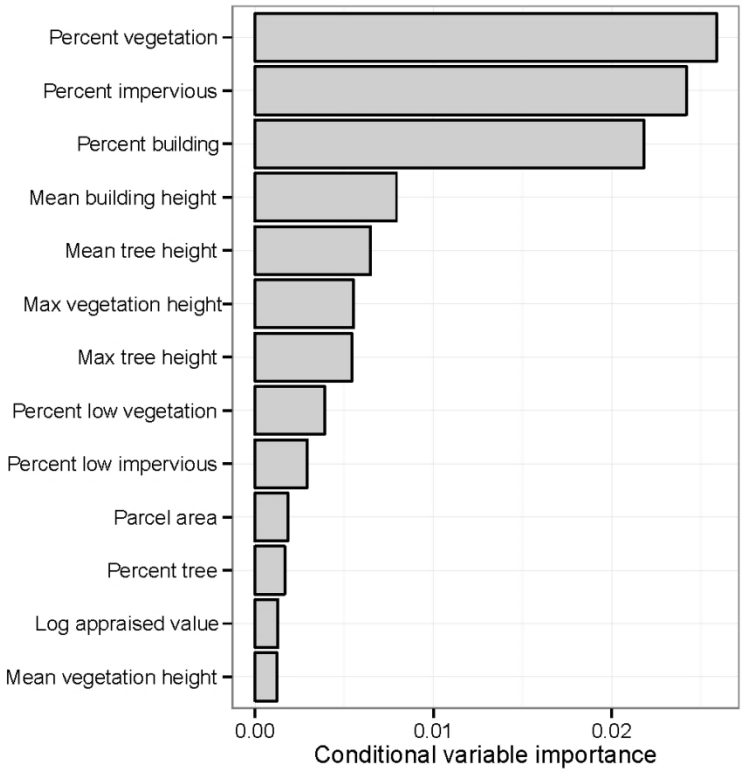

Figure 3-7. Conditional variable importance plot for combined land cover composition, vertical structure, socioeconomic/demographic variables from Random Forest analysis of 2005 vegetated area-adjusted census block group outdoor water use. Bars for variables with conditional variable importance less than 0.002 are not displayed

4. INFLUENCE OF LAND COVER COMPOSITION AND VERTICAL STRUCTURE ON LAND SURFACE TEMPERATURE IN A SEMI-ARID SUBURBAN AREA

Introduction

The majority of the world's population now lives in cities (Crane and Kinzig 2005), and in many regions, rates of urban expansion are rising significantly (Alig et al. 2004, Cohen 2006). Dramatic changes in land cover composition and spatial structure accompany urbanization with important consequences for ecological and hydrologic functioning (Oke 1989, McDonnell et al. 1997, Walsh et al. 2005). Asphalt, concrete, and buildings in the urban landscape more effectively store incident solar radiation than vegetation. In addition, transpiration by vegetation moderates temperatures through latent heat exchange (Campbell and Norman 1998), so when urbanization leads to the conversion of vegetation to impervious cover, increases in ambient temperature are commonly observed (Owen et al. 1998, Small 2006).

This phenomenon, commonly termed the urban heat island (UHI) (Oke 1982, Arnfield 2003), has broad consequences for human comfort and energy consumption, residential water use, and a range of ecohydrological processes (Guhathakurta and Gober 2007, Luber and McGeehin 2008, Gober et al. 2012, Halper et al. 2012, Sawka et al. 2013). The Park Cool Island is a related phenomenon, where irrigated areas with high vegetation cover are cooler than surrounding urban areas, the result of shading and latent heat exchange (Chow et al. 2011, Declet-Barreto et al. 2013). Land surface temperature (LST) patterns have important consequences for urban sustainability, particularly critical in light of projected climate changes, but our understanding of the landscape factors influencing LST remains weak.

Vegetation is an important factor shaping urban LST. The Normalized Difference Vegetation Index (NDVI)(Rouse et al. 1973) , a widely used proxy for vegetation abundance and condition, is correlated with LST (Gallo et al. 1993, Weng et al. 2004). Other measures of vegetation abundance such as the vegetation fraction or indices of impervious cover have also been evaluated (Owen et al. 1998, Yuan and Bauer 2007, Yue et al. 2007). For example, Yuan and Bauer (2007) applied a spectral mixture analysis of NDVI and percent impervious surface to evaluate LST patterns in the Minneapolis-St. Paul metropolitan area. They found a pronounced and seasonally-invariant relationship between LST and the percent cover of impervious surfaces, as well as seasonally varying correlations between LST and NDVI. Patch-based metrics of landscape structure have also been correlated with LST (Li et al. 2011, Zhou et al. 2011), demonstrating the broad importance of vegetation abundance and landscape structure on LST patterns. For example, Li et al. (2011) found positive correlations between mean LST and common landscape metrics such as percent of land use (PLAND) and edge density (ED). While previous analyses provide general relationships between vegetation as a whole and LST, little is known how different types of vegetation (e.g., forests and turfgrass) with different vertical structural characteristics influence urban LST. A more detailed understanding of these effects would provide important information for urban planners and landscape architects.

Trees differ functionally from turfgrass lawns and other urban vegetation types in their effect on local and regional energy balances, carbon and water cycling, and other ecosystem services (Nowak and Crane 2002, Pataki et al. 2006, Pataki et al. 2011a). Maps of tree canopy cover can be relatively easily created by analyzing aerial or satellite imagery; however, a variable like tree cover poorly address the complex vertical structure created by trees that influences boundary layer characteristics and turbulent exchanges with the atmosphere (Oke

1982, Oke 1989, Kanda et al. 2006). The importance of vertical structural characteristics has not been widely examined because comprehensive, landscape-scale data were not available. Advancements in lidar remote sensing now allow explicit analyses of vertical structure (Shugart et al. 2010), facilitating a greater understanding of the influence of urban landscape structure on LST patterns.

In this analysis, I evaluate relationships between urban land cover composition, vertical structure, and summer daytime LST patterns. In particular, I focus on the importance of physiognomic class and measures of vertical structure on LST. Specific research questions include the following: (1) How do patterns of land cover composition and three-dimensional structure vary spatially in my study area? (2) How do patterns of LST differ between urbanized areas and undeveloped native vegetation types? (3) What land cover compositional and vertical structural characteristics best predict summer daytime LST patterns?

Study area

I studied a 287 km^2 area centered on Aurora, Colorado, a rapidly growing suburb adjacent to Denver in the Colorado Front Range region. The study area, which also included portions of Denver, Adams, and Arapahoe counties (Figure 4-1), was converted from shortgrass steppe to dryland and irrigated agriculture beginning in the late-19th century, and has seen rapid population growth and urban expansion in recent decades. The regional climate is semiarid and the area receives approximately 400 mm of precipitation annually, much of it in the form of convective summer thunderstorms. Dominant land uses include low to high density single and multi-family residential, retail commercial and light industrial, and parks/open space, the latter including small neighborhood parks and larger recreational parks and golf courses. Undeveloped portions of the study area that still support native shortgrass steppe communities were used as

reference areas in analyses of LST patterns (Figure 4-1). Dominant urban vegetation cover types include urban forests of varying composition and structure, irrigated lawns in park and residential contexts, and unirrigated native and ruderal communities.

Methods

Land cover analysis and structural characterization

To evaluate land cover and structure characteristics for my study area, I analyzed a high resolution land cover map produced using an object-oriented image analysis (OBIA) approach. Specific details are presented in Chapter 2, but a brief summary of the approach follows. Mapping land cover involved the following steps: (1) data preprocessing; (2) image segmentation; (3) classification; and (4) error analysis. Lidar point cloud and intensity data from April, 2008 were used to generate first return, bare Earth, intensity, and normalized digital surface model (nDSM) rasters. Four-band (blue, green, red, near infrared) imagery was used to derive spectral indices such as the Normalized Difference Vegetation Index (NDVI), and principal components analysis rasters. Layers were combined for image segmentation using a region merging algorithm (Benz et al. 2004) and the mean and standard deviation of pixel values for each image segment was calculated and exported for training and classification. The RandomForest package in R (version 2.15.1) was used with a training data set to assign land cover classes to image segments (Breiman 2001, Liaw and Wiener 2002). A validation data set (n = 767 points) was used to calculate overall accuracy, producer's accuracy (omission error), user's accuracy (commission error), and kappa coefficient (Congalton and Green 1999).

Using the resulting land cover classification, I summarized land cover patterns for the assessment area and produce individual masks for each land cover class. These masks were combined with the lidar-derived nDSM to create multiple data layers describing vertical

structure. For example, a tree canopy height layer was created by extracting nDSM values using the tree cover mask. A gradient-based approach to quantifying vertical structure variables was developed using focal statistics functions in ArcGIS. For key compositional and structural variables (e.g., tree canopy density, tree height, building height), a 3 ha circular moving window was used to derive continuous data layers describing mean neighborhood values. This scale was chosen to approximate that of city blocks. I calculated the difference in mean height between impervious and vegetated cover rasters to provide a general indicator of the dominant land cover compositional elements influencing vertical structure.

Evaluation of LST in relation to land cover composition and structure

I quantified patterns of LST using Landsat 5 TM scenes obtained from the US Geological Survey's Global Visualization Viewer (http://glovis.usgs.gov/). Six late-spring and summer Landsat scenes that were cloud free for the study area extent were selected for analysis from 2005 to 2011. Landsat 5 TM thermal band data (Band 6, 10.45-12.42 μm wavelength) are collected at a resolution of 120 m, but are distributed at a resampled 30 m pixel resolution, the resolution retained in subsequent analyses. Sensor gain and offset values published for the Landsat 5 TM sensors published by Chander (2009) used in the R "landsat" package were used to convert raw digital number (DN) values to radiometric temperature in degrees C (Goslee 2011).

I compared LST patterns in urbanized and undeveloped reference areas by creating polygons supporting shortgrass steppe communities on undeveloped portions of Buckley Air Force base and adjacent open-space lands (Figure 4-1). For a given Landsat scene, mean reference area LST values were calculated using zonal statistics in ArcGIS and subtracted from LST rasters to yield a series of "deviance from reference area temperature" ($LST_{d\ ref}$) grids.

Raster analysis functions in the R package "raster" were used to derive LST grids standardized to scene mean and standard deviation for use in regression analyses. LST patterns were also examined in relationship to land use characteristics using zoning data.

Atmospheric effects can cause systematic biases in remotely-sensed temperature, limiting the interpretability of direct comparisons of scenes acquired at different times and under different atmospheric conditions (Voogt and Oke 2003). Variation in sun-sensor-surface geometry and the three-dimensional structure of urban areas can cause anisotropic effects, an additional source of bias (Voogt and Oke 1998, Lagouarde and Irvine 2008). Also, radiometric surface temperatures often differ from air temperatures due to factors such as advection (Voogt and Oke 2003). As a consequence, I was less interested in comparisons in absolute temperatures between scenes; rather, my focus was on relative spatial patterns exhibited within a scene.

Using 2010 census blocks as units (n= 7490), I calculated means and standard deviations for land cover compositional, vertical structural, and LST rasters using zonal statistics in ArcGIS. I then used these data to evaluate the importance of vertical structural variables versus land cover compositional variables on LST using two approaches. First, I used the Random Forests algorithm in the R "randomForest" package (Liaw and Wiener 2002) in a regression context to compare the variance in LST explained using models fit to different subsets of explanatory variables: land cover compositional variables only, vertical structural variables only, and a full model combining all explanatory variables. To understand the specific influence of NDVI on model performance, subsets were run with and without inclusion of NDVI among explanatory variables. Separate RF models using 500 trees were created for the six Landsat scenes analyzed, with the response variable that scene's LST values. I used the out-of-bag (OOB) estimate produced by the algorithm as an estimate of the error rate.

In addition to generally achieving high predictive accuracy compared with traditional regression approaches, RFs provide a way of ranking the importance of explanatory variables in prediction (Grömping 2009, Genuer et al. 2010), a key objective in my analysis. Using the fully specified model, I compared three variable importance measures. Two traditional variable importance measures were evaluated: %IncMSE and IncNodeImpurity. The first is calculated by permuting OOB data and predictor variables, averaging the difference over all trees constructed (500 in my case), and normalizing by the standard deviation of the differences. The IncNodeImpurity measure assesses the decrease in node impurity from splitting on a particular variable measured using residual sum of squares, averaged for all trees in the ensemble. Recent studies have found that these variable importance measures can sometimes be biased towards highly correlated variables (Strobl et al. 2007). Therefore, I also calculated conditional variable importance estimates using the “cforest” algorithm in the R package "party". This algorithm employs a conditional permutation scheme for the computation of the variable importance that avoids potential bias (Strobl et al. 2007, Strobl et al. 2008). In these conditional permutations, predictor and response variables are shuffled, and the effects on a standardized measure of model accuracy are assessed before and after each permutation. For predictor variables lacking a meaningful relationship with the response, the shuffling of its values will produce little change in model accuracy, while a large drop in accuracy will be observed for predictors showing strong associations with the response variable (Strobl et al. 2007, Strobl et al. 2008). Variable importance measures produced this way reflect both the individual effect of predictor variables and their influence as part of complex interactions, which is challenging to assess in traditional regression approaches (Strobl et al. 2008).

Results

Land cover composition and vertical structure

Land cover classification accuracy over all classes was 92.7%, with a Kappa coefficient of 0.90. The highest producer's accuracy (Congalton and Green 1999) was for the water class, followed by low-impervious, low-vegetation, buildings, trees, and bare soil classes (Table 4-2). The tree class had the highest user's accuracy, followed by buildings, and the low-impervious and low-vegetation classes, each with an accuracy of approximately 93%. Water and bare soil classes had the lowest user's accuracy, but together comprised <5% of the study area (Table 4-2).

The low vegetation class, including irrigated and unirrigated areas, covered the largest proportion of the assessment area at 43.8% (Table 4-2). Low impervious was the second most abundant class at 28.2%, followed by buildings and trees/shrubs at 12.4% and 11.9%, respectively. Land cover was spatially heterogeneous, varying within areas with different land use, zoning, and history of development. Overall, industrial and commercial areas had the highest cover of low impervious land at 37.3%, compared to less than 15% in parks and open space. Total vegetation cover (trees/shrubs and low vegetation classes) was highest in open space at 81.6%, and developed parks at 78.5%. While low vegetation cover was only slightly lower in residential areas than those zoned commercial/industrial (37.5% vs. 40.7%), residential areas had the highest tree cover of 16.9%, more than four times greater than commercial/industrial areas.

Distinct trends in vertical structure occur across the study area reflecting both land-use characteristics and historical land development patterns. Mean tree height was greatest in the north western portion of the study area, where the oldest neighborhoods occur (Figure 4-3). Moving window-derived building height was greatest in a few locations with commercial or

industrial land uses and in more recently developed single-family residential areas (Figure 4-4). Concentrations of sites where mean tree height exceeded building height occurred in areas with higher forest canopy cover, primarily in the northwest portion of the study region (Figure 4-4). Buildings are smaller in older neighborhoods contributing to their higher height differential.

Evaluation of LST in relation to land cover composition and structure

The highest mean LST for the six Landsat scenes analyzed was 40.5 °C on July 10, 2008, and the lowest was 32.9 °C on July 18, 2005. Among individual Landsat scenes, there was considerable variation in LST (Table 3; Figure 4-5, 4-6). The coolest portions of all scenes were water bodies, with temperatures recorded over large reservoirs averaging 14.9°C cooler than commercial/industrial areas and 10.9°C cooler than parks. Residential areas averaged 4.0°C cooler than commercial/industrial areas, and both residential and commercial/industrial areas were cooler than reference areas by 5.2°C and 1.2°C, respectively. Spatial patterns of $LST_{d\ ref}$ varied among Landsat scenes, reflecting differences in both meteorological conditions at the time of Landsat scene acquisition and seasonality (Table 4-3, Figure 4-7).

Regression analyses using the RF algorithm and the full set of explanatory variables explained a mean of 65.0% of the variance in LST among the six Landsat scenes analyzed, ranging from a low of 56.4% for the 2005Jul18 scene to a high of 74.6% for the 2011Jul19 scene (Table 5). In contrast, the mean percent of LST variation explained by the land cover compositional subset of explanatory variables was 50.1%, ranging from 39.7% to 62.9%. Adding NDVI to the land cover compositional subset improved the mean prediction by only 5.6%. The mean % variance explained by the subset of vertical structural variables was 56.7%, improving to 61.6% through inclusion of NDVI. Compared with the model developed using the land cover compositional variables only, the addition of vertical structural variables and NDVI improved

prediction accuracy by an average of 14.9%, ranging from 11.7% to 19.2% for individual Landsat scenes.

Using conditional variable importance values, the tree-building height had the highest mean importance among the six Landsat scenes, followed by tree height and NDVI (Table 4-6). The composite variables % impervious and % vegetation had higher mean importance than individual class abundance variables such as % buildings, although there was variability in relative variable importance rankings among individual Landsat scenes (Figure 4-9). The relative rankings of variables were most similar between the conditional and IncNodeImpurity measures. Using IncNodePurity, the mean height difference between trees and buildings was the highest-ranked variable used. Four of the top six variables ranked using the IncNodePurity metric described some aspect of vertical structure and no single land cover class abundance measure ranked higher than fifth in relative importance using IncNodePurity (Figure 4-10). Averaging across all six dates, NDVI had the highest variable importance using the percent increase in mean standard error (%IncMSE) measure (Table 4-6). The mean height difference between trees and buildings was the second most important variable using the %IncMSE criterion. The mean tree height and tree height standard deviation variables also ranked highly using %IncMSE (Table 6). The aggregate compositional variables % vegetation and % impervious variables were more important than any single-class variables using IncNodePurity but not for %IncMSE.

Discussion

My results highlight the complexity of urban land cover composition and the effect of vertical structure on census block-level LST patterns. The model incorporating vegetation abundance and its proxy NDVI was less effective in predicting LST patterns than models incorporating vertical structural attributes. Measures of vertical structure were consistently

important predictors of LST patterns, while land cover compositional metrics were of relatively low predictive value. Two structural variables were particularly important, tree height and the difference between mean tree height and building height, highlighting the different mechanisms by which vegetation structure can influence LST patterns.

In addition to latent heat exchange processes, trees reduce heating through their effects on boundary layer characteristics and shading (Oke 1989). While transpiration from all vegetation types reduces the fraction of energy going towards sensible heat flux, unlike low vegetation types like turfgrass, trees also influence microclimate by shading adjacent areas. Thus, trees can provide cooling benefits even when plant transpiration rates are relatively low (Chow and Brazel 2012).The high variable importance of the height difference between trees and buildings emphasizes this important function; the net cooling benefit from trees was greatest when they were taller than adjacent buildings.

Comparisons of model accuracy among different subsets of explanatory variables reveal the importance of irrigation on urban LST patterns. The lower variable importance of land cover compositional measures like % vegetation relative to NDVI in my analyses reflects NDVI's integration of both vegetation abundance and vigor. The compositional classes I used did not discriminate between irrigated and non-irrigated areas, information that is partially contained in NDVI. However, in areas with high leaf area like many urban plant communities, NDVI is relatively insensitive to differences in canopy structure (Gamon et al. 1995), and the importance of vertical structural characteristics in my regression analyses reveals the limitations of a single measure like NDVI in predicting urban LST patterns.

The addition of vertical structural variables such as tree height and the difference between tree and building height to regression models based on land cover class abundance alone

improved prediction accuracy by an average of 9.3%. For every Landsat scene analyzed, regression models based only on the subset of vertical structural variables explained more LST variation than models based on land cover class abundance. When vertical structural variables were combined with NDVI, they outperformed the land cover class only classification by 11.5%. These results reveal important mechanisms governing the relationship between land cover composition and structure and urban thermal characteristics.

Empirical and modeling studies broadly highlight the importance of land cover characteristics on urban microenvironment, suggesting ways of addressing the negative effects of urbanization on LST through design decisions at varying spatial scales (Shashua-Bar et al. 2010, Shashua-Bar et al. 2011, Vidrih and Medved 2013). Summertime extremes in LST are likely to increase in severity with climate change (Luber and McGeehin 2008), directly and indirectly affecting human health (Kovats and Hajat 2008). This research points to the particular importance of vertical structure on LST patterns, information that can be used to inform design and planning decisions. Particularly important in my analysis was the height characteristics of urban trees, especially in relation to adjacent buildings. Past research has demonstrated the benefit of shade trees on energy needed to cool individual houses (Rudie and Dewers 1984); my analyses demonstrate the broader benefit of urban forests on urban LST. These benefits are in addition to other ecosystem services like reduced storm water generation, carbon storage, and biodiversity (Hope et al. 2003, Byrne et al. 2008, Dobbs et al. 2011).

Most cities in arid and semi-arid regions have limited water resources and mitigation of UHI effects is one of several considerations driving water use planning decisions. The benefits of vegetation for moderating LST are derived in part from latent heat exchange, supported by supplemental irrigation. From a water conservation standpoint, landscaping with low water use

species has sensibly been promoted, although landscapes dominated by such species may offer less cooling benefit (Chow and Brazel 2012). Efforts to reduce residential water consumption, while simultaneously maintaining a desirable thermal environment, should consider not just the plant water use traits, but vertical structural characteristics.

Mean temperature in all of my urban land use types was lower than native shortgrass steppe, but significant spatial variability occurred in LST_{dref} within each land use class. This reflects differences in land cover composition and vertical structure as well as management characteristics like irrigation. For example, industrial and commercial areas had the highest mean LST values, but mean LST was still cooler than steppe areas because of the predominance of irrigated vegetation, which more than balanced the higher LST created by impervious land cover types. For the six dates analyzed, I did not observe the development of a strong UHI in my study area, although at finer spatial scales, variation in land cover composition and vertical structure led to areas with higher LST than undeveloped reference areas. The vigor of native grasses varies seasonally with precipitation, while cool-season turfgrass remains physiologically active throughout the summer if provided sufficient supplemental irrigation, contributing to evaporative cooling and the seasonal differences in spatial patterns of LST_{dref} evident among different Landsat scenes.

Much of the research on patterns and drivers of UHI in the U.S. has been conducted in the desert Southwest (Baker et al. 2002, Sun et al. 2009, Buyantuyev and Wu 2010, Jenerette et al. 2011, Chow and Brazel 2012). This work illustrates the processes influencing UHI formation, but differences in climate and natural vegetation limit their direct application in semi-arid temperate regions. Shortgrass steppe communities support higher plant biomass and leaf area

than desert communities (Barbour and Billings 2000) and steppe communities are capable of significantly greater latent heat exchange than desert plant communities.

There are limitations to using radiometric temperatures to characterize urban LST. Remotely-sensed measurements generally diverge from air temperatures because of factors like advective transport of heat by complex wind patterns shaped by the spatial configuration and varied aerodynamic roughness characteristics of cities (Voogt and Oke 2003). Atmospheric effects can systematically bias temperature, limited their value in comparisons across time. Spatial anisotrophy in complex structural environments can introduce bias and are difficult to model. However, the broad synoptic view of entire landscapes provided by satellite imagery does provide useful insights for understanding the influence of land cover characteristics on LST patterns across cities.

The study area supports land-use and land cover characteristics typical of many suburban areas, has a varied development history, and is socioeconomically and demographically diverse. However, it is important to recognize the broader regional context. Numerous studies have examined LST patterns along gradients of development ranging from simple linear transects to more complex character-based synthetic gradients (Hahs and McDonnell 2006, McDonnell and Hahs 2008, Berland and Manson 2013). In these studies, as in this study, broad conclusions are shaped by the choice of the spatial grain and extent of analysis.

Conclusions

Land cover compositional data have been effectively used in past studies to predict urban LST patterns. By including vertical structural information derived from lidar, I found that additional predictive accuracy can be obtained. Random forest regression models developed using only vertical structural explanatory variables outperformed those using only land cover compositional variables. In comparisons

of three variable importance measures, two vertical structural variables—tree height and the height difference between trees and buildings—consistently outranked land cover compositional variables in predicting census block-level LST patterns. These results highlight the important benefits from urban vegetation, and especially trees, in mitigating UHI formation and draw attention to the particular role of shading by trees in moderating urban LST.

Table 4-1. Percent user's and producer's accuracy from land cover classification. Because of their low relative abundance, the bare soil and water LC classes were combined into a single "other" class in regression analyses.

Class	User's accuracy (%)	Producer's accuracy (%)	Proportion of study area (%)
Bare	81.8	77.1	2.0
Building	94.9	88.6	12.4
Low Impervious	93.9	95.4	28.2
Low Vegetation	93.1	94.9	43.8
Tree/shrub	95.5	87.5	11.9
Water	81.0	100	1.7

Table 4-2. Summary LST statistics for study area. Daily instrumental mean temperature is from the Denver International Airport weather station (KDEN).

Landsat scene acquisition date	Mean LST (°C)	Minimum LST (°C)	Maximum LST (°C)	Standard Deviation (°C)	Daily Instrumental Max (°C)
2005 Jul 18	31.9	19.4	41.6	2.6	31.7
2008 Jul 10	40.5	22.1	57.4	3.5	36.7
2008 Aug 11	34.6	21.2	48.9	2.7	30.6
2010 May 29	36.8	17.2	49.0	3.2	25.6
2010 Aug 17	34.0	20.8	47.9	3.3	31.1
2011 Jul 19	35.4	21.6	50.1	2.8	27.2

Table 4-3. Summary deviation from reference LST statistics for study area.

Landsat scene acquisition date	Mean $LST_{dev\ ref}$ (°C)	Minimum $LST_{dev\ ref}$ (°C)	Maximum $LST_{dev\ ref}$ (°C)	Standard Deviation (°C)
2005 Jul 18	-3.9	-16.5	5.7	2.6
2008 Jul 10	-1.2	-19.6	15.8	3.5
2008 Aug 11	0.4	-13.0	14.8	2.7
2010 May 29	-2.2	-21.8	10.0	3.2
2010 Aug 17	-7.0	-20.2	6.9	3.3
2011 Jul 19	-2.5	-16.2	12.2	2.8

Table 4-4. Percent variation explained by Random Forest regressions of LST against different combinations of land cover compositional and structural variables. Mean and standard deviation (SD) columns are for the six Landsat scene dates.

Scene Date	2005 Jul 18	2008 Jul 10	2008 Aug 11	2010 May 29	2010 Aug 17	2011 Jul 19	Mean (SD)
LC compositional only	39.7	46.5	52.7	44.2	54.6	62.9	**50.1 (8.3)**
Vertical structural only	41.0	51.8	57.6	58.7	63.2	68.0	**56.7 (9.4)**
LC compositional + NDVI	48.0	53.5	56.5	48.6	61.3	66.2	**55.7 (7.2)**
Vertical structural + NDVI	51.5	57.2	61.2	60.2	67.7	71.9	**61.6 (7.3)**
Full model	56.4	61.1	64.4	63.4	70.2	74.6	**65.0 (6.5)**

Table 4-5. Mean, standard deviation (SD), and rank of variable importance measures for the six Landsat scenes analysed (n=6). Conditional: Conditional variable importance calculated using the "cforest" algorithm; IncNodeImpurity: increase in node impurity calculated using "randomForest" package; %IncMSE: percent increase in mean standard error calculated using "randomForest" package. See methods for description of each variable importance measure.

	Conditional		*IncNodeImpurity*		*%IncMSE*	
	Mean (SD)	**Rank**	**Mean (SD)**	**Rank**	**Mean (SD)**	**Rank**
Tree-Bldg height diff	0.818 (0.51)	1	2431.8 (821.3)	1	35.7 (6.0)	2
Tree height	0.646 (0.37)	2	1337.6 (567.2)	3	27.3 (3.4)	5
NDVI	0.481 (0.29)	3	1564.3 (484.1)	2	44.5 (10.2)	1
% Impervious	0.312 (0.12)	4	1060.5 (422.7)	5	21.7 (4.5)	11
% Vegetation	0.274 (0.09)	5	1076.2 (379.8)	4	26.8 (3.0)	7
% Tree/shrub	0.200 (0.10)	6	656.7 (278.4)	6	17.1 (3.8)	14
% Building	0.170 (0.06)	7	473.9 (127.3)	8	21.3 (4.6)	12
% LowVegetation	0.127 (0.04)	8	467.5 (82.2)	9	27.8 (2.1)	4
nDSM SD	0.105 (0.04)	9	538 (188.1)	7	30.1 (4.5)	3
Prop Imp from LowImp	0.101 (0.03)	10	318.9 (91.9)	15	22.1 (9.1)	9
Prop Veg from LowVeg	0.090 (0.04)	11	349.2 (108.4)	11	16.4 (2.7)	15
Prop Veg from Tree	0.088 (0.04)	12	352.5 (109.2)	10	15.5 (2.5)	16
Prop Imp from Bldg	0.082 (0.03)	13	330.1 (90.5)	14	22.6 (7.4)	8
Tree Bldg height diff SD	0.060 (0.07)	14	344.9 (121.4)	13	20 (10.3)	13
Tree height SD	0.054 (0.03)	15	348.1 (114.8)	12	27.3 (4.2)	6
% Other	0.045 (0.02)	16	278.9 (87.9)	16	22.1 (4.1)	10

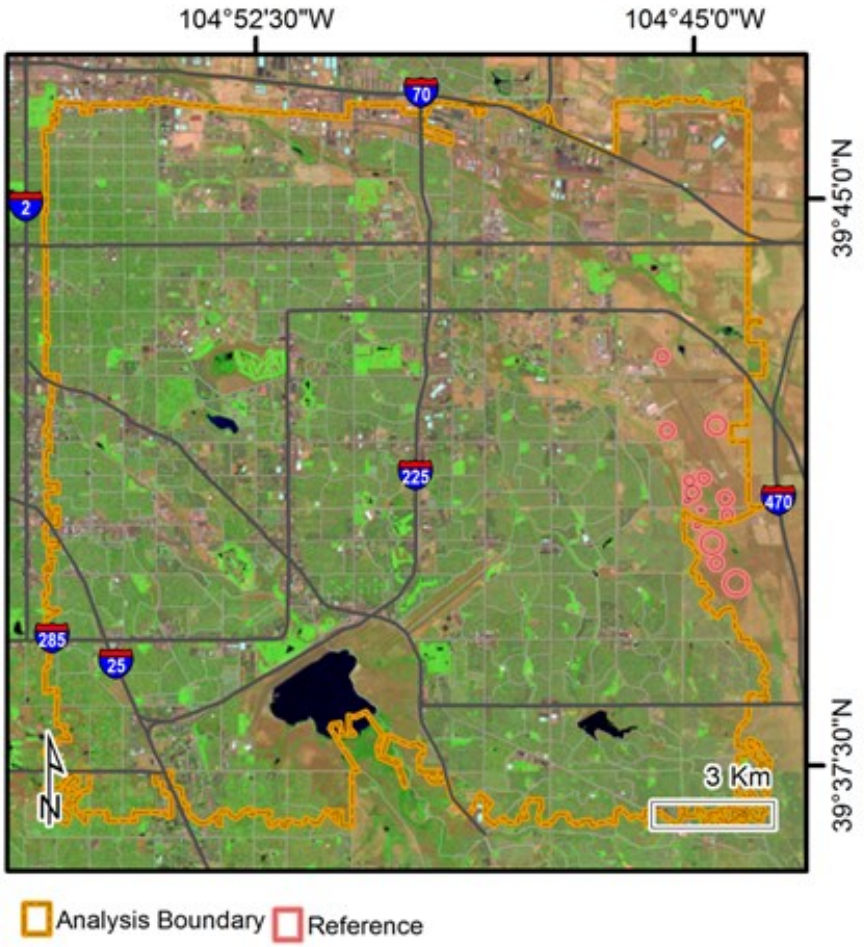

Figure 4-1. Aurora-Denver study area in North Central, Colorado, USA; Bottom panel: Landsat 5 TM (Bands 7,4,2). Reference areas refer to unirrigated shortgrass steppe communities in undeveloped open space in and adjacent to Buckley Air Force base.

Figure 4-2. Portion of study area illustrating the land cover classification (panel A); % vegetation (tree/shrub or low vegetation) for 2010 census blocks (panel B).

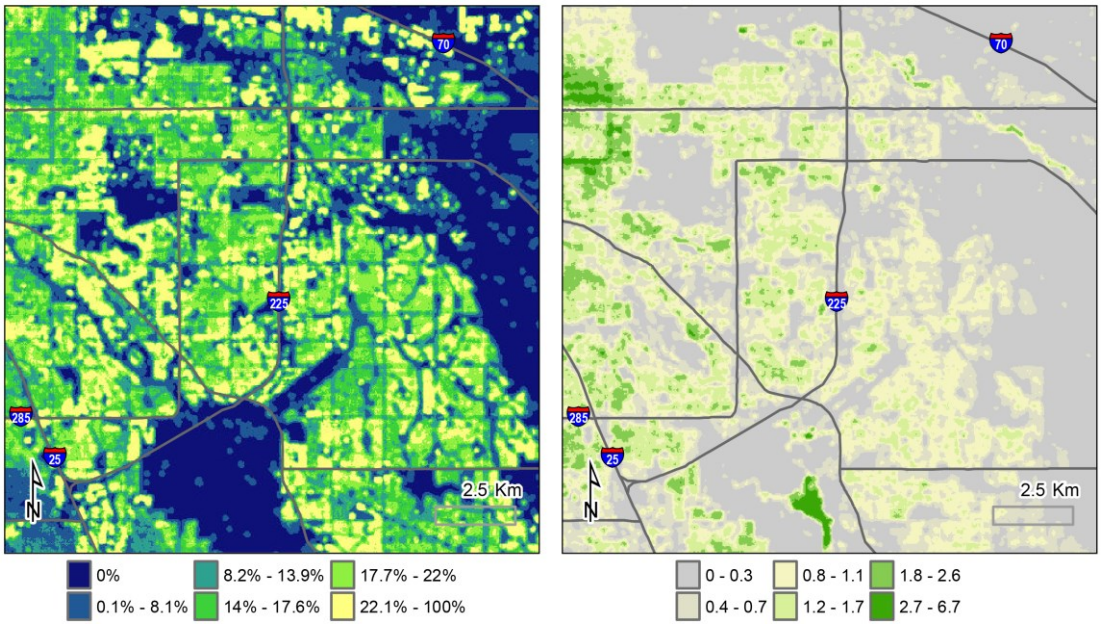

Figure 4-3. Mean tree canopy cover (left panel) and mean tree height (meters; right panel) calculated using a 3 ha moving window.

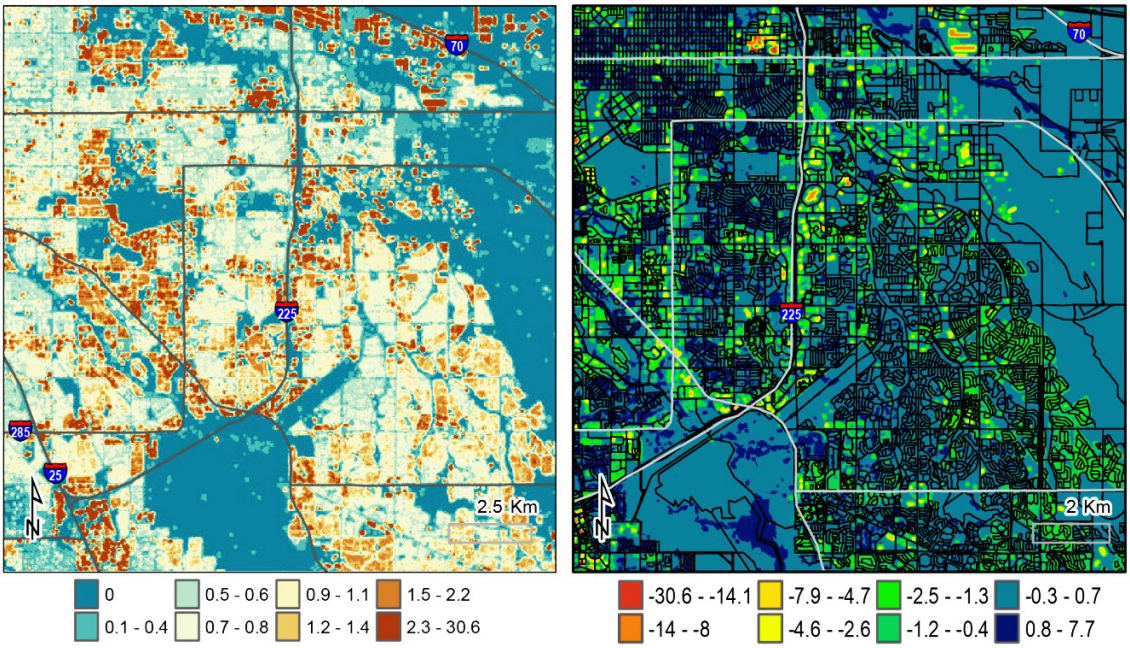

Figure 4-4. Mean building height (panel); difference between mean vegetated and impervious canopy height (m) derived using a 3 ha moving window (right panel). Negative values in right panel indicate that the impervious class forms the tallest height element, while positive values indicate that vegetation classes (usually trees) are dominant.

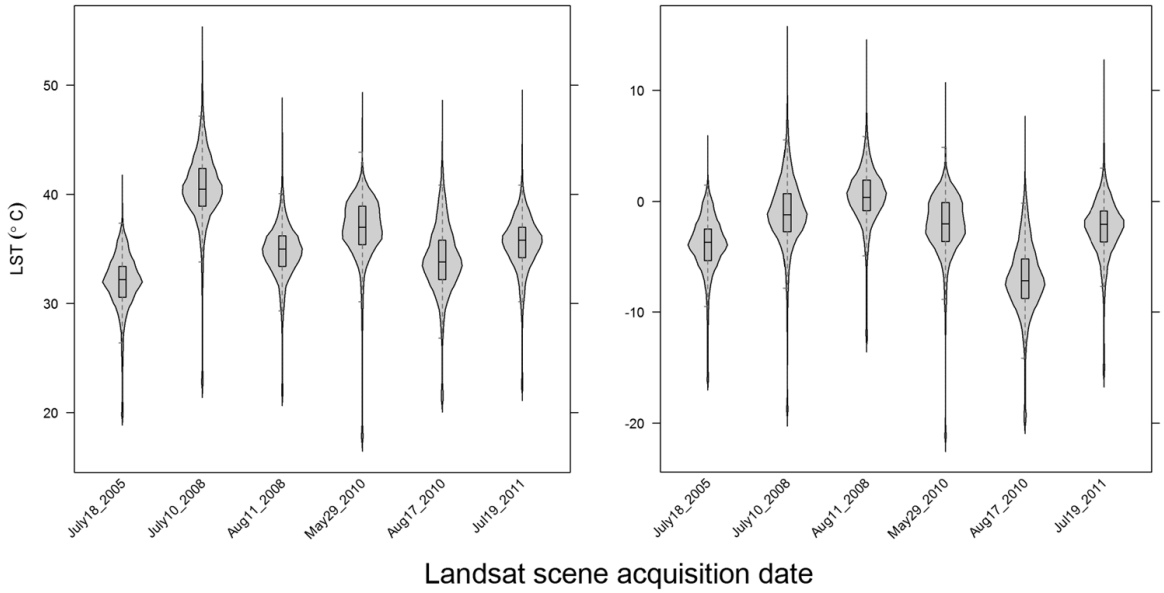

Figure 4-5. Box and whisker plots for LST (left panel) and deviation from reference area temperature (right panel) on different Landsat scene acquisition dates.

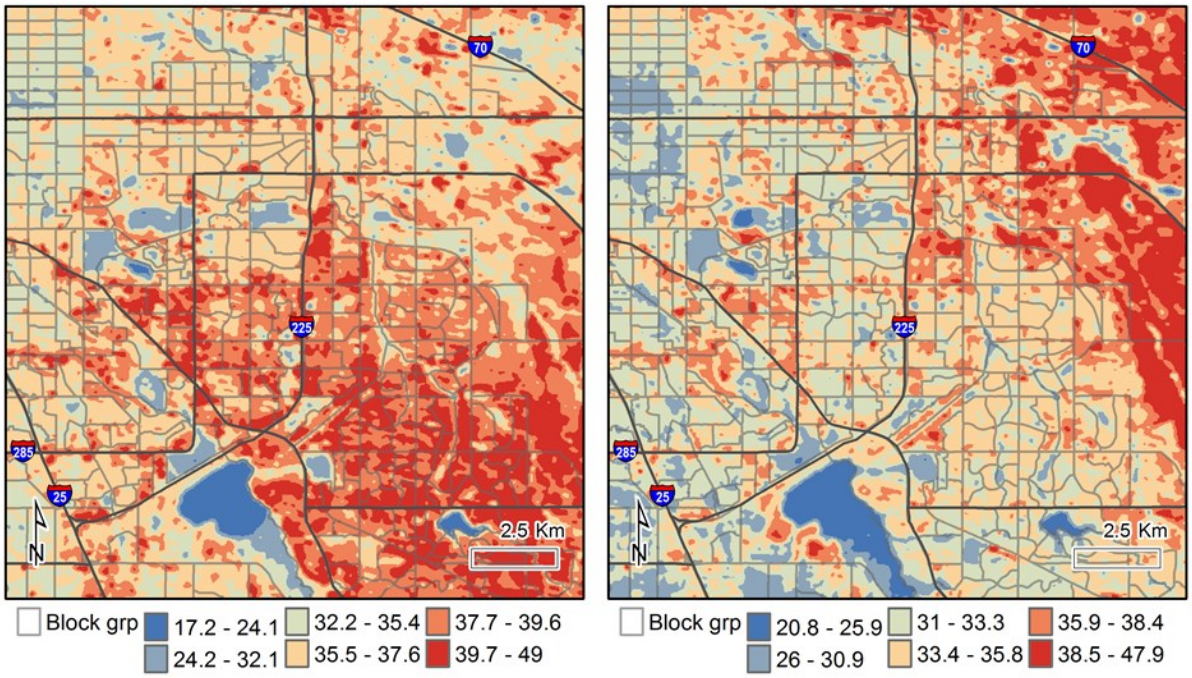

Figure 4-6. Comparison of LST on 5/29/10 (left panel) and 8/17/2010 (right panel).

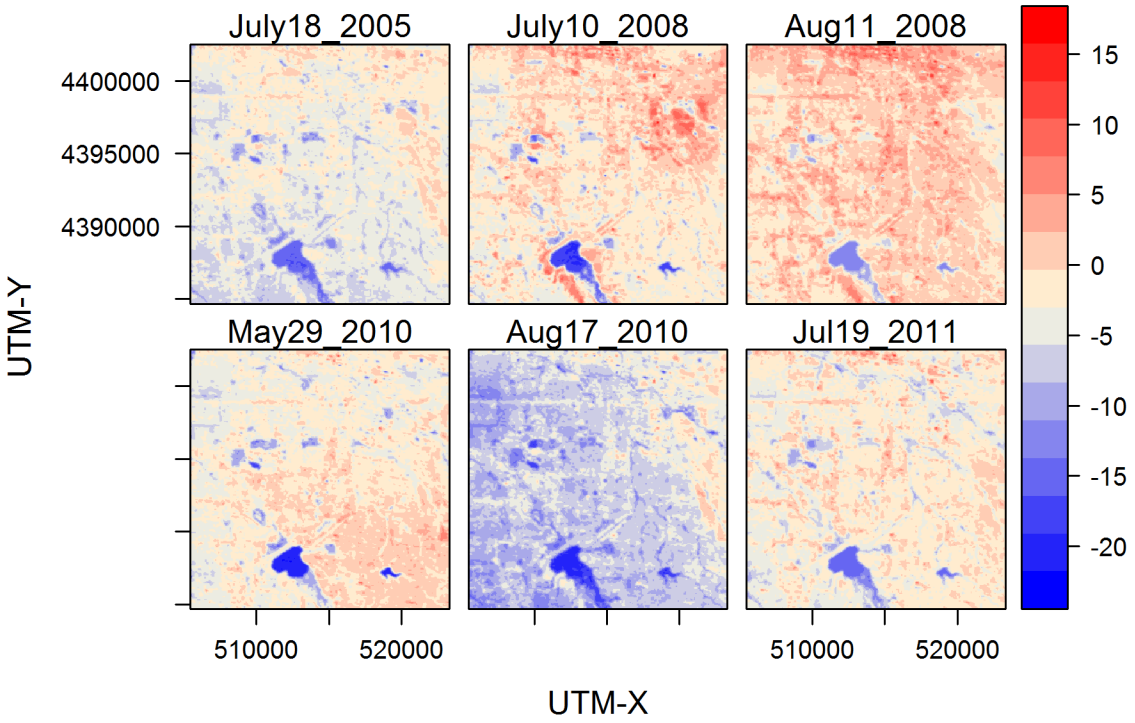

Figure 4-7. Deviation from reference area LST ($LST_{d\ ref}$) for level plot.

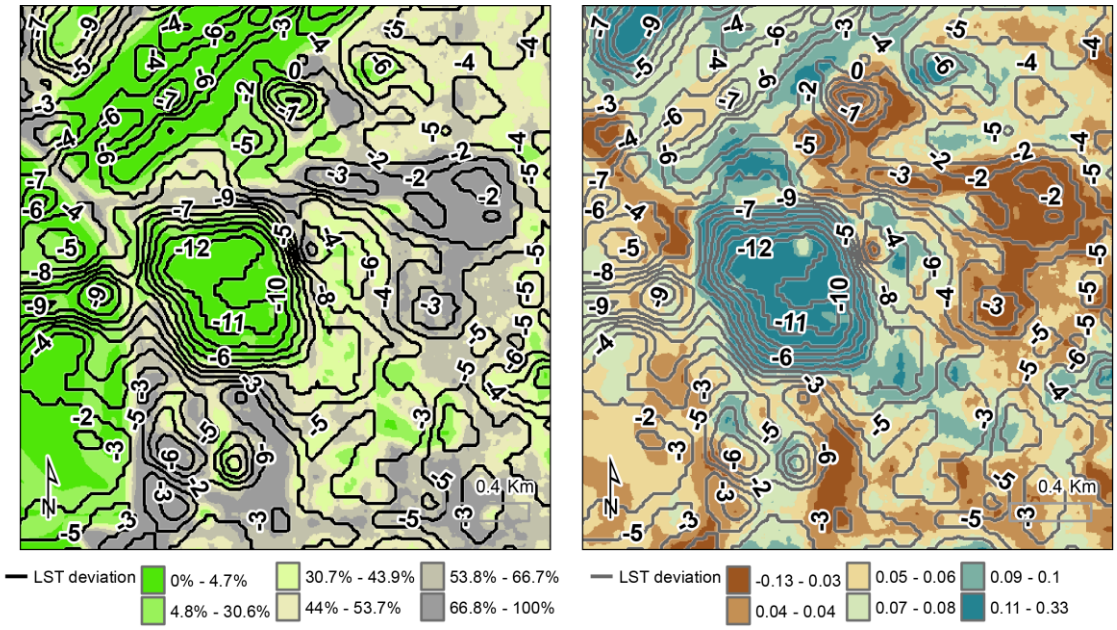

Figure 4-8. Contours of $LST_{d\ ref}$ (°C) from undeveloped reference area for a golf course (left center of figures in both panels) and adjacent residential areas in southeast Aurora overlaid on % impervious cover raster (left panel) and 2008 NDVI (right panel). Contour lines represent 1º C deviation from reference area temperature in 2008Aug11 Landsat scene.

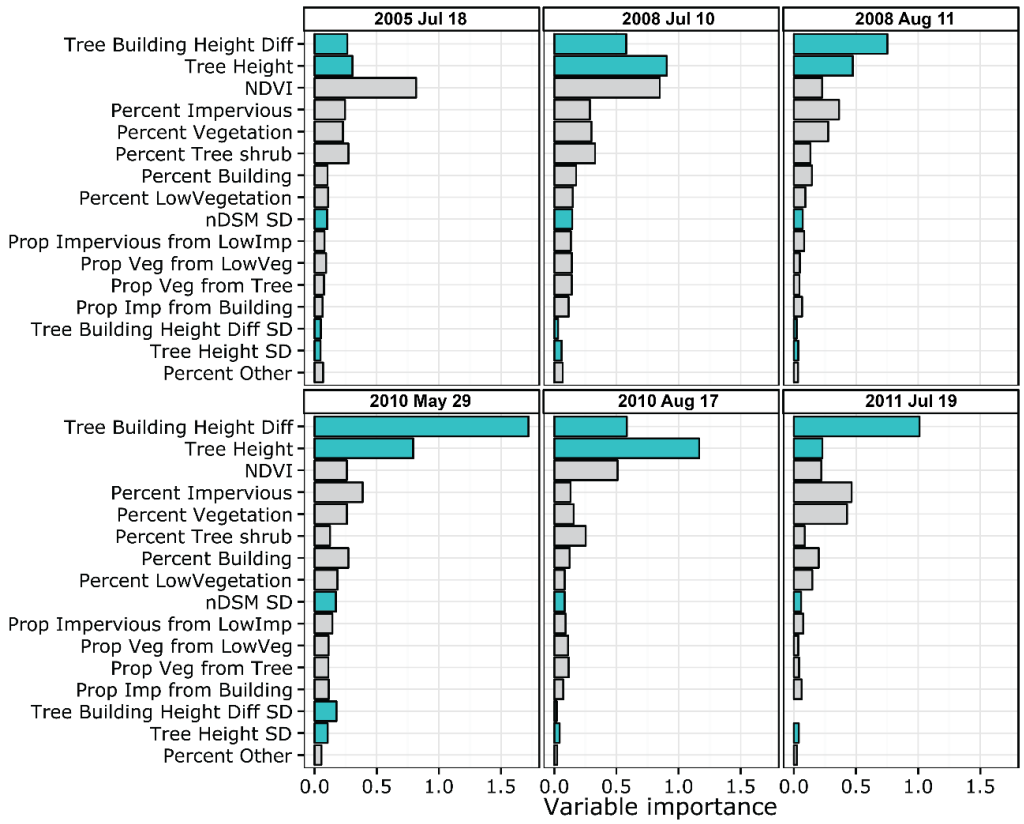

Figure 4-9. Conditional variable importance values for Random Forest analyses of LST and urban land cover compositional (grey bars) and vertical structural (blue bars) variables for individual Landsat scenes.

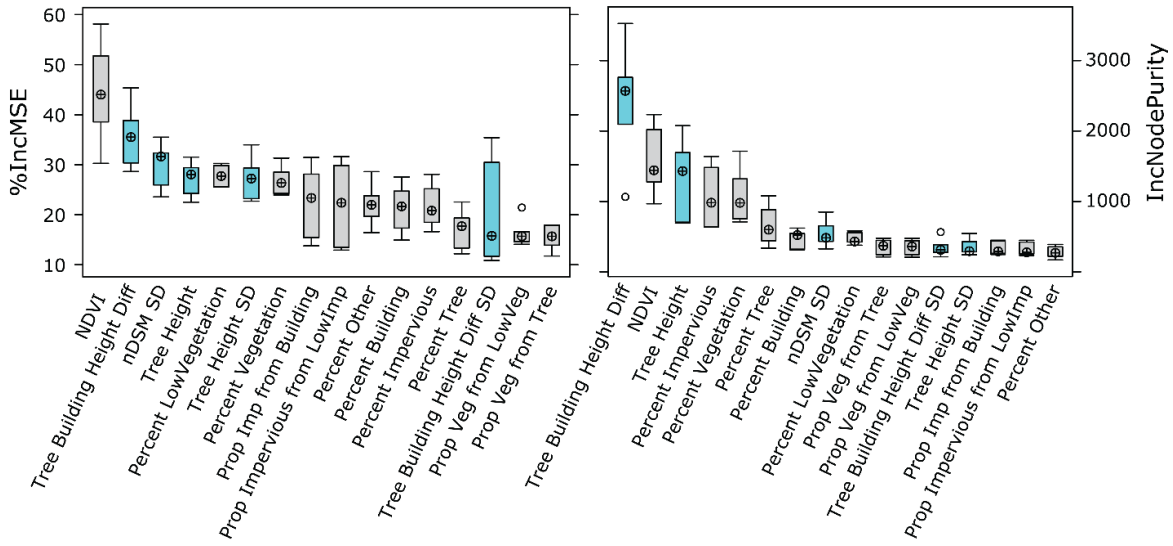

Figure 4-10. Boxplots of variable importance measures from Random Forest analysis of urban land cover compositional (grey bars) and vertical structural (blue bars) variables (n=6).

5. IRRIGATION HETEROGENEITY AND PLANT FUNCTIONAL TYPE EFFECTS ON URBAN VEGETATION WATER USE

Introduction

The establishment of a distinctive urban flora is among the most conspicuous changes accompanying urbanization. From a compositional perspective, the net effect of this transformation is typically to increase homogeneity (Pyšek et al. 2004, McKinney 2006). Turf lawns comprised of near-monocultures of cool-season grasses (e.g., *Poa pratensis*) are the dominant vegetation type in most temperate-zone US cities (Milesi et al. 2005). While trees also contribute significant cover and diversity, the composition of the urban forest is typically skewed towards a relatively small number of species favored because of aesthetic characteristics and an ability to tolerate the stresses of the urban environment (Golubiewski 2006, McHale et al. 2007, Nowak and Greenfield 2010). Urbanization can promote compositional homogeneity, but it remains unclear how functional properties like plant water use vary in relation to land cover composition, structure, and management factors like irrigation.

In arid and semi-arid climates, supplemental irrigation can support plant species with widely differing water use requirements (Nouri et al. 2013). While irrigated urban vegetation provides a range of important ecosystem services (Dobbs et al. 2011, Peters et al. 2011, Berland 2012), this is often at the cost of increased water use relative to unirrigated native cover types (Mcpherson 1992, Pataki et al. 2011b). As cities seek ways to manage limited water supplies, more attention is being given to plant water use and landscape irrigation practices, which accounts for the majority of typical summer household water use (Kenney et al. 2008, Ferguson et al. 2013). However, there remains significant uncertainty about the factors influencing the water use characteristics of urban plants under field conditions.

Individually, tree and turf water use have been extensively researched (Feldhake et al. 1983, Vrecenak and Herrington 1984, Jiang et al. 1998, Kjelgren and Montague 1998, Wang et al. 2008, Pataki et al. 2011a). However, few studies have looked at water use in combined tree and turf land cover types in urban landscapes. In many natural settings, trees have been found to use more water than herbaceous

species (Zhang et al. 2001, Huxman et al. 2005), but whether this is true in urban contexts is unclear. Urban trees can support large canopies and are generally well-coupled with the atmosphere (Oke 1989), which can result in greater transpiration than herbaceous urban land covers (Devitt et al. 1995), but other studies have found the reverse to be true (St. Hilaire et al. 2008, Peters et al. 2011), creating uncertainty.

A variety of important functional differences between trees and turf can affect water use. Trees have deeper and more laterally extensive root systems than grasses (Canadell et al. 1996, Jackson et al. 1996, Bijoor et al. 2012). Through shading and effects on the boundary layer, trees influence light, temperature, and humidity under their canopies, thereby influencing water use of surrounding vegetation (Jo and Mcpherson 2001, Shashua-Bar et al. 2011, Litvak et al. 2013). Turf commonly extends under the canopy of trees, and transpiration from both canopy layers must be accounted for when estimating total vegetation water use. ET could be expected to be greater in such dual canopy situations because of greater transpiring leaf area, but through shading, tree canopies may have the net effect of reducing ET. For example, the addition of trees to irrigated turfgrass lawns reduced total water consumption in one California study (Litvak et al. 2013). In another study from Israel, analysis of lysimeter and sap flux measurements indicated that total ET was lower in yards supporting small shade trees compared to those covered by turfgrass alone (Shashua-Bar et al. 2009, Shashua-Bar et al. 2011). However, it is unclear whether similar effects occur with cool-season turf and urban tree species in other climatic region.

In contrast to the general uniformity of turf, urban forests support different tree species of varying age, size and basic functional characteristics (Kendal et al. 2014). These can result in differences in average and peak transpiration rates and the particular response to environmental drivers of water use (Bush et al. 2008, McCarthy and Pataki 2010, Pataki et al. 2011a). Stomatal sensitivity to atmospheric drivers of ET varies between tree species, as well as between broader functional groups that can be defined by differences in plant physiology, xylem anatomy, root distribution, and phenology (Hacke and Sperry 2001, Bowden and Bauerle 2008, Peters et al. 2010, Chen et al. 2012, Litvak et al. 2012). For example, xylem anatomy, which refers to the size and frequency distribution of xylem vessels in a tree's sapwood, has been correlated with various aspects of tree water transport (Sperry et al. 1988, Sperry and

Sullivan 1992, Tyree and Zimmermann 2002, Pataki and Oren 2003, Bovard et al. 2005). Ring-porous species, including many common urban trees (e.g., *Celtis occidentalis*, *Gleditisa triacanthos*, *Quercus rubra*), have large diameter xylem vessels that are efficient at transporting water, but are more vulnerable to drought-induced cavitation than diffuse-porous trees (e.g., *Populus deltoides*, *Acer* spp.) or trees with tracheid xylem anatomy (conifers)(Hacke et al. 2007, Sperry et al. 2008, Litvak et al. 2012). Urban trees include all of these broad functional groups, but little is known about how water use characteristics differ between groups in an urban context.

Other functional characteristics like plant phenology can influence tree water use. For example, evergreen trees may use less water during mid-summer than deciduous trees, but have higher total annual transpiration because they are capable of transpiring for a longer period (Peters et al. 2010, Peters et al. 2011). In contrast, Catovsky et al. (2002) found that broad-leaved red oak and red maple trees had two- to four-fold greater annual water fluxes per ground area than coniferous eastern hemlock trees. Deciduous birch trees had stand level ET rates 1.6 times those of coniferous hemlocks in a study in the Northeastern US, even though ET rates were higher in the hemlock stand during the dormant season (Daley et al. 2007). With a few exceptions (Peters and McFadden 2010, Peters et al. 2010, Pataki et al. 2011a), differences between transpiration in evergreen and deciduous tree species have not been examined in urban areas, despite their potential importance to vegetation water use. If functional differences can be generalized and inferences made to landscape-scale distribution patterns, a truer accounting of vegetation's role in urban ecohydrological processes may be possible.

Objectives

This paper seeks to improve understanding of the factors influencing water use by irrigated urban vegetation. In particular, I contrast water use between turfgrass and tree vegetation types, evaluate differences in water use between tree species and functional groups, and assess the importance of fine-scale variation in irrigation application on turfgrass water use. I ask the following questions: (1) How does fine-scale variation in the amount of irrigation applied affect the condition and water use by *Poa pratensis* turf? (2) Does turf water use differ significantly between full sun and tree-shaded settings? (3)

How do transpiration rates differ among common urban tree species and functional types and in comparison to turf? These analyses add to the limited pool of data on water use by urban vegetation and contribute to a broader understanding of the importance of variation in plant composition and management on a key component of the urban water balance.

Methods

Study area

I conducted my analyses in Aurora, Colorado, a rapidly expanding suburb adjacent to Denver in the Colorado Front Range region (Figure 5-1). The population of Aurora has grown rapidly from 74,974 residents in 1970 to 325,078 residents in 2010 (City of Aurora 2012), driving urban expansion into agricultural areas and native shortgrass steppe. Land use changes in the last half-century have resulted in neighborhoods of varying age and land cover characteristics, and an urban forest of varied composition and age structure. Low to high-density single and multi-family residential, retail, commercial and light industrial land uses predominate. In parks and residential areas, vegetation is dominated by irrigated *Poa pratensis* lawns and urban forests comprised of primarily of introduced conifers and broad-leaved deciduous species. Aurora has a semiarid climate, with mean annual precipitation of 402 mm, most of this occurring from April-September (National Weather Service; Station ID: KDEN; 1980-2010 normals). At the site level, I analyzed 5 city-owned parks and recreation areas: Del Mar Par (DM), Canterbury Park (CB), Rocky Ridge (RR), Meadow Hills (MH), and Sagebrush Park (SG) (Figure 5-1, Table 5-2).

Weather, irrigation, and soil moisture

Average air temperature and relative humidity were measured at study sites using a CS105 probe (Campbell Scientific, Logan, Utah, USA). Values were recorded every 30 minutes on a CR1000 datalogger (Campbell Scientific) and used to calculate vapor pressure deficit. Precipitation was recorded using a Texas Instruments tipping-bucket rain gauge with a sensitivity of 0.254 mm, and events were summed to yield daily precipitation totals. Because of instrument failures and vandalism, data were

supplemented with meteorological data from a standard reference ET (ET_o) weather station at the Aurora Town Hall (ATH) in central Aurora.

To quantify spatial patterns of irrigation application access my study areas, I installed a network of cylindrical plastic jars (100 cm^3 volume, 15.2 cm^2 aperture) placed into PVC sleeves installed flush with the ground surface to act as catch cans. Mineral oil was added to prevent evaporation between measurements. On approximately a weekly basis, I measured the contents of each catch can using a graduated cylinder, reset the cans, and replenished them with more mineral oil. To calculate a depth of application, I divided the volume of water captured (cm^3) by the area of the opening (cm^2). These data were summed on a monthly and seasonal basis and interpolated using the inverse distance weighting (IDW) technique in the ArcGIS Spatial Analyst extension (version 10.1; ESRI, Redlands, CA).

Changes in volumetric soil water content (θ_v) were measured in 2 vertical arrays per site, one located under tree canopy and one in an open turf setting. Each array consisted of 3 capacitance soil moisture sensors (EC-5; Decagon, Inc.) installed at 0.1 m, 1 m, and 2m depths (Figure 5-2). Volumetric water content (θ_v) was recorded on an hourly basis using an Em5b data logger (Decagon, Inc., Pullman, WA). Because soil moisture can be highly variable spatially, I also made periodic manual measurements of near surface θ_v using an EC-5 probe at the locations of lysimeters and catch cans.

Turfgrass water use

To measure turfgrass ET, drainage lysimeters were installed following the general design in Oad et al. (1997)(Figure 5-2). Two lysimeters were installed under the canopy of each tree instrumented with sap flow sensors, one south and one north of the trunk, and were used to represent shaded turf. To represent turf ET in unshaded locations, additional lysimeters were installed in open turfgrass areas lacking trees (Figure 5-2). On a weekly basis, I used a vacuum pump to remove water from the storage reservoir at the bottom of each lysimeter and measured the volume using a graduated cylinder. ET of grass in the lysimeters was then calculated by subtracting the collected volume of water from an estimate of the volume of water application (natural precipitation plus supplemental irrigation provided by sprinkler irrigation). Irrigation volume was calculated as the product of irrigation application depth

measured using catch cans that were installed flush with the ground surface adjacent to the lysimeters (Figure 5-2). Catch cans were filled with a small amount of mineral oil to prevent evaporation and measured concurrently with lysimeters.

Visual assessments of my sites in the field and in aerial imagery revealed considerable spatial variation in the color and condition of turf. To evaluate potential consequences for turf water use, I measured water flux using a 0.95 L clear Lexan chamber attached to a portable gas exchange system (LI-6400; LICOR, Inc., Lincoln, NE). The interior of the chamber was coated with clear Teflon tape to reduce sorption of water to the chamber sides. I sampled turf at 2 m increments along a transect spanning a range of irrigation application levels on cloudless days in mid-summer 2012 at the DM site. The gas exchange measurements were not adjusted for leaf area; rather, the fixed footprint of the chamber was used as the denominator in normalizing water vapor flux measurements on the IRGA. Thus, differences in measurements were a function of multiple factors inside the chamber including leaf area and plant condition, and were interpreted as a relative index of transpiration rather than an absolute value. At each plot, I measured turf height and recorded the condition of turf using a three-point qualitative scale (poor, fair, good) based on tiller density and color. Volumetric soil water content (θ_v) in the upper 10 cm of the soil was measured using a capacitance soil moisture sensor (EC-5; Decagon, Inc.). In addition, I collected radiometric temperature measurements of the turf canopy using a non-contact infrared thermometer (Model 60275; Centech, Inc.). Radiometric and surface temperatures can diverge because of a variety of environmental and equipment factors (Gardner et al. 1992); therefore, I interpreted measurements as a gross index of plant stress, and not as an absolute temperature.

From a height of ~1 m, I also collected a photograph perpendicular to the ground surface using a Canon 8 MP digital camera. Images were collected under cloudless conditions at mid-day. Raw images were transformed from the Red-Green-Blue (RGB) color space model captured by the camera to the Hue-Saturation-Brightness (HSB) model (Karcher and Richardson 2003, Ali et al. 2013) and the mean pixel values of each image calculated using the ImageJ software package (http://imagej.nih.gov/ij/)(Abràmoff

et al. 2004). Statistical properties of images were then analyzed along with Li-Cor and ancillary measurements of turf condition in the R statistical program.

Tree water use

In each study site, tree transpiration was measured in 7-10 trees using 20 mm Granier thermal dissipation (TDP) sap flow probes inserted radially into the outer sapwood tissue (Granier 1985, Lu et al. 2004). Each sensor was comprised of two probes vertically spaced ~15 cm apart and connected to a multiplexer and CR1000 datalogger. The upper probe was heated continuously with 0.2 W of power provided by a solar panel and battery, while the lower probe was used for monitoring the reference temperature of the stem. Covers constructed of closed-cell foam and HVAC reflective foil tape were placed over sensors to reduce ambient thermal effects. Output from sap flux sensors was logged every 30 s and recorded as 30-min averages for analysis. New sensors were installed whenever data were null, out of range, or if probes showed evidence of damage. Sap flux density for the 20 mm length of the sensor (J_o) was calculated using the empirical form developed by Granier (1985):

$$J_O = a(\frac{\Delta T_M - \Delta T}{\Delta T})^b$$

Where J_o is sap flux density (g m^{-2} s^{-1}) in the outer 2 cm of sapwood (where the sensor was installed), a and b are empirical coefficients, and ΔT_M and ΔT is the temperature difference between heated and unheated reference probes. Baseline calculations and sap flux density were calculated using BaseLiner (version 3.1, Hydro-Ecology Group, Duke University). Data were processed using the original coefficients identified by Granier (a =0. 0119, b = 1.231) for tree species with diffuse-porous species and conifers. However, recent work suggests that different coefficients should be used when processing TDP data for ring-porous species (Steppe and Lemeur 2007, Bush et al. 2008), which includes many common species found in urban forests and my study sites. Since individual coefficients were not available for many ring porous species in my analysis, I used coefficients published by Bush et al. (2010) for the common urban tree *Gleditsia triacanothos* (a = 0.309 , b = 0.87) to calculate sap flux density for all ring-porous species.

For diffuse-porous and coniferous species, sapwood depth was assessed by visually evaluating color and moisture content of cores extracted using an increment borer. Tree diameter, bark thickness, and sapwood depth measurements were then used to calculate total sapwood area (A_s, cm^2). Because water transport in ring-porous species is typically restricted to the current year's vessels (Hacke and Sperry 2001, Taneda and Sperry 2008, Bush et al. 2010), sapwood area in these species was assessed using measurements of the current annual growth from tree cores. Sap flux measurements were then multiplied by sapwood area to calculate daily whole tree transpiration (E_T; kg d^{-1}) after applying a correction based on Gaussian equations developed by Pataki et al. (2011a) to account for radial variation in sap flux density. Canopy area-adjusted transpiration (E_C; kg m^{-2} d^{-1}) was calculated by dividing individual tree transpiration by projected canopy area digitized from high resolution (0.15 m GSD) aerial imagery.

Results

Weather, irrigation, and soil moisture

Temperature and vapor pressure showed a similar seasonal pattern among sites. For example, mean vapor pressure deficit at the DM site was highest in August, 2012 (3.03 KPa), followed by July (2.76 KPa) and June (2.49 KPa)(Figure 5-3). Significant precipitation was limited to mid-May and early July, with a dry June and August (Figure 5-4). At all sites, volumetric soil water at depths of 1 m and 2 m was generally invariant seasonally. However, near surface (0.1 m depth) soil moisture water contents were more dynamic, showing a clear signal from both natural precipitation and irrigation events (Figure 5-4). Spatial patterns of moisture content were positively correlated with surface irrigation readings from catch cans.

Catch can analyses demonstrated significant spatial variation in irrigation application rates within and between parks (Figure 5-5). The highest mean seasonal application was at the SG study site, with 129 cm of application in 2011, compared to 87 cm at the CB site (Table 5-2). The ranking of water use among sites matched observations on the condition of vegetation in the parks, with the drier sites such as CB exhibiting poorer turf condition. Specific spatial patterns varied from site to site as a function of irrigation

design characteristics such as the size and location of sprinkler heads. Distinct areas of high and low application were associated with the interaction of sprinkler spray patterns and tree trunks and foliage. Some sites (e.g. MH) showed distinct gradients in application, while in others were more irregular (Figure 5-5). Together, the sites demonstrate that complex, fine-scale heterogeneity in irrigation is typical.

Turfgrass water use

Turfgrass water use was spatially variable. The highest mean seasonal (May to October) turfgrass ET of 115 cm occurred at the RR site, with similar mean ET at SG and DM (114 and 112 cm, respectively.) The CB and MH sites had significantly lower ET of 85 and 91 cm. The effect of tree canopy cover on turf water use in lysimeters was inconsistent among sites (Figure 5-6). This variance reflects the broader heterogeneity of irrigation application and turf water use observed in the study sites. For example, mean May-October water use by turf in the open lysimeters at the SG, MH, and CB sites was greater than water use in lysimeters under tree canopies. However, when examined on a monthly basis, the patterns were more complex and showed evidence of change over the season (Figure 5-6).

Turf water use from lysimeters was positively correlated with irrigation application, although the slope decreased at the highest application rates. ET increased linearly over low to moderate application rates, with the slope of the ET-application line declining at higher application rates (Figure 5-6). For lysimeters at lower irrigation application rates, ET accounted for all or most measured application. However, at intermediate to high application levels, the marginal increase in ET with additional application declined (Figure 5-6).

Chamber measurements of instantaneous turfgrass transpiration diverged between plots with different turf condition (Figure 5-7). Turf plots rated in “good” condition had nearly twice the water flux rate of plots in the “fair” condition class, and four times that of plots rated as “poor”. As flux measurements were made relative to chamber area, these patterns reflect differences in several factors including physiological condition, leaf area, tiller density, and grass height. While all plots were mown on the same schedule, significant spatial variability in growth rates was observed during the summer. Early in the growing season, turf in open locations had a faster growth rate than turf under tree canopies. In

addition, there was relatively little variability in growth or condition evident in the areas of open-grown turf. However, this pattern reversed itself during the summer and the spatial heterogeneity in turf condition increased as soil moisture became more limiting. Spatial differences in turf condition were correlated with volumetric soil moisture content measurements. Plots with low soil moisture on the sampling date were those in either the poor or fair condition class (Figure 5-8). Measurements of canopy temperature using a noncontact IR thermometer demonstrated clear differences in canopy temperature between turf in different condition, with turf plots with lower water flux rates having higher canopy temperatures. Analyses of digital photos showed strong correlations between color and transpiration rates. The specific correlation differed depending on whether image brightness, hue, or saturation was considered. The image hue had the strongest correlation with transpiration ($r^2 = 0.77$), followed by saturation ($r^2 = 0.68$), and brightness ($r^2 = 0.59$). Plots visually assigned to different turf condition classes were distinctly clustered together in image space, suggesting this approach may provide an effective means of rapidly assigning condition.

Tree water use

Tree composition and structural characteristics differed among sites (Figure 5-10). So too did water use, with differences depending on the water use metric (e.g., J_s, E_T, E_c) and species (Figure 5-11). Ring-porous species had the highest J_o values, as expected given their hydraulic architecture. For instance, the ring-porous species *Gledistia triacanthos* had mean daily summertime (June-August) J_o of 1445 g cm^{-2} d^{-1}, compared with 212 g cm^{-2} d^{-1} for the conifer *Pinus ponderosa* or 176 g cm^{-2} d^{-1} for the diffuse-porous *Populus deltoides*. However, because sapwood depth and sapwood area (A_{sw}) are so much smaller in ring-porous species, this did not translate into consistently higher E_T or E_C.

Whole tree water use (E_T) rates differed among species and individual trees, but the highest E_T rates were generally associated with the largest trees. For example, the highest seasonal mean daily E_T (170 .7 kg d^{-1}) was observed in a large *Pinus ponderosa* at the DM site, followed by a large *Gleditsia triacanthos* at the MH. The lowest mean daily E_T of 18.0 kg d^{-1} occurred with a small *Acer negundo* tree located partially under the canopy of an adjacent tree. Mean summer daily whole tree water use (E_T)

across all trees for the summer months was 54.3 kg d^{-1}. Ring-porous species had a lower mean water use (49.9 kg d^{-1}) than diffuse-porous species and conifers (53.8 and 57.5 kg d^{-1}, respectively).

While larger trees generally used more water on an individual tree (E_T) basis, different patterns occurred when analyses were scaled to canopy area (E_C). For example, mean summertime daily E_T by *Populus deltoides* at the DM site was 130.7 kg d^{-1}, twice the 65.4 kg d^{-1} of the conifer *Pinus sylvestris*. However, the pine used more water on a canopy area basis (E_c) because of its more compact crown (3.6 kg m^{-2} d^{-1} versus 1.8 kg m^{-2} d^{-1}). Mean daily E_c varied between species with a particular wood anatomy type. For instance, at the CB site, ring-porous *Fraxinus pennsylvanica* had a seasonal average daily E_c of 1.1 kg m^2 d^{-1}, compared to 0.42 kg m^{-2} d^{-1} for *Quercus rubra.* Diffuse-porous species had the highest mean daily E_C of 2.6 kg m^{-2} d^{-1}, compared with 2.4 kg m^{-2} d^{-1} for conifers and 1.1 kg m^{-2} d^{-1} for ring-porous species.

Differences in water use were likely influenced by the variability among sites in tree composition and size. For example, 80% of the trees at the RR site were *Pinus nigra*, but this species was measured at only one other site. Ring-porous species were most abundant in my sample, comprising 43% of all trees sampled. Conifers accounted for 40% of trees, followed by diffuse porous deciduous species at 17%. Mean tree diameter and tree canopy area was highest for ring-porous species at 41.9 cm and 70.0 m^2, followed by conifers and diffuse-porous deciduous species. Conifers had the largest mean sapwood depth of 11.1 cm compared to only 0.2 cm for ring porous species (Figure 5-10). Because of their large tree size and deep sapwood, conifers had the highest mean A_{sw} of 724.5 cm^2, nearly twice that of diffuse-porous angiosperms and an order or magnitude greater than ring-porous species. Species composition and variation in the relative proportion of trees with different functional characteristics (e.g., wood anatomy) likely contributed to variation among sites in sap flow and total tree water use.

Discussion

The most common view of urbanization's effect on vegetation emphasizes compositional homogeneity. However, from a functional perspective, urban vegetation is highly heterogeneous, a consequence of spatially variable management practices and differences in water use between species and

basic plant functional types. My analyses highlight the important functional differences between trees and turfgrass vegetation types, as well as the large differences in water use from tree to tree. When coupled with the high spatial variability in turfgrass water use I observed, these analyses draw attention to the complexity of urban vegetation and the potential consequences for water use.

Water use by turf was associated with large variability in effective irrigation. This variability has important consequences for ecological and hydrologic function. In arid and semi-arid climates, vegetation productivity is typically constrained by low water availability (Parton et al. 1981), and supplemental irrigation significantly expands the range of water availability occurring on the landscape. Results also demonstrate that inefficiencies inherent to irrigation infrastructure and management practices create a spatially heterogeneous pattern of water availability, even at relatively fine spatial scales. These patterns are likely important drivers of variability in ecosystem functions like soil carbon accumulation (Golubiewski 2003) and groundwater recharge (Newcomer et al. 2014), in addition to their importance for vegetation water use.

Data from lysimeters and instantaneous measurements of ET from chamber measurements demonstrate significant variability in turfgrass water use within and among sites. Results suggest that differences in irrigation application are the primary driver of this variation. Analyses of chamber measurements showed strong correlations between irrigation application and turf condition, which were in turn correlated with quantitative color characteristics extracted from digital images. These results support previous research indicating the promise of image analysis for quickly assessing turf condition and potential turf ET (Karcher and Richardson 2003, Karcher and Richardson 2005). However, there are important limitations that must be noted. Specific image signatures will vary widely in response to many factors such as fertilization, turf type, time of day, and camera equipment, drastically reducing the utility of comparisons among sites. The approach cannot provide quantitative estimates of actual ET. Rather, its value is as a rapid and easily implemented site-level index of variability in irrigation application and potential water use.

Turf water use estimates from lysimeters in my study areas fit within the broad range of previously published values for *Poa pratensis* turf. For example, Green (1991) reported *P. pratensis* ET of 1.24 cm d^{-1} in a Texas lysimeter study. In Colorado, Feldhake (1983) reported daily lysimeter ET estimates for *P. pratensis* of 0.58 cm d^{-1}. This is lower than the mean daily July ET of 0.72 cm d^{-1} among my Aurora sites, but higher than the 0.49 cm d^{-1} rate observed at the CB site. Lysimeter estimates of turfgrass ET rates were greater than published estimates of native shortgrass steppe water use (Parton et al. 1981, Sala et al. 1992), highlighting the ecohydrological importance of a common vegetation conversion that occurs with urbanization in the Front Range region.

Similar to results from my turfgrass analyses, I found significant tree-to-tree variation in individual water use (E_T) and canopy area-adjusted transpiration (E_C). I generally found higher individual transpiration rates in coniferous species and lower rates in ring-porous trees, but patterns varied between species and sites due in part to differences in size. Other researchers have also documented variability in water use rates between tree functional types. For example, Poyotos et al. (2005) found water use by a *Pinus sylvestris* forest was nearly twice that of a nearby oak-dominated stand. Sap flux and whole tree water use rates were higher in diffuse-porous species than ring-porous hardwoods in a study of the temporal dynamics of water storage in different species (Köcher et al. 2013), as in urban areas in Utah and California (Bush et al. 2008, Taneda and Sperry 2008, Litvak et al. 2012). Coniferous species used significantly more water in a Minneapolis study water use by of urban trees (Peters et al. 2010). Results from this study support the idea that functional differences among urban trees contribute to broader patterns of variability in vegetation water use.

All study sites were city-owned parks or recreation areas and were professionally managed by city staff. The heterogeneity in irrigation I observed was not the purposeful result of management, rather, the result of irrigation system factors like sprinkler head type, number, and distribution. Clear spatial patterns in turf color and condition aligned with spray patterns from sprinkler heads and were observable in aerial images collected in different years. In the case of in-ground irrigation systems, these inefficiencies are effectively fixed for the lifetime of the irrigation system. Because water availability is a

critical factor limiting plant productivity, water and carbon cycling will differ between areas with chronically low application versus higher application rates, with potentially large effects at broad landscape scales (Golubiewski 2006). Similarly, areas with high irrigation rates in excess of plant consumptive use could be important loci for deep drainage and groundwater recharge (Lerner 2002, Healy and Scanlon 2010).

As the lysimeter data demonstrate, the influence of trees on turf water use can vary. I hypothesized that shade from tree canopies would reduce turf water use, since tree canopies or buildings reduce net incoming radiation (Feldhake et al. 1983, Shashua-Bar et al. 2011, Litvak et al. 2013). However, chamber measurements and lysimeter data highlight the importance of water availability as a conditioning variable influencing the effects of shade. Partial shade can mitigate the development of turf water stress and the accompanying increase in stomatal regulation of water loss. While too much shade can be detrimental to turf condition (Feldhake 1981, Beard 1997), most parks and yards do not support completely closed canopies. Anecdotal observations of greater turf regrowth and height between mowing in areas with partial tree cover suggest there may be facilitative effects from tree canopy shading that should be considered in future research.

From a functional perspective, my results run counter to the common perception that urban vegetation is homogenous (Polsky et al. 2014). Recognizing the differences in water use between plant functional types can be used to improve prediction of ET patterns among neighborhoods and cities and to explore effects of altered climate, land use, or vegetation composition patterns on urban water use. Identifying the particular contribution of different plant functional types requires information on both their relative fractional cover and specific water use characteristics (Peters et al. 2011), but models that can effectively integrate tree functional type into their predictions should be more accurate than those that assume homogenous functional traits.

Low water use is a desirable trait in urban trees, but is not the only factor to consider when evaluating the cost/benefit of individual species. Ecosystem services like land surface temperature moderation, species' habitat, and rainfall interception are directly related to tree size and productivity

(Dwyer et al. 1992, McCarthy et al. 2011, Xiao and McPherson 2011, Asgarzadeh et al. 2012, Inkiläinen et al. 2013). While I focused on relative water use, future analyses that can incorporate growth properties to allow assessment of water use efficiency may provide an improved basis for ranking species from an ecosystem services perspective.

Conclusions

While urbanization may increase the homogeneity of vegetation from a compositional perspective, my results highlight the functional heterogeneity characteristic of urban vegetation. This can be attributed to functional differences among species and vegetation types, as well as high spatial variability in irrigation. This functional heterogeneity may affect water use at broad spatial scales and should be used to inform landscape planning decisions in semi-arid cities facing limited water supplies.

Table 5-1. Abbreviations used in paper

Abbreviation	Quantity
A_i	sapwood area at depth *i* (cm^2)
A_{sw}	Sapwood area (cm^2)
D	vapor-pressure deficit (kPa)
E_C	canopy transpiration ($mm\ d^{-1}$)
E_T	tree transpiration ($kg\ tree^{-1}\ d^{-1}$)
I	Combined irrigation and precipitation application (cm)
J_i	sap-flux density at depth *i* ($g \cdot cm^{-2} \cdot d^{-1}$)
J_O	sap-flux density in the outer 2 cm of sapwood ($g \cdot cm^{-2} \cdot d^{-1}$)
J_S	sap-flux density across the active sapwood ($g \cdot cm^{-2} \cdot d^{-1}$)
θ_v	Volumetric water content ($m^3\ m^{-3}$)

Table 5-2. Tree species and biometric variables. Where n for a species is greater than 1, standard deviation is presented in parentheses.

Site	Species	n	Canopy area (m^2)	Sapwood Depth (cm)	A_{sw} (cm^2)
CB	*Celtis occidentalis*	1	46.2	0.2	17.9
	Fraxinus americana	1	24.7	0.2	11.8
	Fraxinus pennsylvanica	4	36.1 (2.6)	0.2 (0.1)	2.7 (1.6)
	Picea pungens	1	43.6	1.0	997.9
	Quercus rubra	1	51.6	0.2	19.5
DM	*Gleditsia triacanthos*	4	102.3 (9.3)	0.3	28.3
	Pinus ponderosa	1	57.5	14.9	113.6
	Pinus sylvestris	2	18.0	6.8	320.0
	Populus deltoides	1	126.8	5.5	741.8
MH	*Acer negundo*	2	12.2	6.4 (0.5)	281.7 (64.8)
	Celtis occidentalis	1	51.5	0.1	11.6
	Gleditsia triacanthos	2	101.5 (22.3)	0.2 (0.2)	35.2 (3.2)
	Pinus nigra	1	23.7	9.9	293.9
	Pinus sylvestris	1	33.5	1.1	445.3
RR	*Picea pungens*	1	5.2	8.2	271.6
	Pinus nigra	8	34.6 (2.5)	11.7 (1.8)	811.6 (164.4)
SG	*Pinus nigra*	3	31.3 (2.3)	15.0 (2.3)	945.4 (27.8)
	Quercus rubra	2	30.9 (6.3)	0.4 (0.4)	34.2 (3.6)
	Tilia cordata	4	11.6 (2.3)	1.3 (1.0)	383.6 (81.7)

Table 5-3. Summary statistics for 2011 application (sprinkler irrigation plus precipitation) for inverse distance weighted (IDW) interpolated rasters derived from seasonal (May-Oct) catch can data.

Site	Mean (cm)	Std Dev	Median (cm)	Area (m^2)
CB	87.0	16.5	83.9	4463
DM	115.4	18.8	108.6	5929
MH	94.7	12.0	93.6	3150
RR	127.5	12.2	129.0	2481
SG	128.5	14.5	126.7	4010

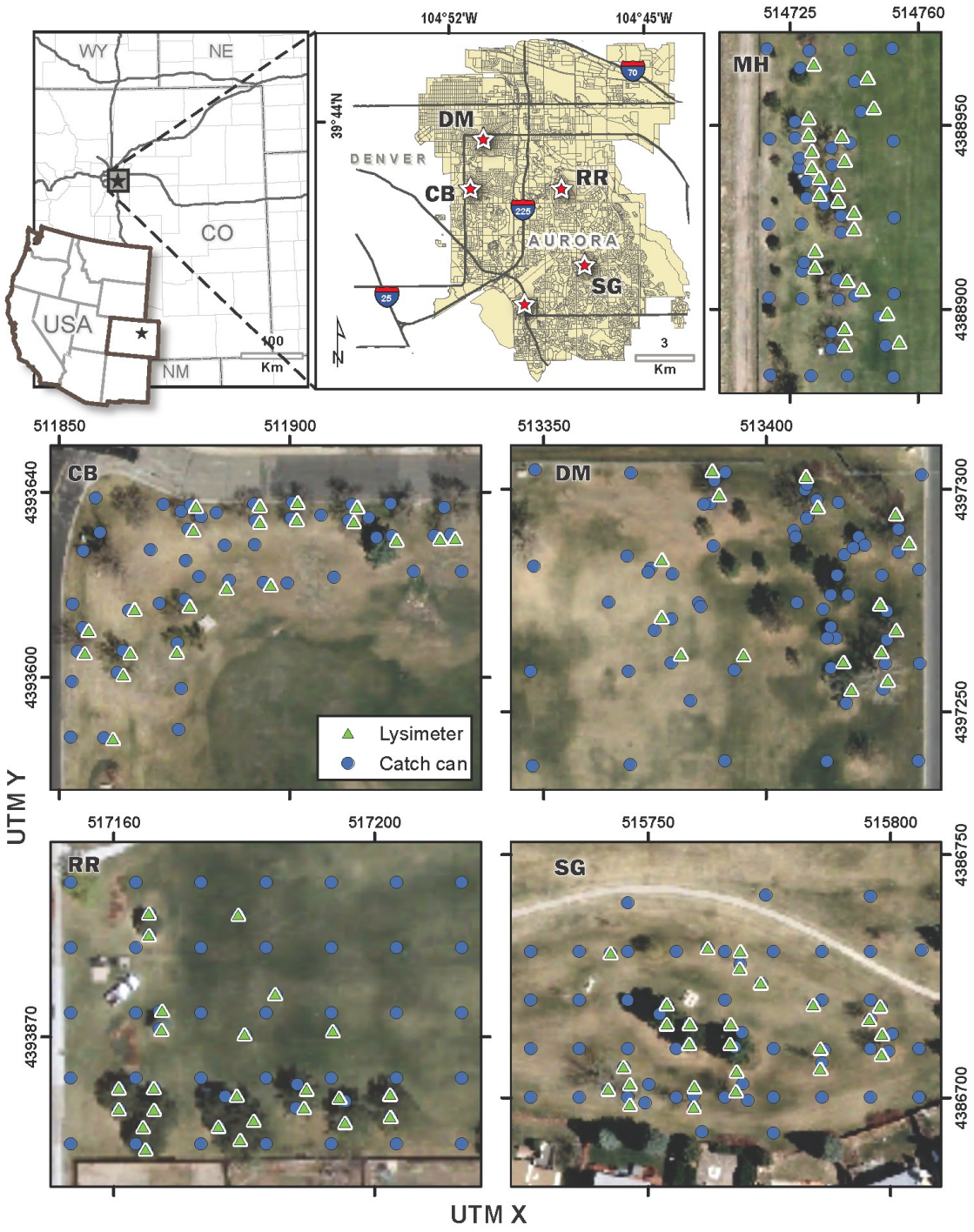

Figure 5-1. Regional and local context for study (top left). Study sites used in tree and turf water use analyses are indicated in by stars and are labelled as follows: CB = Canterbury Park, DM= Del Mar Park, MH = Meadow Hills, RR = Rocky Ridge, SG = Sagebrush. The remaining panels illustrate the distribution of catch cans and lysimeters in each study site.

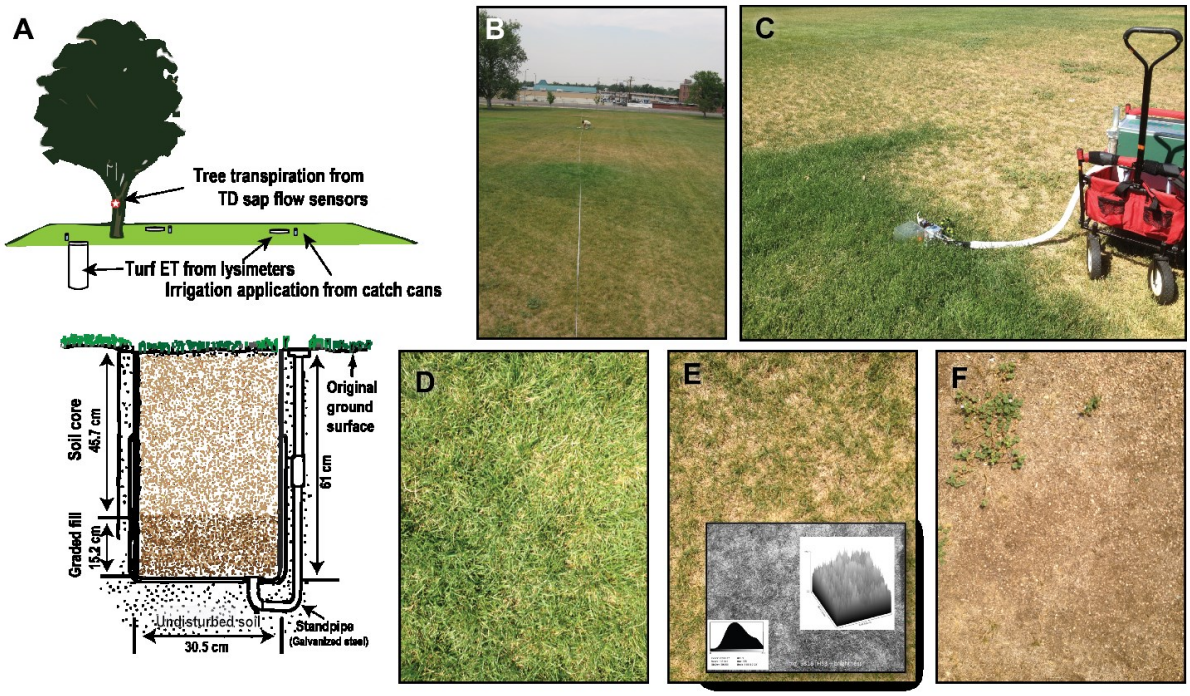

Figure 5-2. Schematic of study site instrumentation and lysimeter design (panel A) used to estimate turf water use. Transect in DM study site (panel B), along which chamber transpiration measurements were made using a chamber affixed to a LiCor 6400 (C). Turf was visually rated as good (D), fair (E), or poor (F) based on tiller density and color and photographed for quantitative image analysis. Inset in panel E show Brightness band and histogram of image, as calculated in ImageJ.

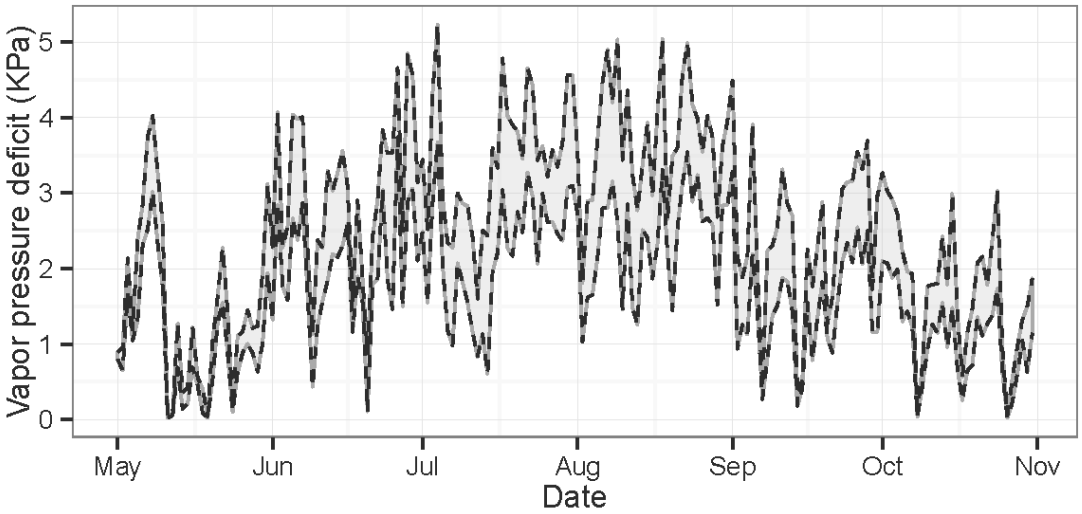

Figure 5-3. Seasonal variation in vapor pressure deficit (KPa) in 2011 (DM site).

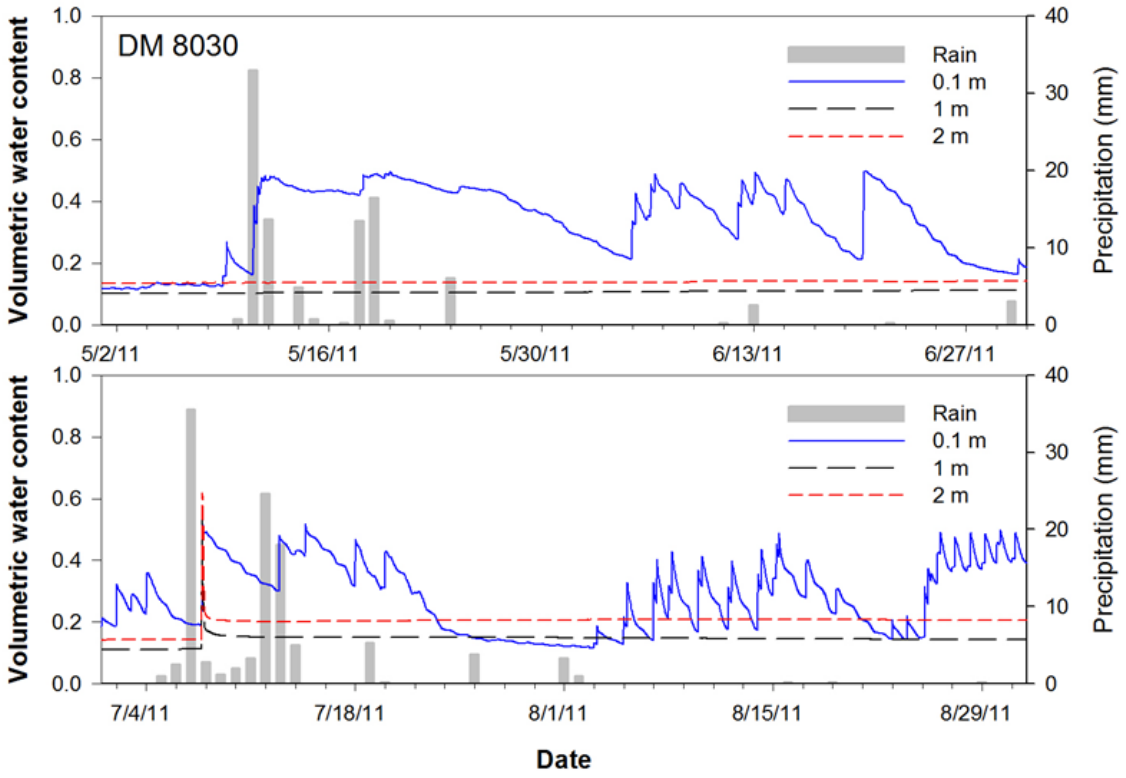

Figure 5-4. Volumetric soil moisture content (θ_v) from representative soil moisture probe array at Del Mar Park. Deep soil moisture sensors (1m and 2 m) similarly showed little temporal variation relative to near surface soil moisture contents.

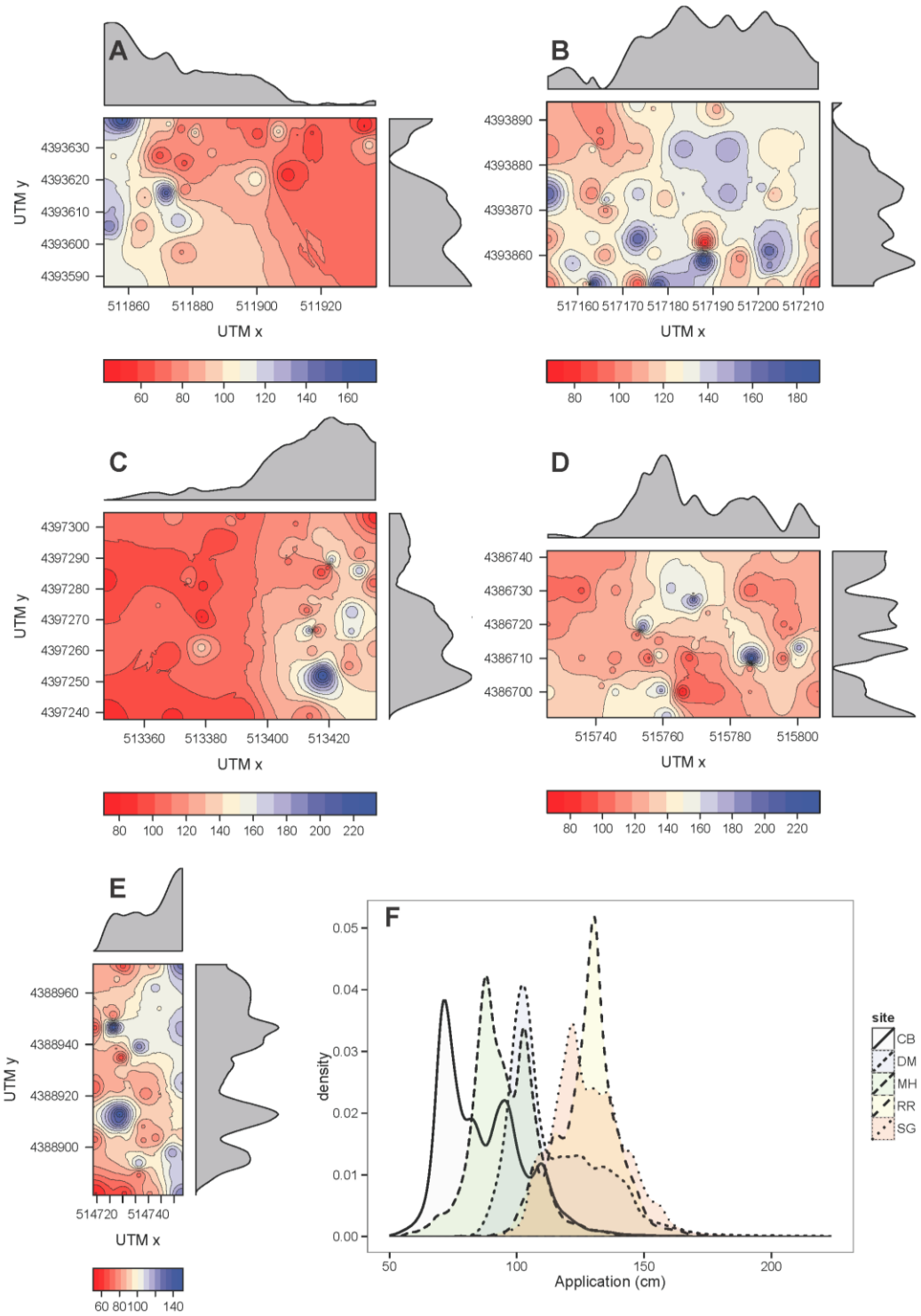

Figure 5-5. Maps of May-October application (irrigation and precipitation; cm) generated using inverse distance weighting interpolation of catch can data installed at Canterbury (CB, Panel A), Rocky Ridge (RR; panel B); Del Mar Park (DM, panel C), Sagebrush Park (SG; panel D), Meadow Hills (MH; Panel E). Marginal plots in panels A-E depict the mean irrigation value. Density plot of application for all sites (panel F).

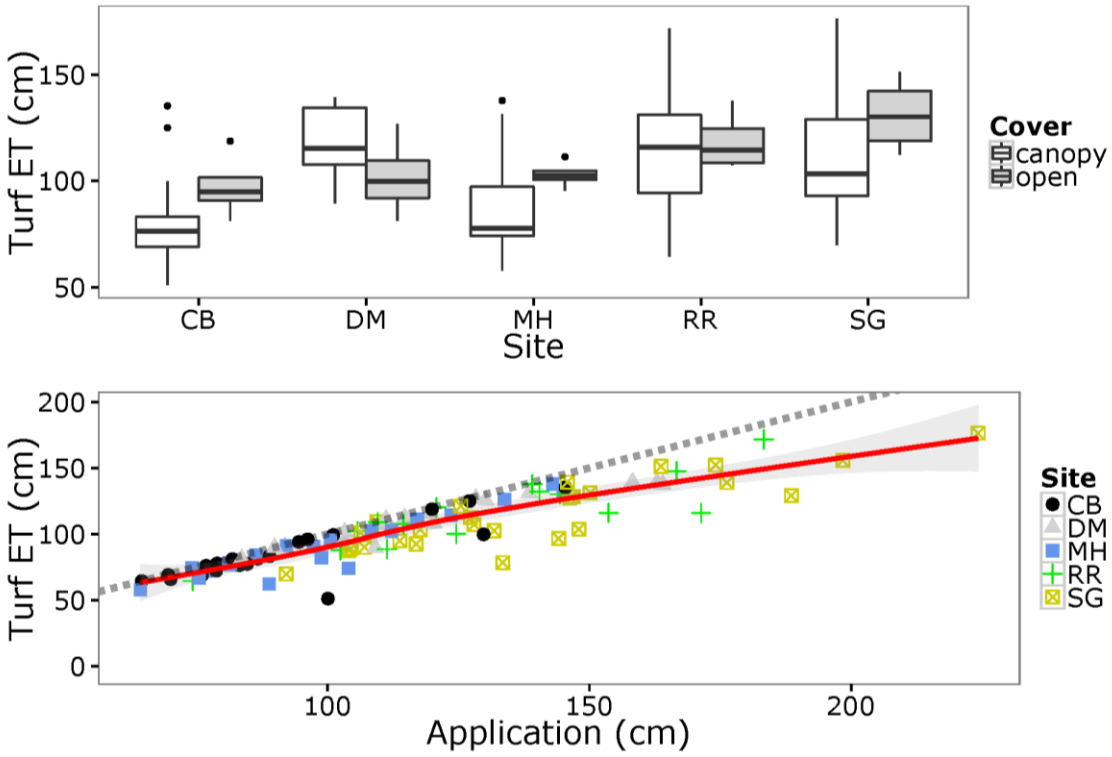

Figure 5-6. Boxplots comparing 2011 seasonal estimates (May to October) of turf ET from lysimeters under tree canopies (white bars, "canopy") versus those in open locations (grey bars, "open") at study sites (middle panel). Turf ET plotted versus irrigation application measured using catch cans installed adjacent to lysimeters (bottom panel). Dashed line represents a 1:1 line for ET and application.

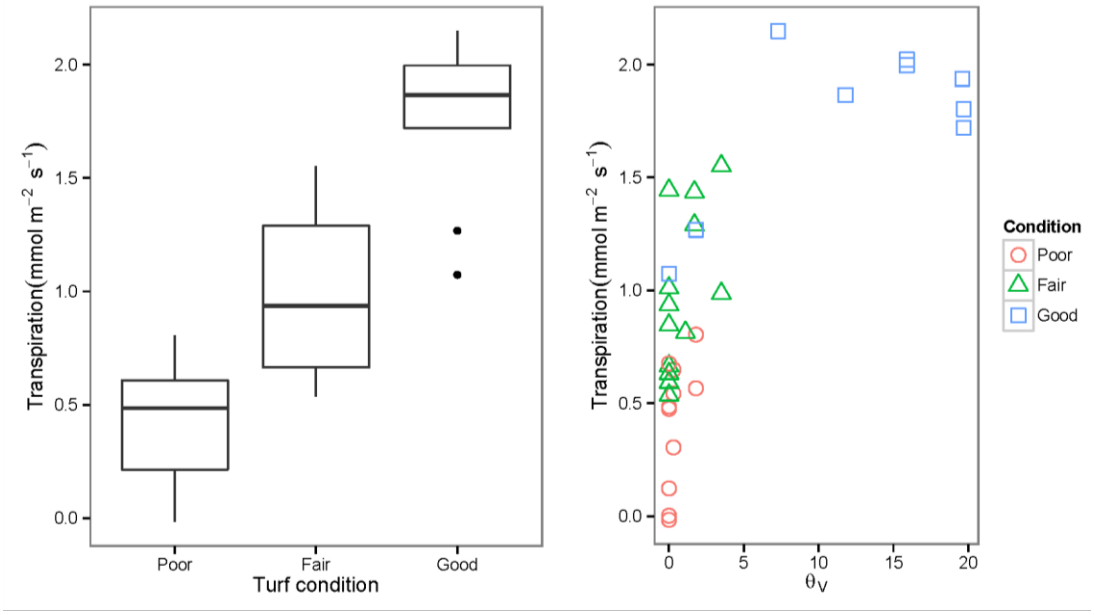

Figure 5-7. Relationship between instantaneous turf transpiration measured using LiCor 6400 and turf condition class (left panel) and volumetric soil water content measured using a soil capacitance probe (right panel).

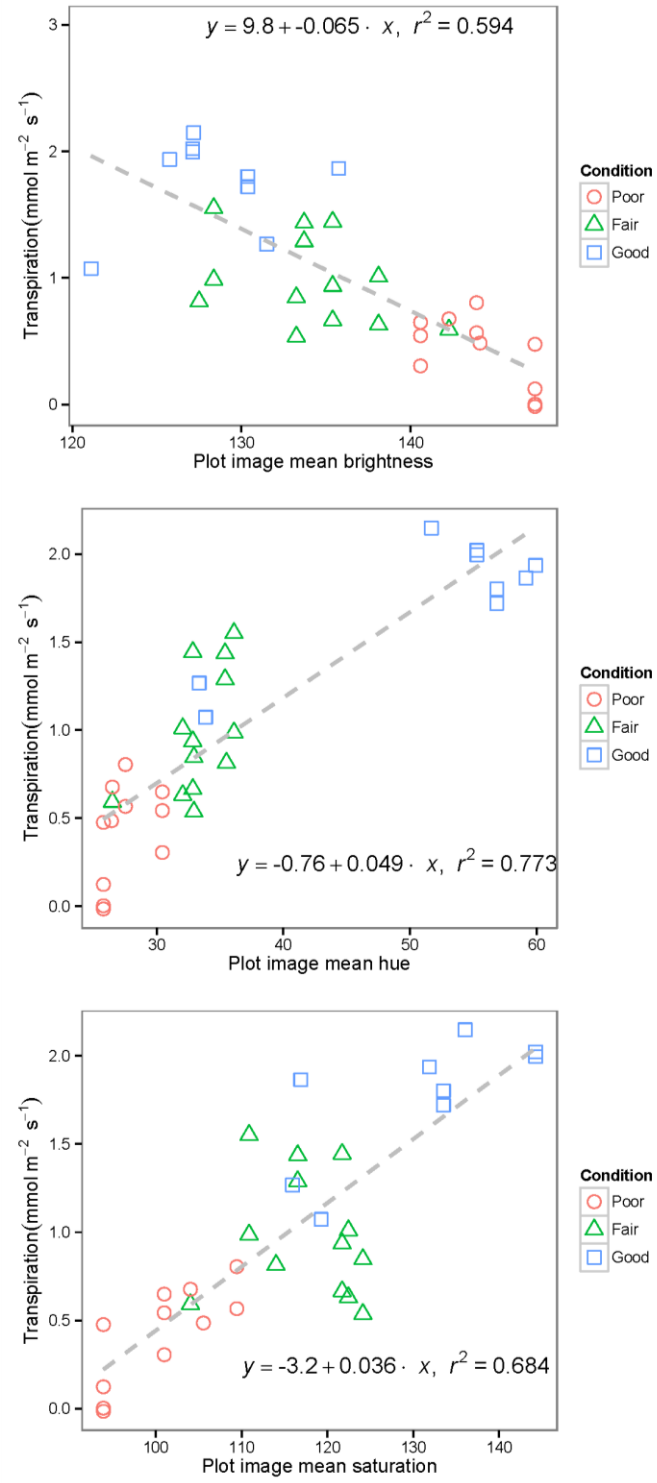

Figure 5-8. Instantaneous turfgrass transpiration plotted versus plot image brightness (top panel), hue (middle panel), and saturation (bottom panel) for plots rates as poor (circles), fair (triangles), or good (square) condition. Note that transpiration is relative to ground (chamber) area, not leaf area.

Figure 5-9. Oblique image of the DM site oriented to the North illustrating the location of the transect used for turf gas exchange measurements and digital image analysis. Note variable pattern of turf condition associated with the location of sprinkler heads (Imagery source: Google Earth)

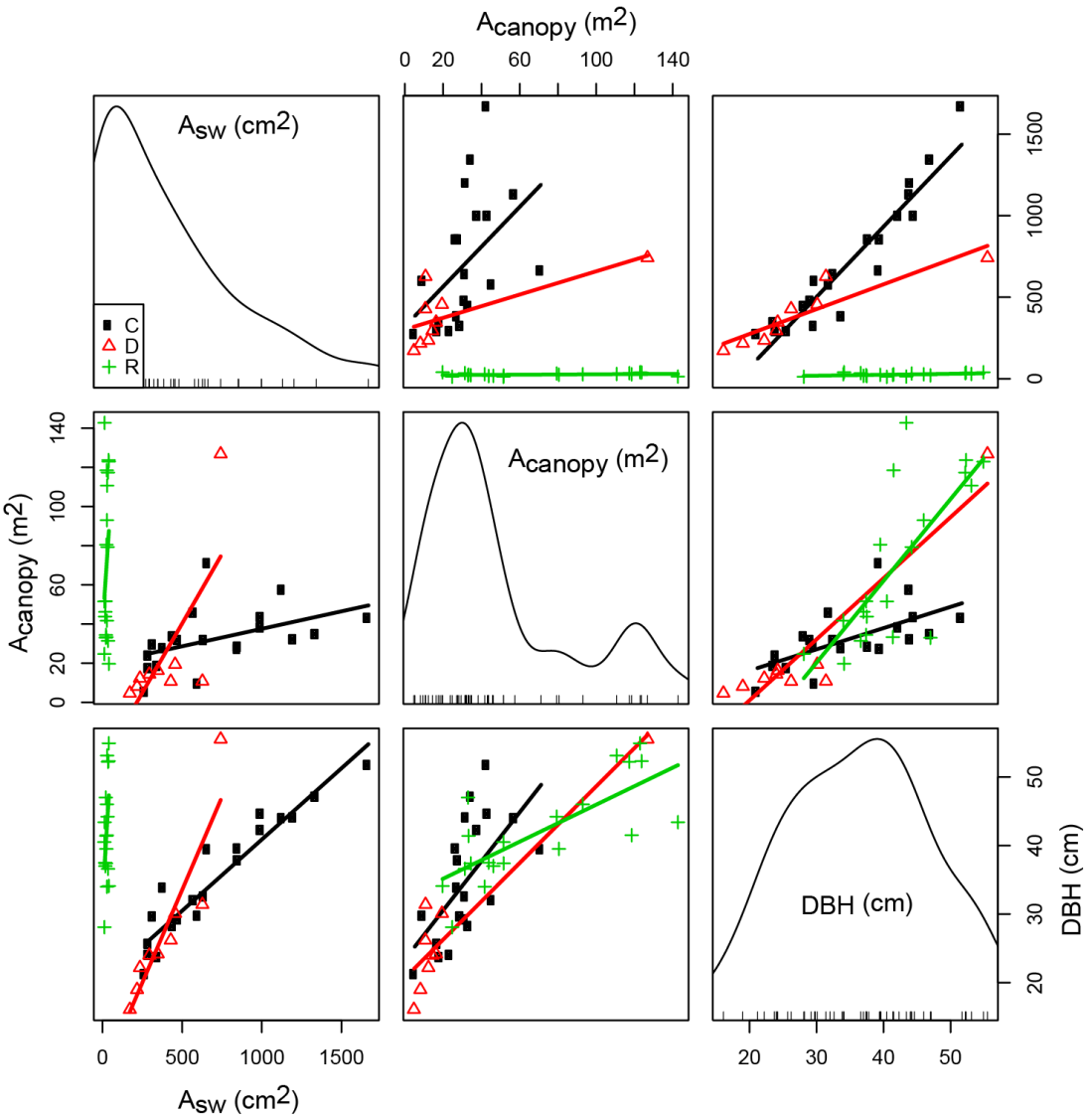

Figure 5-10. Scatterplots, least-squares regression lines, and density plots for tree sapwood area, canopy area, and diameter for ring porous (R, green lines), diffuse-porous (D, red lines) and coniferous species (C, black lines).

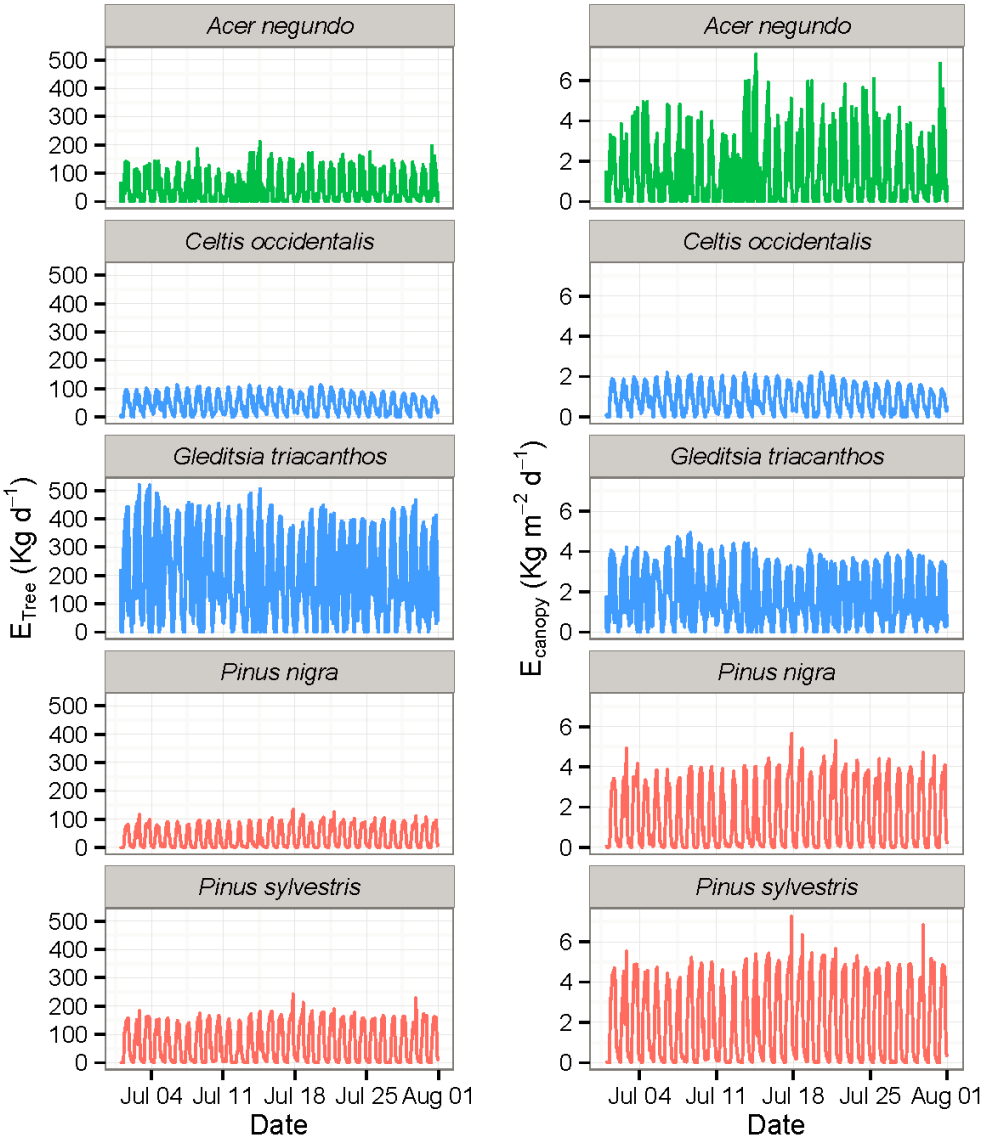

Figure 5-11. Representative daily sap flux traces from July 2011 averaged by species for MH trees expressed as mass flux (E_T, kg/d) and canopy area adjusted flux (E_{canopy}; kg/m^2 d). Line color indicates wood anatomy type (C: coniferous, D: diffuse porous, R: ring porous).

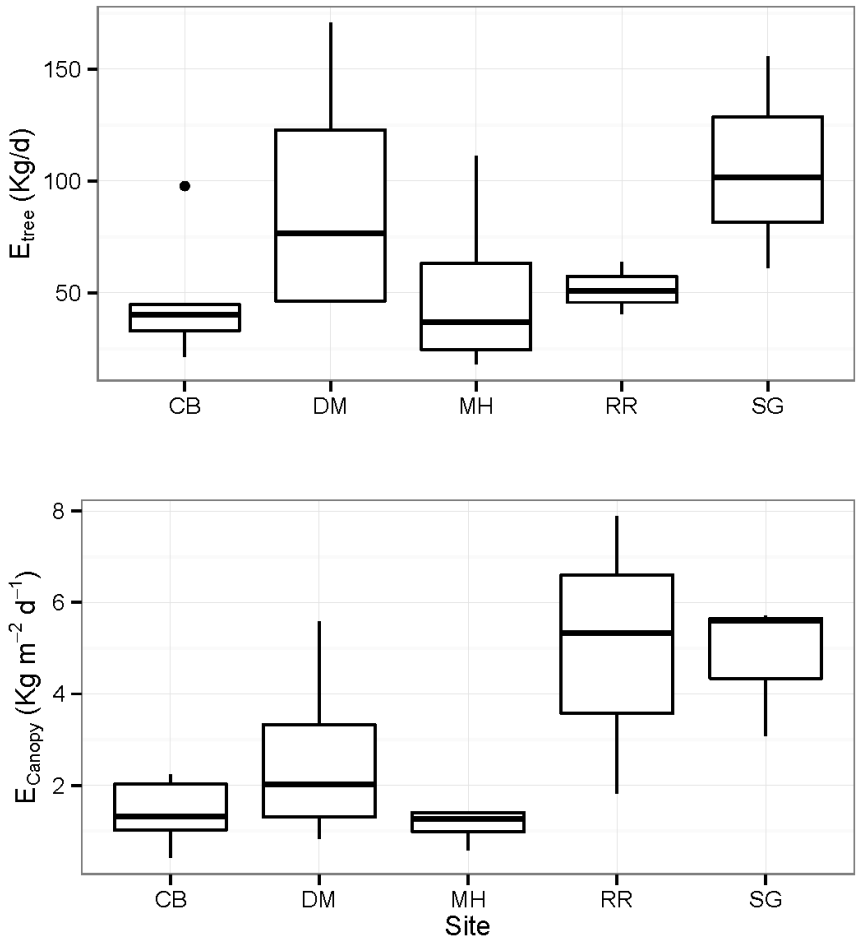

Figure 5-12. Boxplots of mean daily individual tree water use (E_T, top panel) and canopy-area-adjusted water use (E_C, bottom panel) at each study site during the summer of 2011 (Jun-Aug) for all species combined. The high E_C at the RR is due to the prevalence of conifers at that site.

6. SYNTHESIS

Cities are focal points for economic growth, innovation, and employment (Cohen 2006). The long-term sustainability for cities is tied to how well they are designed and managed. The results of my analyses provide clear evidence that urban vegetation composition and structure are important characteristics that should be addressed by planners, water managers, and individual residents.

I documented significant heterogeneity in land cover composition and vertical structural characteristics in my study area. Although spatially variable, these patterns were not random, but were correlated with age of development. This structural heterogeneity is not unique to Aurora, CO; it is a hallmark of urbanized areas across the world. This heterogeneity has important consequences for ecosystem services.

At broad scales, urbanization tends to homogenize vegetation and reduce biodiversity (McKinney 2006, Smart et al. 2006, Williams et al. 2009). However, I found that from a functional perspective, urban vegetation is highly complex. Spatial heterogeneity in the structure and composition or urban vegetation coupled with variable management practices like irrigation and fertilization, supports functionally diverse and sometimes novel environments (Oberndorfer et al. 2007, Lundholm and Richardson 2010, Robinson and Lundholm 2012, Polsky et al. 2014).

My results highlight the inefficiencies common in landscape irrigation practices, both at fine and coarse spatial scales. While land cover and structure characteristics predicted some of the variability in water use, there was significant variation within similarly configured residential parcels. A variety of factors may contribute to this variation such as inefficiencies in the irrigation system design or issues with operations. While many homes have in-ground irrigation systems with timers, most of these systems still lack integration of soil moisture or rain sensors to turn sprinklers off in the event of precipitation. More widespread use of smart irrigation controllers, i.e., controllers capable of utilizing weather conditions,

current and historic evapotranspiration, or soil moisture levels to control water applications, will enable significant water savings (Haley et al. 2007, Bijoor et al. 2014).

The basic profile of ecosystem services provided in tree versus turf cover types differs. For example, trees store more carbon above ground (McHale et al. 2007), but well-irrigated and fertilized turf can contribute more soil carbon over time (Golubiewski 2003). Because of their extensive leaf and canopy area, interception from trees can have a significant hydrologic effect (Grimmond 1989, Xiao et al. 1998, Xiao et al. 2000, Inkiläinen et al. 2013, Livesley et al. 2013). This can be viewed negatively, in that water lost to ET is "consumptively used" and not available to recharge soil moisture and support plant growth. However, canopy evaporation can help moderate land surface temperatures through latent heat exchange, thereby having a positive effect on thermal comfort. In addition, interception by trees can help moderate storm water runoff, critical for moderating floods (Walsh et al. 2005).

Summertime extremes in LST are likely to increase in severity with climate change (Luber and McGeehin 2008), with important implication for human health (Kovats and Hajat 2008). By reducing UHI formation, the promotion of structurally diverse vegetation communities can mitigate ozone production, reduce deaths from extreme heat events, and decrease energy expenditures for cooling buildings (JC et al. 1996, Manning 2008). These benefits are in addition to those derived from other ecosystem services like reduced storm water generation, carbon storage, and biodiversity (Hope et al. 2003, Byrne et al. 2008, Dobbs et al. 2011). My results suggest ways that planning decisions, particularly those aimed at promoting structural complexity, can positively influence the urban environment.

Aurora includes a diverse range of land use and land cover characteristics and is representative of urban-suburban areas throughout the region. However, it is important to recognize the broader regional context. LST patterns have been shown to vary along gradients of development (Hahs and McDonnell 2006, McDonnell and Hahs 2008, Berland and Manson 2013). In these studies as well as my own, the results are influenced by the choice of spatial grain and extent of analysis. Future work should aim to more explicitly examined gradients in land cover compositional and vertical structural characteristics at additional scales, including broader regional ones, to explore the generality of correlations.

The establishment and maintenance of urban vegetation entails costs that should be considered alongside potential benefits. Most species planted in arid and semiarid urban landscapes require supplemental irrigation. Water to support these plants is economically expensive and is drawn from regional supplies also needed for direct human consumption, agriculture, and to maintain water in streams and rivers (Pataki et al. 2011b, Bodini et al. 2012). However, irrigated urban vegetation also provides a range of provisioning and regulating ecosystem services that may offset the costs incurred for irrigation. For example, a large deciduous shade tree may be a profligate user of water, but it provides some services (e.g., shading, bird habitat, etc.) to much greater effect than a small-statured xeriscape shrub. Further research is needed to identify these tradeoffs and to incorporate them into design and planning.

Plant selection is a particularly important consideration for new construction, since replacement rates for long-lived woody species are generally slow (Roman et al. 2014). While there are examples of more dramatic changes to urban forest composition such as the spread of Dutch elm disease (Karnosky 1979, Subburayalu and Sydnor 2012) or the Emerald Ash Borer (Poland and McCullough 2006), changes in urban forests are generally gradual. More typically, canopy cover, tree height, and canopy volume change slowly as trees mature. As my analyses illustrate, these changes are linked with patterns of historical development, providing a framework for understanding landscape-scale variation in tree cover, tree height, and canopy volume.

Further analyses should more closely compare water requirements of different vegetation types and actual irrigation practices. There is often a large disconnect between actual irrigation practices and consumptive use requirements. Under low to moderate irrigation applications, urban trees may consume water at rates comparable to that of cool-season turf, but because of their more extensive root systems, trees are better able to acquire water across parcel boundaries and at greater soil depth (Gerhold and Johnson 2003). These differences have important implications water conservation, since the greatest water conservation gains are possible where actual landscape water requirements and outdoor watering practices are brought into alignment. Providing a since the greatest gains in efficiency are possible where actual landscape water requirements and outdoor watering practices are brought into alignment.

The values, beliefs, and norms or residents interact with property attributes such as household and structure size to influence watering behavior (Cook et al. 2012), but my analyses also highlight the importance of land cover composition, and to a lesser extent, vertical structure on outdoor irrigation behavior. Irrigation practices reflect the individual attitudes and social characteristics of homeowners; however, my results also demonstrate significant clustering of residences with high and low relative water use.

Collectively, my results demonstrate the importance of physical characteristics such as the amount, type, and three-dimensional structure of vegetation on water use. Because these variables change through time as landscapes age, understanding this trajectory provides insights useful for forecasting future changes in water demand and the provisioning of important ecosystem services. These results suggest that compositional and structural variables may be useful additions to decision support systems aimed at improving planning and decision-making (Xie 2009).

LITERATURE CITED

Abràmoff, M. D., P. J. Magalhães, and S. J. Ram. 2004. Image processing with ImageJ. Biophotonics international **11**:36-43.

Ahern, J. 2013. Urban landscape sustainability and resilience: the promise and challenges of integrating ecology with urban planning and design. Landscape Ecology **28**:1203-1212. *10.1007/s10980-012-9799-z*.

Al Fugara, A., B. Pradhan, and T. Ahmed Mohamed. 2009. Improvement of land-use classification using object-oriented and fuzzy logic approach. Applied Geomatics **1**:111-120. *10.1007/s12518-009-0011-3*.

Ali, A., J. C. Streibig, J. Duus, and C. Andreasen. 2013. Use of image analysis to assess color response on plants caused by herbicide application. Weed Technology **27**:604-611. *10.1614/WT-D-12-00136.1*.

Alig, R. J., J. D. Kline, and M. Lichtenstein. 2004. Urbanization on the US landscape: looking ahead in the 21st century. Landscape and Urban Planning **69**:219-234.

Anderson, J., E. Hardy, J. Roach, and R. Witmer. 1976. A land use and land cover classification system for use with remote sensor data. Geological Survey Professional Paper 964, USDI Geological Survey.

Anselin, L. 1995. Local indicators of spatial association—LISA. Geographical Analysis **27**:93-115.

Arbués, F., M. a. A. García-Valiñas, and R. Martínez-Espiñeira. 2003. Estimation of residential water demand: a state-of-the-art review. The Journal of Socio-Economics **32**:81-102. *10.1016/S1053-5357(03)00005-2*.

Arnfield, A. J. 2003. Two decades of urban climate research: a review of turbulence, exchanges of energy and water, and the urban heat island. International Journal of Climatology **23**:1-26.

Asgarzadeh, M., A. Lusk, T. Koga, and K. Hirate. 2012. Measuring oppressiveness of streetscapes. Landscape and Urban Planning **107**:1-11. *10.1016/j.landurbplan.2012.04.001*.

Baker, L., A. Brazel, N. Selover, C. Martin, N. McIntyre, F. Steiner, A. Nelson, and L. Musacchio. 2002. Urbanization and warming of Phoenix (Arizona, USA): Impacts, feedbacks and mitigation. Urban Ecosystems **6**:183-203.

Balling, R. C., and H. C. Cubaque. 2009. Estimating future residential water consumption in Phoenix, Arizona based on simulated changes in climate. Physical Geography **30**:308-323.

Balling, R. C., P. Gober, and N. Jones. 2008. Sensitivity of residential water consumption to variations in climate: An intraurban analysis of Phoenix, Arizona. Water Resources Research **44**:W10401. *10.1029/2007wr006722*.

Barbour, M. G., and W. D. Billings. 2000. North American terrestrial vegetation. Cambridge University Press, New York, NY.

Barnett, T. P., D. W. Pierce, H. G. Hidalgo, C. Bonfils, B. D. Santer, T. Das, G. Bala, A. W. Wood, T. Nozawa, A. A. Mirin, D. R. Cayan, and M. D. Dettinger. 2008. Human-induced changes in the hydrology of the western United States. Science **319**:1080-1083. *10.1126/science.1152538*.

Beard, J. 1997. Shade stresses and adaptation mechanisms of turfgrasses. International Turfgrass Society Research Journal **8**:1186-1195.

Benz, U. C., P. Hofmann, G. Willhauck, I. Lingenfelder, and M. Heynen. 2004. Multi-resolution, object-oriented fuzzy analysis of remote sensing data for GIS-ready information. ISPRS Journal of Photogrammetry and Remote Sensing **58**:239-258.

Berland, A. 2012. Long-term urbanization effects on tree canopy cover along an urban–rural gradient. Urban Ecosystems **15**:721-738. *10.1007/s11252-012-0224-9*.

Berland, A., and S. M. Manson. 2013. Patterns in residential urban forest structure along a synthetic urbanization gradient. Annals of the Association of American Geographers **103**:749-763. *10.1080/00045608.2013.782598*.

Bijoor, N., H. McCarthy, D. Zhang, and D. Pataki. 2012. Water sources of urban trees in the Los Angeles metropolitan area. Urban Ecosystems **15**:195-214. *10.1007/s11252-011-0196-1*.

Bijoor, N., D. Pataki, D. Haver, and J. Famiglietti. 2014. A comparative study of the water budgets of lawns under three management scenarios. Urban Ecosystems:1-23. *10.1007/s11252-014-0361-4*.

Blöschl, G., and M. Sivapalan. 1995. Scale issues in hydrological modelling: A review. Hydrological Processes **9**:251-290. *10.1002/hyp.3360090305*.

Bodini, A., C. Bondavalli, and S. Allesina. 2012. Cities as ecosystems: Growth, development and implications for sustainability. Ecological Modelling **245**:185-198. *10.1016/j.ecolmodel.2012.02.022*.

Boone, C., M. Cadenasso, J. Grove, K. Schwarz, and G. Buckley. 2010. Landscape, vegetation characteristics, and group identity in an urban and suburban watershed: why the 60s matter. Urban Ecosystems **13**:255-271. *10.1007/s11252-009-0118-7*.

Bovard, B. D., P. S. Curtis, C. S. Vogel, H. B. Su, and H. P. Schmid. 2005. Environmental controls on sap flow in a northern hardwood forest. Tree physiology **25**:31-38.

Bowden, J. D., and W. L. Bauerle. 2008. Measuring and modeling the variation in species-specific transpiration in temperate deciduous hardwoods. Tree physiology **28**:1675-1683.

Breiman, L. 2001. Random Forests. Machine Learning **45**:5-32.

Brookshire, D. S., B. Colby, M. Ewers, and P. T. Ganderton. 2004. Market prices for water in the semiarid West of the United States. Water Resources Research **40**:W09S04. *10.1029/2003wr002846*.

Brown, T. C. 2006. Trends in water market activity and price in the western United States. Water Resources Research **42**:W09402. *10.1029/2005wr004180*.

Bush, S. E., K. R. Hultine, J. S. Sperry, and J. R. Ehleringer. 2010. Calibration of thermal dissipation sap flow probes for ring- and diffuse-porous trees. Tree physiology **30**:1545-1554. *10.1093/treephys/tpq096*.

Bush, S. E., D. E. Pataki, K. R. Hultine, A. G. West, J. S. Sperry, and J. R. Ehleringer. 2008. Wood anatomy constrains stomatal responses to atmospheric vapor pressure deficit in irrigated, urban trees. Oecologia **156**:13-20. *10.1007/s00442-008-0966-5*.

Buyantuyev, A., and J. Wu. 2010. Urban heat islands and landscape heterogeneity: linking spatiotemporal variations in surface temperatures to land-cover and socioeconomic patterns. Landscape Ecology **25**:17-33.

Byrne, L. B., M. A. Bruns, and K. C. Kim. 2008. Ecosystem properties of urban land covers at the aboveground-belowground interface. Ecosystems **11**:1065-1077. *10.1007/s10021-008-9179-3*.

Campbell, G. S., and J. M. Norman. 1998. Introduction to Environmental Biophysics. Springer Verlag, New York, NY.

Campbell, J. B., and R. H. Wynne. 2002. Introduction to Remote Sensing. The Guilford Press, New York, NY.

Canadell, J., R. B. Jackson, J. R. Ehleringer, H. A. Mooney, O. E. Sala, and E. D. Schulze. 1996. Maximum rooting depth of vegetation types at the global scale. Oecologia **108**:583-595.

Catovsky, S., N. M. Holbrook, and F. A. Bazzaz. 2002. Coupling whole-tree transpiration and canopy photosynthesis in coniferous and broad-leaved tree species. Canadian Journal of Forest Research **32**:295-309. *10.1139/x01-199*.

Chander, G., B. L. Markham, and D. L. Helder. 2009. Summary of current radiometric calibration coefficients for Landsat MSS, TM, ETM+, and EO-1 ALI sensors. Remote Sensing of Environment **113**:893-903.

Chen, L., Z. Zhang, and B. E. Ewers. 2012. Urban tree species show the same hydraulic response to vapor pressure deficit across varying tree size and environmental conditions. PLoS ONE **7**:e47882.

Chen, Y. H., W. Su, J. Li, and Z. P. Sun. 2009. Hierarchical object oriented classification using very high resolution imagery and LIDAR data over urban areas. Advances in Space Research **43**:1101-1110. *10.1016/j.asr.2008.11.008*.

Chow, W. L., R. Pope, C. Martin, and A. Brazel. 2011. Observing and modeling the nocturnal park cool island of an arid city: horizontal and vertical impacts. Theoretical and Applied Climatology **103**:197-211. *10.1007/s00704-010-0293-8*.

Chow, W. T. L., and A. J. Brazel. 2012. Assessing xeriscaping as a sustainable heat island mitigation approach for a desert city. Building and Environment **47**:170-181. *10.1016/j.buildenv.2011.07.027*.

City of Aurora. 2012. Who is Aurora? An overview of demographic and social data and trends. City of Aurora, Planning & Development Services Department.

Clark, D. 2003. Urban World/Global City. Routledge, New York, NY.

Clinton, N., A. Holt, J. Scarborough, L. Yan, and P. Gong. 2010. Accuracy assessment measures for object-based image segmentation goodness. Photogrammetric Engineering and Remote Sensing **76**:289-299.

Cohen, B. 2006. Urbanization in developing countries: Current trends, future projections, and key challenges for sustainability. Technology in Society **28**:63-80. *10.1016/j.techsoc.2005.10.005*.

Congalton, R. G., and K. Green. 1999. Assessing the accuracy of remotely sensed data: principles and practices. Lewis Publishers, Boca Raton, FL.

Cook, E. M., S. J. Hall, and K. L. Larson. 2012. Residential landscapes as social-ecological systems: a synthesis of multi-scalar interactions between people and their home environment. Urban Ecosystems **15**:19-52. *10.1007/s11252-011-0197-0*.

Corbella, H. M., and D. S. Pujol. 2009. What lies behind domestic water use?: a review essay on the drivers of domestic water consumption. Boletín de la Asociación de Geógrafos Españoles **50**:297-314.

Crane, P., and A. Kinzig. 2005. Nature in the metropolis. Science **308**:1225.

Cromwell, J. E., J. B. Smith, and R. S. Raucher. 2007. Implications of Climate Change for Urban Water Utilities. Association of Metropolitan Water Agencies, Washington, D.C.

Daley, M. J., N. G. Phillips, C. Pettijohn, and J. L. Hadley. 2007. Water use by eastern hemlock (*Tsuga canadensis*) and black birch (*Betula lenta*): implications of effects of the hemlock woolly adelgid. Canadian Journal of Forest Research **37**:2031-2040. *10.1139/x07-045*.

Declet-Barreto, J., A. Brazel, C. Martin, W. L. Chow, and S. Harlan. 2013. Creating the park cool island in an inner-city neighborhood: heat mitigation strategy for Phoenix, AZ. Urban Ecosystems **16**:617-635. *10.1007/s11252-012-0278-8*.

Devitt, D., and R. Morris. 2009. Sustainable water use in urban landscapes in the 21st century: A Las Vegas perspective. Acta Hort. (ISHS) **881**:483-486.

Devitt, D., D. Neuman, D. Bowman, and R. Morris. 1995. Comparative water use of turfgrasses and ornamental trees in an arid environment. Journal of Turfgrass Management **1**:47-63.

Diaz-Uriarte, R., and S. Alvarez de Andres. 2006. Gene selection and classification of microarray data using random forest. BMC Bioinformatics **7**:3. *10.1186/1471-2105-7-3*.

Dimoudi, A., and M. Nikolopoulou. 2003. Vegetation in the urban environment: microclimatic analysis and benefits. Energy and Buildings **35**:69-76. *10.1016/S0378-7788(02)00081-6*.

Doan, H. T. X., and G. M. Foody. 2007. Increasing soft classification accuracy through the use of an ensemble of classifiers. International Journal of Remote Sensing **28**:4609-4623.

Dobbs, C., F. J. Escobedo, and W. C. Zipperer. 2011. A framework for developing urban forest ecosystem services and goods indicators. Landscape and Urban Planning **99**:196-206. *10.1016/j.landurbplan.2010.11.004*.

Doesken, N. J., R. A. Pielke, and O. A. P. Bliss. 2003. Climatography of the United States No. 60. Colorado Climate Center, Atmospheric Science Department, Colorado State University, Fort Collins, CO.

Dwyer, J. F., E. G. McPherson, H. W. Schroeder, and R. A. Rowntree. 1992. Assessing the benefits and costs of the urban forest. Journal of Arboriculture **18**:227-227.

Feldhake, C. M. 1981. Turfgrass evapotranspiration and urban microenvironment interaction. Ph.D. dissertation. Colorado State University, Fort Collins, CO.

Feldhake, C. M., R. E. Danielson, and J. D. Butler. 1983. Turfgrass evapotranspiration 1. Factors influencing rate in urban environments. Agronomy Journal **75**:824-830.

Ferguson, B. C., N. Frantzeskaki, and R. R. Brown. 2013. A strategic program for transitioning to a water sensitive city. Landscape and Urban Planning **117**:32-45. *10.1016/j.landurbplan.2013.04.016*.

Fielding, K. S., S. Russell, A. Spinks, and A. Mankad. 2012. Determinants of household water conservation: The role of demographic, infrastructure, behavior, and psychosocial variables. Water Resources Research **48**:W10510. *10.1029/2012wr012398*.

Franczyk, J., and H. Chang. 2009. Spatial analysis of water use in Oregon, USA, 1985–2005. Water Resources Management **23**:755-774. *10.1007/s11269-008-9298-9*.

Galea, S. 2002. Urbanization, urbanicity, and health. Journal of Urban Health **79**:S1-S12.

Gallo, K. P., A. L. McNab, T. R. Karl, J. F. Brown, J. J. Hood, and J. D. Tarpley. 1993. The use of a vegetation index for assessment of the urban heat island effect. International Journal of Remote Sensing **14**:2223-2230. *10.1080/01431169308954031*.

Gamon, J. A., C. B. Field, M. L. Goulden, K. L. Griffin, A. E. Hartley, G. Joel, J. Penuelas, and R. Valentini. 1995. Relationships between NDVI, canopy structure, and photosynthesis in 3 Californian vegetation types. Ecological Applications **5**:28-41.

Gardner, B., D. Nielsen, and C. Shock. 1992. Infrared thermometry and the crop water stress index. II. Sampling procedures and interpretation. Journal of Production Agriculture **5**:466-475.

Genuer, R., J.-M. Poggi, and C. Tuleau-Malot. 2010. Variable selection using random forests. Pattern Recognition Letters **31**:2225-2236. *10.1016/j.patrec.2010.03.014*.

Gerhold, H., and A. Johnson. 2003. Root dimensions of landscape tree cultivars. Journal of Arboriculture **29**:322-326.

Getis, A., and J. K. Ord. 1992. The analysis of spatial association by use of distance statistics. Geographical Analysis **24**:189-206.

Githinji, L. J. M., J. H. Dane, and R. H. Walker. 2009. Water-use patterns of tall fescue and hybrid bluegrass cultivars subjected to ET-based irrigation scheduling. Irrigation Science **27**:377-391. *10.1007/s00271-009-0153-4*.

Gober, P., A. Middel, A. Brazel, S. Myint, H. Chang, J. D. Duh, and L. House-Peters. 2012. Tradeoffs between water conservation and temperature amelioration in phoenix and portland: implications for urban sustainability. Urban Geography **33**:1030-1054. *10.2747/0272-3638.33.7.1030*.

Golubiewski, N. 2003. Carbon in conurbations: afforestation and carbon storage as consequences of urban sprawl in Colorado's Front Range. PhD dissertation. University of Colorado, Boulder, Colorado.

Golubiewski, N. 2006. Urbanization increases grassland carbon pools: Effects of landscaping in Colorado's Front Range. Ecological Applications **16**:555-571.

Goodwin, N. R., N. C. Coops, T. R. Tooke, A. Christen, and J. A. Voogt. 2009. Characterizing urban surface cover and structure with airborne lidar technology. Canadian Journal of Remote Sensing **35**:297-309.

Goslee, S. C. 2011. Analyzing remote sensing data in R: the landsat package. Journal of Statistical Software **43**:1-25.

Grafton, R. Q., M. B. Ward, H. To, and T. Kompas. 2011. Determinants of residential water consumption: Evidence and analysis from a 10-country household survey. Water Resources Research **47**:W08537. *10.1029/2010wr009685*.

Granier, A. 1985. A new method of sap flow measurement in tree stems. Annales Des Sciences Forestieres **42**:193-200.

Green, R., S. Sifers, C. Atkins, and J. Beard. 1991. Evapotranspiration rates of eleven Zoysia genotypes. HortScience **26**:264-266.

Grimmond, C. S. B. 1989. An evaporatranspiration-interception model for urban areas. Ph.D. dissertation. The University of British Columbia (Canada), Canada.

Grömping, U. 2009. Variable importance assessment in regression: linear regression versus random forest. The American Statistician **63**:308-319. *10.1198/tast.2009.08199*.

Guan, H., J. Li, M. Chapman, F. Deng, Z. Ji, and X. Yang. 2013. Integration of orthoimagery and lidar data for object-based urban thematic mapping using random forests. International Journal of Remote Sensing **34**:5166-5186. *10.1080/01431161.2013.788261*.

Guhathakurta, S., and P. Gober. 2007. The impact of the Phoenix Urban Heat Island on residential water use. Journal of the American Planning Association **73**:317-329.

Hacke, U. G., and J. S. Sperry. 2001. Functional and ecological xylem anatomy. Perspectives in Plant Ecology Evolution and Systematics **4**:97-115.

Hacke, U. G., J. S. Sperry, T. S. Feild, Y. Sano, E. H. Sikkema, and J. Pittermann. 2007. Water transport in vesselless angiosperms: conducting efficiency and cavitation safety. International Journal of Plant Sciences **168**:1113-1126. *10.1086/520724*.

Hahs, A. K., and M. J. McDonnell. 2006. Selecting independent measures to quantify Melbourne's urban–rural gradient. Landscape and Urban Planning **78**:435-448. *10.1016/j.landurbplan.2005.12.005*.

Haley, M. B., M. D. Dukes, and G. L. Miller. 2007. Residential irrigation water use in Central Florida. Journal of Irrigation and Drainage Engineering-ASCE **133**:427-434. *10.1061/(asce)0733-9437*.

Halper, E. B., C. A. Scott, and S. R. Yool. 2012. Correlating vegetation, water use, and surface temperature in a semiarid city: A multiscale analysis of the impacts of irrigation by single-family residences. Geographical Analysis **44**:235-257. *10.1111/j.1538-4632.2012.00846.x*.

Hansen, A., R. Rasker, B. Maxwell, J. Rotella, J. Johnson, A. Parmenter, U. Langner, W. Cohen, R. Lawrence, and M. Kraska. 2002. Ecological causes and consequences of demographic change in the New West. Bioscience **52**:151-162.

Hansen, M. C., and T. R. Loveland. 2012. A review of large area monitoring of land cover change using Landsat data. Remote Sensing of Environment **122**:66-74. *10.1016/j.rse.2011.08.024*.

Hapfelmeier, A., and K. Ulm. 2013. A new variable selection approach using Random Forests. Computational Statistics & Data Analysis **60**:50-69. *10.1016/j.csda.2012.09.020*.

Harlan, S. L., S. T. Yabiku, L. Larsen, and A. J. Brazel. 2009. Household water consumption in an arid city: affluence, affordance, and attitudes. Society & Natural Resources **22**:691-709. *10.1080/08941920802064679*.

Hastie, T., R. Tibshirani, and J. Friedman. 2009. Random Forests. Pages 587-604 The Elements of Statistical Learning. Springer, New York, NY.

Healy, R. W., and B. R. Scanlon. 2010. Estimating groundwater recharge. Cambridge University Press, Cambridge, UK.

Herold, M., J. Scepan, A. Muller, and S. Gunther. 2003. Object-oriented mapping and analysis of urban land use/cover using IKONOS data. Pages 531-538 *in* T. Benes, editor. 22nd Earsel Symposium Geoinformation for European-Wide Integration, Prague, Czech Republic.

Holland, D. E., J. A. Berglund, J. P. Spruce, and R. D. McKellip. 2008. Derivation of effective aerodynamic surface roughness in urban areas from airborne Lidar terrain data. Journal of Applied Meteorology and Climatology **47**:2614-2626. *10.1175/2008jamc1751.1*.

Hope, D., C. Gries, W. Zhu, W. Fagan, C. Redman, N. Grimm, A. Nelson, C. Martin, and A. Kinzig. 2003. Socioeconomics drive urban plant diversity. Proceedings of the National Academy of Sciences of the United States of America **100**:8788–8792. *doi: 10.1073/pnas.1537557100*.

House-Peters, L., B. Pratt, and H. Chang. 2010. Effects of urban spatial structure, sociodemographics, and climate on residential water consumption in Hillsboro, Oregon. Journal of the American Water Resources Association **46**:461-472. *10.1111/j.1752-1688.2009.00415.x*.

House-Peters, L. A., and H. Chang. 2011. Urban water demand modeling: Review of concepts, methods, and organizing principles. Water Resources Research **47**:W05401. *10.1029/2010wr009624*.

Huang, M. J., S. W. Shyue, L. H. Lee, and C. C. Kao. 2008. A knowledge-based approach to urban feature classification using aerial imagery with lidar data. Photogrammetric Engineering and Remote Sensing **74**:1473-1485.

Huxman, T. E., B. P. Wilcox, D. D. Breshears, R. L. Scott, K. A. Snyder, E. E. Small, K. Hultine, W. T. Pockman, and R. B. Jackson. 2005. Ecohydrological implications of woody plant encroachment. Ecology **86**:308-319.

Inkiläinen, E. N. M., M. R. McHale, G. B. Blank, A. L. James, and E. Nikinmaa. 2013. The role of the residential urban forest in regulating throughfall: A case study in Raleigh, North Carolina, USA. Landscape and Urban Planning **119**:91-103. *10.1016/j.landurbplan.2013.07.002*.

Jabareen, Y. R. 2006. Sustainable urban forms their typologies, models, and concepts. Journal of Planning Education and Research **26**:38-52. *10.1177/0739456X05285119*.

Jackson, R. B., J. Canadell, J. R. Ehleringer, H. A. Mooney, O. E. Sala, and E. D. Schulze. 1996. A global analysis of root distributions for terrestrial biomes. Oecologia **108**:389-411. *10.1007/BF00333714*.

Janmaat, J. 2013. Spatial patterns and policy implications for residential water use: An example using Kelowna, British Columbia. Water Resources and Economics **1**:3-19. *10.1016/j.wre.2013.03.003*.

JC, S., R. CH, F. KH, S. JD, and F. WD. 1996. Heat-related deaths during the July 1995 heat wave in Chicago. N. Engl. J. Med. **335**:84.

Jenerette, G. D., S. L. Harlan, W. L. Stefanov, and C. A. Martin. 2011. Ecosystem services and urban heat riskscape moderation: water, green spaces, and social inequality in Phoenix, USA. Ecological Applications **21**:2637-2651. *10.1890/10-1493.1*.

Jensen, J. R., and D. C. Cowen. 1999. Remote sensing of urban suburban infrastructure and socio-economic attributes. Photogrammetric Engineering and Remote Sensing **65**:611-622.

Jiang, H. F., J. D. Fry, and S. C. Wiest. 1998. Variability in turfgrass water requirements on a golf course. HortScience **33**:689-691.

Jo, H. K., and E. G. Mcpherson. 2001. Indirect carbon reduction by residential vegetation and planting strategies in Chicago, USA. Journal of Environmental Management **61**:165-177.

Jobin, B., S. Labrecque, M. Grenier, and G. Falardeau. 2008. Object-based classification as an alternative approach to the traditional pixel-based classification to identify potential habitat of the Grasshopper Sparrow. Environmental Management **41**:20-31. *10.1007/s00267-007-9031-0*.

Kanda, M., R. Moriwaki, and F. Kasamatsu. 2006. Spatial variability of both turbulent fluxes and temperature profiles in an urban roughness layer. Boundary-layer meteorology **121**:339-350. *10.1007/s10546-006-9063-7*.

Karcher, D. E., and M. D. Richardson. 2003. Quantifying turfgrass color using digital image analysis. Crop Science **43**:943-951. *10.2135/cropsci2003.9430*.

Karcher, D. E., and M. D. Richardson. 2005. Batch analysis of digital images to evaluate turfgrass characteristics. Crop Science **45**:1536-1539.

Karnosky, D. F. 1979. Dutch Elm Disease: A Review of the History, Environmental Implications, Control, and Research Needs. Environmental Conservation **6**:311-322. *10.1017/S037689290000357X*.

Ke, Y., L. J. Quackenbush, and J. Im. 2010. Synergistic use of QuickBird multispectral imagery and LIDAR data for object-based forest species classification. Remote Sensing of Environment **114**:1141-1154. *10.1016/j.rse.2010.01.002*.

Kendal, D., C. Dobbs, and V. I. Lohr. 2014. Global patterns of diversity in the urban forest: is there evidence to support the 10/20/30 rule? Urban Forestry & Urban Greening. *10.1016/j.ufug.2014.04.004*.

Kenney, D. S., C. Goemans, R. Klein, J. Lowrey, and K. Reidy. 2008. Residential water demand management: lessons from Aurora, Colorado. Journal of the American Water Resources Association **44**:192-207. *10.1111/j.1752-1688.2007.00147.x*.

Kjelgren, R., and T. Montague. 1998. Urban tree transpiration over turf and asphalt surfaces. Atmospheric Environment **32**:35-41.

Köcher, P., V. Horna, and C. Leuschner. 2013. Stem water storage in five coexisting temperate broad-leaved tree species: significance, temporal dynamics and dependence on tree functional traits. Tree physiology **33**:817-832.

Kovats, R. S., and S. Hajat. 2008. Heat stress and public health: a critical review. Annual Review of Public Health **29**:41-55. *10.1146/annurev.publhealth.29.020907.090843*.

Kressler, F., T. Bauer, and K. Steinnocher. 2002. Object-oriented per-parcel land use classification of very high resolution images. Pages 164-167 *in* Remote Sensing and Data Fusion over Urban Areas, IEEE/ISPRS Joint Workshop. IEEE, Rome, Italy.

Lach, S. R., J. P. Kerekes, and X. F. Fan. 2009. Fusion of multiple image types for the creation of radiometrically-accurate synthetic scenes. Journal of Applied Remote Sensing **3**. *10.1117/1.3075896*.

Lackner, M., and T. M. Conway. 2008. Determining land-use information from land cover through an object-oriented classification of IKONOS imagery. Canadian Journal of Remote Sensing **34**:77-92.

Lagouarde, J.-P., and M. Irvine. 2008. Directional anisotropy in thermal infrared measurements over Toulouse city centre during the CAPITOUL measurement campaigns: first results. Meteorology and atmospheric physics **102**:173-185.

Larson, K., E. Cook, C. Strawhacker, and S. Hall. 2010. The influence of diverse values, ecological structure, and geographic context on residents' multifaceted landscaping decisions. Human Ecology **38**:747-761. *10.1007/s10745-010-9359-6*.

Lefsky, M. A., W. B. Cohen, G. G. Parker, and D. J. Harding. 2002. Lidar remote sensing for ecosystem studies. Bioscience **52**:19-30.

Lerner, D. 2002. Identifying and quantifying urban recharge: a review. Hydrogeology Journal **10**:143-152. *10.1007/s10040-001-0177-1*.

Levin, S. A. 1992. The problem of pattern and scale in ecology. Ecology **73**:1943-1967.

Li, J., C. Song, L. Cao, F. Zhu, X. Meng, and J. Wu. 2011. Impacts of landscape structure on surface urban heat islands: A case study of Shanghai, China. Remote Sensing of Environment **115**:3249-3263. *10.1016/j.rse.2011.07.008*.

Liaw, A., and M. Wiener. 2002. Classification and regression by randomForest. R News **2**:18-22.

Litvak, E., N. S. Bijoor, and D. E. Pataki. 2013. Adding trees to irrigated turfgrass lawns may be a water-saving measure in semi-arid environments. Ecohydrology. *10.1002/eco.1458*.

Litvak, E., H. R. McCarthy, and D. E. Pataki. 2012. Transpiration sensitivity of urban trees in a semi-arid climate is constrained by xylem vulnerability to cavitation. Tree physiology **32**:373-388. *10.1093/treephys/tps015*.

Livesley, S. J., B. Baudinette, and D. Glover. 2013. Rainfall interception and stem flow by eucalypt street trees – The impacts of canopy density and bark type. Urban Forestry & Urban Greening **13**:192–197. *10.1016/j.ufug.2013.09.001*.

Lu, P., L. Urban, and P. Zhao. 2004. Granier's thermal dissipation probe (TDP) method for measuring sap flow in trees: Theory and practice. Acta Botanica Sinica **46**:631-646.

Luber, G., and M. McGeehin. 2008. Climate change and extreme heat events. American Journal of Preventive Medicine **35**:429-435. *10.1016/j.amepre.2008.08.021*.

Lundholm, J. T., and P. J. Richardson. 2010. Habitat analogues for reconciliation ecology in urban and industrial environments. Journal of Applied Ecology **47**:966-975.

Malinverni, E. S., A. N. Tassetti, A. Mancini, P. Zingaretti, E. Frontoni, and A. Bernardini. 2011. Hybrid object-based approach for land use/land cover mapping using high spatial resolution imagery. International Journal of Geographical Information Science **25**:1025-1043. *10.1080/13658816.2011.566569*.

Manning, W. J. 2008. Plants in urban ecosystems: Essential role of urban forests in urban metabolism and succession toward sustainability. International Journal of Sustainable Development and World Ecology **15**:362-370. *10.3843/SusDev.15.4:12*.

Mayer, P. W., W. B. DeOreo, E. M. Opitz, J. C. Kiefer, W. Y. Davis, B. Dziegielewski, and J. O. Nelson. 1999. Residential end uses of water. American Water Works Association Research Foundation, Denver, CO.

McCarthy, H., and D. Pataki. 2010. Drivers of variability in water use of native and non-native urban trees in the greater Los Angeles area. Urban Ecosystems **13**:393-414. *10.1007/s11252-010-0127-6*.

McCarthy, H. R., D. E. Pataki, and G. D. Jenerette. 2011. Plant water-use efficiency as a metric of urban ecosystem services. Ecological Applications **21**:3115-3127. *10.1890/11-0048.1*.

McDonnell, M., and A. Hahs. 2008. The use of gradient analysis studies in advancing our understanding of the ecology of urbanizing landscapes: current status and future directions. Landscape Ecology **23**:1143-1155. *10.1007/s10980-008-9253-4*.

McDonnell, M., S. Pickett, P. Groffman, P. Bohlen, R. Pouyat, W. Zipperer, R. Parmelee, M. Carreiro, and K. Medley. 1997. Ecosystem processes along an urban-to-rural gradient. Urban Ecosystems **1**:21-36.

McFeeters, S. K. 1996. The use of the Normalized Difference Water Index (NDWI) in the delineation of open water features. International Journal of Remote Sensing **17**:1425-1432. *10.1080/01431169608948714*.

McHale, M., E. Gregory McPherson, and I. Burke. 2007. The potential of urban tree plantings to be cost effective in carbon credit markets. Urban Forestry & Urban Greening **6**:49-60.

McKinney, M. L. 2006. Urbanization as a major cause of biotic homogenization. Biological Conservation **127**:247-260. *10.1016/j.biocon.2005.09.005*.

Mcpherson, E. G. 1992. Accounting for benefits and costs of urban greenspace. Landscape and Urban Planning **22**:41-51.

Milesi, C., S. Running, C. Elvidge, J. Dietz, B. Tuttle, and R. Nemani. 2005. Mapping and modeling the biogeochemical cycling of turf grasses in the United States. Environmental Management **36**:426-438. *10.1007/s00267-004-0316-2*.

Mitchell, V., H. Cleugh, C. Grimmond, and J. Xu. 2008. Linking urban water balance and energy balance models to analyse urban design options. Hydrological Processes **22**:2891-2900.

Myint, S. W. 2006. Urban vegetation mapping using sub-pixel analysis and expert system rules: a critical approach. International Journal of Remote Sensing **27**:2645-2665.

Myint, S. W., P. Gober, A. Brazel, S. Grossman-Clarke, and Q. Weng. 2011. Per-pixel vs. object-based classification of urban land cover extraction using high spatial resolution imagery. Remote Sensing of Environment **115**:1145-1161. *10.1016/j.rse.2010.12.017*.

Newcomer, M. E., J. J. Gurdak, L. S. Sklar, and L. Nanus. 2014. Urban recharge beneath low impact development and effects of climate variability and change. Water Resources Research **50**:1716-1734. *10.1002/2013WR014282*.

Nieswiadomy, M. L. 1992. Estimating urban residential water demand - effects of price structure, conservation, and education. Water Resources Research **28**:609-615. *10.1029/91wr02852*.

Nouri, H., S. Beecham, A. M. Hassanli, and F. Kazemi. 2013. Water requirements of urban landscape plants: A comparison of three factor-based approaches. Ecological Engineering **57**:276-284. *10.1016/j.ecoleng.2013.04.025*.

Nowak, D. J., and D. E. Crane. 2002. Carbon storage and sequestration by urban trees in the USA. Environmental Pollution **116**:381-389.

Nowak, D. J., and E. J. Greenfield. 2010. Urban and community forests of the Mountain region: Arizona, Colorado, Idaho, Montana, Nevada, New Mexico, Utah, Wyoming. U.S. Department of Agriculture, Forest Service, Northern Research Station, Newtown Square, PA.

O'Neil-Dunne, J. P. M., S. W. MacFaden, A. R. Royar, and K. C. Pelletier. 2012. An object-based system for LiDAR data fusion and feature extraction. Geocarto International **28**:227-242.

Oad, R., K. Lusk, and T. Podmore. 1997. Consumptive use and return flows in urban lawn water use. Journal of Irrigation and Drainage Engineering **123**:62-70.

Oberndorfer, E., J. Lundholm, B. Bass, R. R. Coffman, H. Doshi, N. Dunnett, S. Gaffin, M. Kohler, K. K. Y. Liu, and B. Rowe. 2007. Green roofs as urban ecosystems: ecological structures, functions, and services. Bioscience **57**:823-833.

Oke, T. R. 1982. The energetic basis of the urban heat island. Quarterly Journal of the Royal Meteorological Society **108**:1-24.

Oke, T. R. 1989. The micrometeorology of the urban forest. Philosophical Transactions of the Royal Society of London B Biological Sciences **324**:335-349.

Owen, T. W., T. N. Carlson, and R. R. Gillies. 1998. An assessment of satellite remotely-sensed land cover parameters in quantitatively describing the climatic effect of urbanization. International Journal of Remote Sensing **19**:1663-1681.

Parton, W., W. Lauenroth, and F. Smith. 1981. Water loss from a shortgrass steppe. Agricultural Meteorology **24**:97-109.

Pascual, C., A. Garcia-Abril, L. G. Garcia-Montero, S. Martin-Fernandez, and W. B. Cohen. 2008. Object-based semi-automatic approach for forest structure characterization using lidar data in heterogeneous *Pinus sylvestris* stands. Forest Ecology and Management **255**:3677-3685. *10.1016/j.foreco.2008.02.055*.

Pataki, D., H. McCarthy, E. Litvak, and S. Pincetl. 2011a. Transpiration of urban forests in the Los Angeles metropolitan area. Ecological Applications **21**:661–677. *doi:10.1890/09-1717.1*.

Pataki, D. E., R. J. Alig, A. S. Fung, N. E. Golubiewski, C. A. Kennedy, E. G. Mcpherson, D. J. Nowak, R. V. Pouyat, and P. R. Lankao. 2006. Urban ecosystems and the North American carbon cycle. Global Change Biology **12**:2092-2102.

Pataki, D. E., C. G. Boone, T. S. Hogue, G. D. Jenerette, J. P. McFadden, and S. Pincetl. 2011b. Ecohydrology bearings - invited commentary: Socio-ecohydrology and the urban water challenge. Ecohydrology **4**:341-347. *10.1002/eco.209*.

Pataki, D. E., and R. Oren. 2003. Species differences in stomatal control of water loss at the canopy scale in a mature bottomland deciduous forest. Advances in Water Resources **26**:1267-1278. *10.1016/j.advwatres.2003.08.001*.

Peters, E., R. Hiller, and J. McFadden. 2011. Seasonal contributions of vegetation types to suburban evapotranspiration. Journal of Geophysical Research **116**:G01003. *10.1029/2010jg001463*.

Peters, E., and J. McFadden. 2010. Influence of seasonality and vegetation type on suburban microclimates. Urban Ecosystems **13**:443-460. *10.1007/s11252-010-0128-5*.

Peters, E. B., J. P. McFadden, and R. A. Montgomery. 2010. Biological and environmental controls on tree transpiration in a suburban landscape. Journal of Geophysical Research **115**:G04006.

Pickett, S., M. Cadenasso, J. M. Grove, C. G. Boone, P. M. Groffman, E. Irwin, S. S. Kaushal, V. Marshall, B. P. McGrath, and C. H. Nilon. 2011. Urban ecological systems: Scientific foundations and a decade of progress. Journal of Environmental Management **92**:331-362.

Pickett, S., M. Cadenasso, and B. McGrath. 2013. Resilience in Ecology and Urban Design - Linking Theory and Practice for Sustainable Cities. Springer, New York, NY.

Pickett, S. T., and M. L. Cadenasso. 1995. Landscape ecology: spatial heterogeneity in ecological systems. Science:331-334.

Poland, T. M., and D. G. McCullough. 2006. Emerald ash borer: Invasion of the urban forest and the threat to North America's ash resource. Journal of Forestry **104**:118-124.

Polebitski, A. S., and R. N. Palmer. 2009. Seasonal residential water demand forecasting for census tracts. Journal of Water Resources Planning and Management **136**:27-36.

Polsky, C., J. M. Grove, C. Knudson, P. M. Groffman, N. Bettez, J. Cavender-Bares, S. J. Hall, J. B. Heffernan, S. E. Hobbie, K. L. Larson, J. L. Morse, C. Neill, K. C. Nelson, L. A. Ogden, J. O'Neil-Dunne, D. E. Pataki, R. Roy Chowdhury, and M. K. Steele. 2014. Assessing the homogenization of urban land management with an application to US residential lawn care. Proceedings of the National Academy of Sciences. *10.1073/pnas.1323995111*.

Poyatos, R., P. Llorens, and F. Gallart. 2005. Transpiration of montane *Pinus sylvestris* L. and *Quercus pubescens* Willd. forest stands measured with sap flow sensors in NE Spain. Hydrology and Earth System Sciences **9**:493-505.

Priestnall, G., J. Jaafar, and A. Duncan. 2000. Extracting urban features from LiDAR digital surface models. Computers, Environment and Urban Systems **24**:65-78.

Pyšek, P., Z. Chocholousková, A. Pyšek, V. Jarošík, M. Chytrý, and L. Tichý. 2004. Trends in species diversity and composition of urban vegetation over three decades. Journal of Vegetation Science **15**:781-788. *10.1111/j.1654-1103.2004.tb02321.x*.

R Core Team. 2013. R: A Language and Environment for Statistical Computing version 2.15. R Foundation for Statistical Computing, Vienna, Austria.

Robinson, S., and J. Lundholm. 2012. Ecosystem services provided by urban spontaneous vegetation. Urban Ecosystems **15**:545-557. *10.1007/s11252-012-0225-8*.

Rodriguez-Galiano, V. F., M. Chica-Olmo, F. Abarca-Hernandez, P. M. Atkinson, and C. Jeganathan. 2012. Random Forest classification of Mediterranean land cover using multi-seasonal imagery and multi-seasonal texture. Remote Sensing of Environment **121**:93-107. *10.1016/j.rse.2011.12.003*.

Roman, L., J. Battles, and J. McBride. 2014. The balance of planting and mortality in a street tree population. Urban Ecosystems **17**:387-404. *10.1007/s11252-013-0320-5*.

Rouse, J. W., Jr., R. H. Haas, J. A. Schell, and D. W. Deering. 1973. Monitoring the vernal advancement and retrogradation (green wave effect) of natural vegetation. Prog. Rep. RSC 1978-1, Remote Sensing Center, Texas A&M University, College Station, TX.

Rudie, R., and R. Dewers. 1984. Effects of tree shade on home cooling requirements. Journal of Arboriculture **10**:320-322.

Russell, S., and K. Fielding. 2010. Water demand management research: A psychological perspective. Water Resources Research **46**:W05302. *10.1029/2009wr008408*.

Sala, O., W. Lauenroth, and W. Parton. 1992. Long-term soil water dynamics in the shortgrass steppe. Ecology:1175-1181.

Sawka, M., A. A. Millward, J. McKay, and M. Sarkovich. 2013. Growing summer energy conservation through residential tree planting. Landscape and Urban Planning **113**:1-9. *10.1016/j.landurbplan.2013.01.006*.

Schiewe, J. 2002. Segmentation of high-resolution remotely sensed data-concepts, applications and problems. International Archives of Photogrammetry Remote Sensing and Spatial Information Sciences **34**:380-385.

Seo, S. 2003. Model-based automatic building extraction from lidar and aerial imagery. Ph.D. dissertation. The Ohio State University, Columbus, OH.

Shashua-Bar, L., D. Pearlmutter, and E. Erell. 2009. The cooling efficiency of urban landscape strategies in a hot dry climate. Landscape and Urban Planning **92**:179-186. *10.1016/j.landurbplan.2009.04.005*.

Shashua-Bar, L., D. Pearlmutter, and E. Erell. 2011. The influence of trees and grass on outdoor thermal comfort in a hot-arid environment. International Journal of Climatology **31**:1498-1506. *10.1002/joc.2177*.

Shashua-Bar, L., O. Potchter, A. Bitan, D. Boltansky, and Y. Yaakov. 2010. Microclimate modelling of street tree species effects within the varied urban morphology in the Mediterranean city of Tel Aviv, Israel. International Journal of Climatology **30**:44-57. *10.1002/joc.1869*.

Shugart, H., S. Saatchi, and F. Hall. 2010. Importance of structure and its measurement in quantifying function of forest ecosystems. Journal of Geophysical Research. G. Biogeosciences **115**. *10.1029/2009JG000993*.

Small, C. 2006. Comparative analysis of urban reflectance and surface temperature. Remote Sensing of Environment **104**:168-189. *10.1016/j.rse.2005.10.029*.

Smardon, R. C. 1988. Perception and aesthetics of the urban environment: Review of the role of vegetation. Landscape and Urban Planning **15**:85-106. *10.1016/0169-2046(88)90018-7*.

Smart, S. M., K. Thompson, R. H. Marrs, M. G. Le Duc, L. C. Maskell, and L. G. Firbank. 2006. Biotic homogenization and changes in species diversity across human-modified ecosystems. Proceedings of the Royal Society B: Biological Sciences **273**:2659-2665.

Smith, A. 2010. Image segmentation scale parameter optimization and land cover classification using the Random Forest algorithm. Journal of Spatial Science **55**:69-79.

Sperry, J. S., J. R. Donnelly, and M. T. Tyree. 1988. A method for measuring hydraulic conductivity and embolism in xylem. Plant Cell and Environment **11**:35-40.

Sperry, J. S., F. C. Meinzer, and K. A. McCulloh. 2008. Safety and efficiency conflicts in hydraulic architecture: scaling from tissues to trees. Plant Cell and Environment **31**:632-645. *10.1111/j.1365-3040.2007.01765.x*.

Sperry, J. S., and J. E. M. Sullivan. 1992. Xylem embolism in response to freeze-thaw cycles and water-stress in ring-porous, diffuse-porous, and conifer species. Plant Physiology **100**:605-613.

St. Hilaire, R., M. A. Arnold, D. C. Wilkerson, D. A. Devitt, B. H. Hurd, B. J. Lesikar, V. I. Lohr, C. A. Martin, G. V. McDonald, R. L. Morris, D. R. Pittenger, D. A. Shaw, and D. F. Zoldoske. 2008. Efficient water use in residential urban landscapes. HortScience **43**:2081-2092.

Steppe, K., and R. Lemeur. 2007. Effects of ring-porous and diffuse-porous stem wood anatomy on the hydraulic parameters used in a water flow and storage model. Tree physiology **27**:43-52.

Strobl, C., A.-L. Boulesteix, T. Kneib, T. Augustin, and A. Zeileis. 2008. Conditional variable importance for random forests. BMC Bioinformatics **9**:1-11. *10.1186/1471-2105-9-307*.

Strobl, C., A.-L. Boulesteix, A. Zeileis, and T. Hothorn. 2007. Bias in random forest variable importance measures: Illustrations, sources and a solution. BMC Bioinformatics **8**:1-21. *10.1186/1471-2105-8-25*.

Strobl, C., J. Malley, and G. Tutz. 2009. An introduction to recursive partitioning: rationale, application and characteristics of classification and regression trees, bagging and random forests. Psychological methods **14**:323–348. *10.1037/a0016973*.

Subburayalu, S., and T. D. Sydnor. 2012. Assessing street tree diversity in four Ohio communities using the weighted Simpson index. Landscape and Urban Planning **106**:44-50. *10.1016/j.landurbplan.2012.02.004*.

Sun, C. Y., A. J. Brazel, W. T. L. Chow, B. C. Hedquist, and L. Prashad. 2009. Desert heat island study in winter by mobile transect and remote sensing techniques. Theoretical and Applied Climatology **98**:323-335. *10.1007/s00704-009-0120-2*.

Taneda, H., and J. S. Sperry. 2008. A case-study of water transport in co-occurring ring- versus diffuse-porous trees: contrasts in water-status, conducting capacity, cavitation and vessel refilling. Tree physiology **28**:1641-1651.

Thanapura, P., D. L. Helder, S. Burckhard, E. Warmath, M. O'Neill, and D. Galster. 2007. Mapping urban land cover using QuickBird NDVI and GIS spatial modeling for runoff coefficient determination. Photogrammetric Engineering and Remote Sensing **73**:57-65.

Tooke, T. R., N. C. Coops, N. R. Goodwin, and J. A. Voogt. 2009. Extracting urban vegetation characteristics using spectral mixture analysis and decision tree classifications. Remote Sensing of Environment **113**:398-407. *10.1016/j.rse.2008.10.005*.

Tyree, M. T., and M. H. Zimmermann. 2002. Xylem Structure and the Ascent of Sap. 2nd edition. Springer, New York, NY.

Tzoulas, K., K. Korpela, S. Venn, V. Yli-Pelkonen, A. Kaźmierczak, J. Niemela, and P. James. 2007. Promoting ecosystem and human health in urban areas using Green Infrastructure: A literature review. Landscape and Urban Planning **81**:167-178. *10.1016/j.landurbplan.2007.02.001*.

Vidrih, B., and S. Medved. 2013. Multiparametric model of urban park cooling island. Urban Forestry & Urban Greening **12**:220-229. *10.1016/j.ufug.2013.01.002*.

Voogt, J. A., and T. R. Oke. 1998. Effects of urban surface geometry on remotely-sensed surface temperature. International Journal of Remote Sensing **19**:895-920. *10.1080/014311698215784*.

Voogt, J. A., and T. R. Oke. 2003. Thermal remote sensing of urban climates. Remote Sensing of Environment **86**:370-384. *Doi: 10.1016/s0034-4257(03)00079-8*.

Voss, M., and R. Sugumaran. 2008. Seasonal effect on tree species classification in an urban environment using hyperspectral data, LiDAR, and an object-oriented approach. Sensors **8**:3020-3036. *10.3390/s8053020*.

Vrecenak, A., and L. Herrington. 1984. Estimation of water use of landscape trees. Journal of Arboriculture **10**:313-319.

Walsh, C. J., A. H. Roy, J. W. Feminella, P. D. Cottingham, P. M. Groffman, and R. P. Morgan. 2005. The urban stream syndrome: current knowledge and the search for a cure. Journal of the North American Benthological Society **24**:706-723.

Wang, J., T. A. Endreny, and D. J. Nowak. 2008. Mechanistic simulation of tree effects in an urban water balance model. Journal of the American Water Resources Association **44**:75-85. *10.1111/j.1752-1688.2007.00139.x*.

Watts, J., and R. Lawrence. 2008. Merging random forest classification with an object-oriented approach for analysis of agricultural lands. The International Archives of the Photogrammetry, Remote Sensing and Spatial Information Sciences **37**:579-582.

Weng, Q. H., X. F. Hu, and D. S. Lu. 2008. Extracting impervious surfaces from medium spatial resolution multispectral and hyperspectral imagery: a comparison. International Journal of Remote Sensing **29**:3209-3232. *10.1080/01431160701469024*.

Weng, Q. H., D. S. Lu, and J. Schubring. 2004. Estimation of land surface temperature-vegetation abundance relationship for urban heat island studies. Remote Sensing of Environment **89**:467-483. *10.1016/j.rse.2003.11.005*.

Wentz, E. A., and P. Gober. 2007. Determinants of small-area water consumption for the city of Phoenix, Arizona. Water Resources Management **21**:1849-1863. *10.1007/s11269-006-9133-0*.

West, E. 1998. The contested plains : Indians, goldseekers, & the rush to Colorado. University Press of Kansas, Lawrence, KA.

Wheeler, S. M. 2008. The evolution of built landscapes in metropolitan regions. Journal of Planning Education and Research **27**:400-416.

Williams, N. S. G., M. W. Schwartz, P. A. Vesk, M. A. McCarthy, A. K. Hahs, S. E. Clemants, R. T. Corlett, R. P. Duncan, B. A. Norton, K. Thompson, and M. J. McDonnell. 2009. A conceptual framework for predicting the effects of urban environments on floras. Journal of Ecology **97**:4-9. *10.1111/j.1365-2745.2008.01460.x*.

Witten, I. H., F. Eibe, and M. A. Hall. 2011. Data Mining Practical Machine Learning Tools and Techniques. Third edition. Morgan Kaufman, Amsterdam, Netherlands.

Wood, E. F., M. Sivapalan, K. Beven, and L. Band. 1988. Effects of spatial variability and scale with implications to hydrologic modeling. Journal of Hydrology **102**:29-47. *10.1016/0022-1694(88)90090-x*.

Wu, J. 2014. Urban ecology and sustainability: The state-of-the-science and future directions. Landscape and Urban Planning. *10.1016/j.landurbplan.2014.01.018*.

Xiao, Q., and E. McPherson. 2011. Rainfall interception of three trees in Oakland, California. Urban Ecosystems **14**:755-769. *10.1007/s11252-011-0192-5*.

Xiao, Q., E. G. McPherson, J. R. Simpson, and S. L. Ustin. 1998. Rainfall interception by Sacramento's urban forest. Journal of Arboriculture **24**:235-244.

Xiao, Q. F., E. G. Mcpherson, S. L. Ustin, M. E. Grismer, and J. R. Simpson. 2000. Winter rainfall interception by two mature open-grown trees in Davis, California. Hydrological Processes **14**:763-784.

Xie, H. J. 2009. Using remote sensing and GIS technology for an improved decision support: a case study of residential water use in El Paso, Texas. Civil Engineering and Environmental Systems **26**:53-63. *10.1080/10286600802003666*.

Yang, L. M., L. M. Jiang, H. Lin, and M. S. Liao. 2009. Quantifying sub-pixel urban impervious surface through fusion of optical and InSAR imagery. GIScience & Remote Sensing **46**:161-171. *10.2747/1548-1603.46.2.161*.

Yu, Q., P. Gong, N. Clinton, G. Biging, M. Kelly, and D. Schirokauer. 2006. Object-based detailed vegetation classification. with airborne high spatial resolution remote sensing imagery. Photogrammetric Engineering and Remote Sensing **72**:799-811.

Yuan, F., and M. E. Bauer. 2007. Comparison of impervious surface area and normalized difference vegetation index as indicators of surface urban heat island effects in Landsat imagery. Remote Sensing of Environment **106**:375-386. *10.1016/j.rse.2006.09.003*.

Yue, W., J. Xu, W. Tan, and L. Xu. 2007. The relationship between land surface temperature and NDVI with remote sensing: application to Shanghai Landsat 7 ETM+ data. International Journal of Remote Sensing **28**:3205-3226.

Zhang, L., W. R. Dawes, and G. R. Walker. 2001. Response of mean annual evapotranspiration to vegetation changes at catchment scale. Water Resources Research **37**:701-708. *10.1029/2000WR900325*.

Zhou, W., G. Huang, and M. L. Cadenasso. 2011. Does spatial configuration matter? Understanding the effects of land cover pattern on land surface temperature in urban landscapes. Landscape and Urban Planning **102**:54-63. *10.1016/j.landurbplan.2011.03.009*.

Zhou, W., and A. Troy. 2008. An object-oriented approach for analysing and characterizing urban landscape at the parcel level. International Journal of Remote Sensing **29**:3119-3135. *10.1080/01431160701469065*.